

N70 - 27351

NASA TECHNICAL
MEMORANDUM



NASA TM X-1989

NASA TM X-1989

CASE FILE
COPY



ATLAS-CENTAUR AC-16 FLIGHT
PERFORMANCE EVALUATION FOR
THE ORBITING ASTRONOMICAL
OBSERVATORY OAO-II MISSION

*Staff of Lewis Research Center
Cleveland, Ohio*

1. Report No. NASA TM X-1989	2. Government Accession No.	3. Recipient's Catalog No.	
4. Title and Subtitle ATLAS-CENTAUR AC-16 FLIGHT PERFORMANCE EVALUATION FOR THE ORBITING ASTRONOMICAL OBSERVATORY OAO-II MISSION		5. Report Date May 1970	6. Performing Organization Code
		8. Performing Organization Report No. E-5306	
7. Author(s) Staff of Lewis Research Center		10. Work Unit No. 491-02	11. Contract or Grant No.
9. Performing Organization Name and Address Lewis Research Center National Aeronautics and Space Administration Cleveland, Ohio 44135		13. Type of Report and Period Covered Technical Memorandum	
		14. Sponsoring Agency Code	
12. Sponsoring Agency Name and Address National Aeronautics and Space Administration Washington, D.C. 20546			
15. Supplementary Notes			
16. Abstract The Atlas-Centaur AC-16 vehicle successfully launched the Orbiting Astronomical Observatory OAO-II into a nearly circular Earth orbit at an altitude of 772 km using a direct (single burn) mode of ascent. This report discusses the flight performance of the AC-16 launch vehicle from lift-off through the Centaur retro-maneuver after spacecraft separation.			
17. Key Words (Suggested by Author(s)) Launch vehicles Centaur applications Atlas applications Earth orbiting observatory Orbiting astronomical observatory		18. Distribution Statement Unclassified - unlimited	
19. Security Classif. (of this report) Unclassified	20. Security Classif. (of this page) Unclassified	21. No. of Pages 157	22. Price* \$3.00

*For sale by the Clearinghouse for Federal Scientific and Technical Information
Springfield, Virginia 22151

CONTENTS

	Page
I. <u>SUMMARY</u>	1
II. <u>INTRODUCTION</u>	3
III. <u>LAUNCH VEHICLE DESCRIPTION</u> by Eugene E. Coffey and Joseph A. Ziemianski	5
VI. <u>MISSION PERFORMANCE</u> by William A. Groesbeck	13
<u>ATLAS FLIGHT PHASE</u>	13
<u>CENTAUR FLIGHT PHASE</u>	14
<u>SPACECRAFT SEPARATION</u>	15
<u>CENTAUR RETROMANEUVER</u>	15
V. <u>TRAJECTORY AND PERFORMANCE</u> by John J. Nieberding	19
<u>MISSION PLAN.</u>	19
<u>TRAJECTORY RESULTS</u>	19
Lift-off Through Atlas Booster Phase	19
Atlas Sustainer Phase	20
Centaur Main Engine Firing Phase	20
Centaur Retromaneuver.	22
VI. <u>LAUNCH VEHICLE SYSTEM ANALYSIS</u>	29
<u>PROPULSION SYSTEMS</u> by Kenneth W. Baud, Charles H. Kerrigan, Ronald W. Ruedelee, and Donald B. Zelten	29
Atlas	29
Centaur Main Engines	30
Centaur Boost Pumps	32
Hydrogen Peroxide Engine and Supply System	33
<u>PROPELLANT LOADING AND PROPELLANT UTILIZATION</u> by Richard C. Kalo	54
Level Indicating System for Propellant Loading	54
Atlas Propellant Utilization System	54
Centaur Propellant Utilization System	55
<u>PNEUMATIC SYSTEMS</u> by Eugene J. Fourney and Merle L. Jones	64
Atlas	64
Centaur	66
<u>HYDRAULIC SYSTEMS</u> by Eugene J. Cieslewicz and Eugene J. Fourney	75
Atlas	75
Centaur	76

VEHICLE STRUCTURES by James F. Harrington, Robert C. Edwards, and Dana H. Benjamin	80
Atlas Structures	80
Centaur Structures	80
Vehicle Dynamic Loads	82
SEPARATION SYSTEMS by Thomas L. Seeholzer, Charles W. Eastwood, and William M. Prati	96
Stage Separation	96
Jettisonable Structures	97
ELECTRICAL SYSTEMS by John M. Bulloch and John B. Nechvatal	112
Power Sources and Distribution	112
Instrumentation and Telemetry	113
Tracking System	115
Range Safety Command System	116
GUIDANCE AND FLIGHT CONTROL SYSTEMS by Paul W. Kuebeler, William J. Middendorf, and Corrine Rawlin	125
Guidance System	126
Flight Control Systems	131
VII. <u>CONCLUDING REMARKS</u>	147
<u>APPENDIXES</u>	
A - SUPPLEMENTAL LAUNCH AND WEIGHTS DATA	
by John J. Nieberding	149
B - CENTAUR ENGINE PERFORMANCE CALCULATION	
by Ronald W. Ruedelee	153
REFERENCES	154

I. SUMMARY

The Atlas-Centaur (AC-16) with the Orbiting Astronomical Observatory-II (OAO-II) spacecraft was successfully launched from the Eastern Test Range Complex 36B on December 7, 1968, at 0340:09 eastern standard time. The direct-ascent flight profile was considerably more lofted than those employed in previous Atlas-Centaur flights. The vehicle was programmed to a flight azimuth of 60° in order not to violate the range safety protective zone around Bermuda. To achieve this flight azimuth the Atlas vehicle roll program was 5 seconds longer than for previous Atlas-Centaur flights. After it cleared the Bermuda protective zone, the Centaur was yawed to the right to achieve the desired orbital inclination of 35° to the equator. All Atlas and Centaur systems performed properly, and the spacecraft was injected into the desired 772-kilometer (417-n-mi) near-circular Earth orbit at the desired inclination.

The AC-16 was the first vehicle in which the Centaur flight control system provided the Atlas with both rate and position signal during the Atlas sustainer phase of flight. The OAO nose fairing, flown for the first time on an Atlas-Centaur vehicle, adequately protected the spacecraft during ascent and was jettisoned successfully. Because of the increased weight of the payload and fairing, the Atlas holddown time on the launch pad was extended 1.76 seconds to achieve the desired minimum thrust-to-weight ratio of 1.2 at lift-off.

This report presents an evaluation of the Atlas-Centaur system in support of the OAO-II.

II. INTRODUCTION

by John J. Nieberding

The purpose of the Orbiting Astronomical Observatory-II (OAO-II) was to make precision telescopic measurements from above the Earth's atmosphere. Specific areas of interest were mapping and studying the emission and absorption characteristics of the Sun, stars, planets, nebulae, and interplanetary and interstellar media in the relatively unexplored ultraviolet region of the spectrum.

The primary objective of the AC-16 flight was to inject the OAO-II spacecraft into a circular Earth orbit at an altitude of 772 kilometers (417 n mi) and at an orbital inclination to the equator of 35° . The launch vehicle was also required to perform a retro-maneuver to minimize the periods the Centaur would be in view of the spacecraft optical sensors and to minimize contamination of the spacecraft from Centaur exhaust products.

The AC-16 launch vehicle and the launch vehicle/spacecraft integration effort to support the OAO program were under the direction of the Lewis Research Center. OAO-II was the second of four OAO satellites currently planned to be launched. OAO-I was successfully launched on April 8, 1966, by an Atlas-Agena launch vehicle. OAO-III and -IV are currently planned for 1970 and 1971 launches, respectively.

The AC-16 used a direct (single burn) mode of ascent to inject the spacecraft into the desired orbit. Because of the required orbital altitude of 772 kilometers (417 n mi), the flight profile was considerably steeper than on previous Atlas-Centaur flights. The vehicle was programmed to a flight azimuth of 60° in order to avoid the protective zone around Bermuda imposed by Range Safety at the Eastern Test Range. Then, after it cleared the Bermuda protective zone, the Centaur was yawed to the right to achieve the desired orbital inclination of 35° to the equator. This report evaluates the performance of the Atlas-Centaur launch vehicle, in support of OAO-II, from lift-off through spacecraft separation and completion of the Centaur retromaneuver following spacecraft separation.

III. LAUNCH VEHICLE DESCRIPTION

by Eugene E. Coffey and Joseph A. Ziemianski

The Atlas-Centaur is a two-stage launch vehicle consisting of an Atlas first stage and a Centaur second stage connected by an interstage adapter. Both stages are 3.05 meters (10 ft) in diameter, and the composite vehicle is 41.8 meters (135 ft) in length. The vehicle weight at lift-off is approximately 147 255 kilograms (324 656 lbm). The basic structure of the Atlas and the Centaur stages utilizes thin-wall, pressure-stabilized, main propellant tank sections of monocoque construction. Figure III-1 shows the Atlas-Centaur lifting off with the OAO-II spacecraft.

The first-stage SLV-3C Atlas (fig. III-2) is 21.03 meters (69 ft) long. It is powered by an MA-5 propulsion system consisting of a booster engine with two thrust chambers and with a total thrust at sea level of 1494×10^3 newtons (336×10^3 lbf), a sustainer engine with a thrust at sea level of 258×10^3 newtons (58×10^3 lbf), and two vernier engines with a thrust at sea level of 2980 newtons (670 lbf) each.

All engines use liquid oxygen and RP-1 (kerosene) as propellants and are ignited prior to lift-off. The booster engine thrust chambers are gimballed for pitch, yaw, and roll control during the booster engine phase of the flight. This phase is completed at booster engine cutoff, which occurs when the vehicle acceleration reaches about 5.7 g's, and the booster engine section is jettisoned 3.1 seconds later. The sustainer engine and the vernier engines continue to burn for the Atlas sustainer phase of the flight. During this phase, the sustainer engine is gimballed for pitch and yaw control, while the vernier engines are gimballed for roll control only. The sustainer and vernier engines fire until propellant depletion. The Atlas is severed from the Centaur by the firing of a shaped charge system located on the forward end of the interstage adapter. The firing of a retrorocket system then separates the Atlas - interstage adapter from the Centaur.

The Centaur second stage (fig. III-3) is about 9.1 meters (30 ft) long. It is a high-performance stage (specific impulse, 442 sec) powered by two RL10A-3-3 engines which generate a total sea-level thrust of approximately 133.45×10^3 newtons (30 000 lbf). These engines use liquid hydrogen and liquid oxygen as propellants. The Centaur main engines are gimballed to provide pitch, yaw, and roll control during Centaur powered flight. Fourteen hydrogen peroxide engines, mounted on the aft periphery of the tank, provide various thrust levels for attitude control after Centaur main engine cutoff and for vehicle reorientation after spacecraft separation.

The Centaur hydrogen tank is shielded with four insulation panel sections, each 2.54 centimeters (1 in.) thick. Each section consists of a polyurethane-foam-filled honeycomb core, covered with fiber glass lamination. The nose fairing system

(fig. III-4) is 12.2 meters (40 ft) long and consists of a jettisonable section (fiber glass honeycomb core nose fairing and metallic split fairing) and a fixed metallic fairing and fiber glass honeycomb core barrel section. It is used to provide an aerodynamic shield for the OAO-II spacecraft, for the Centaur guidance equipment, and for the Centaur electronic packages during ascent.

This nose fairing system flown for the first time on Atlas-Centaur is similar to the Surveyor nose fairing except it is 5.5 meters (18 ft) longer and uses a mechanical spring system instead of a gas thruster system to jettison the fairing. The fixed fairing and the barrel section remain with the Centaur after jettison of the nose fairing. The insulation panels are jettisoned during the Atlas sustainer phase, and the nose fairing is jettisoned shortly after Centaur main engine start. The OAO-II spacecraft is shown in figure III-5.



Figure III-1. - Atlas-Centaur lifting off with OAO-11.

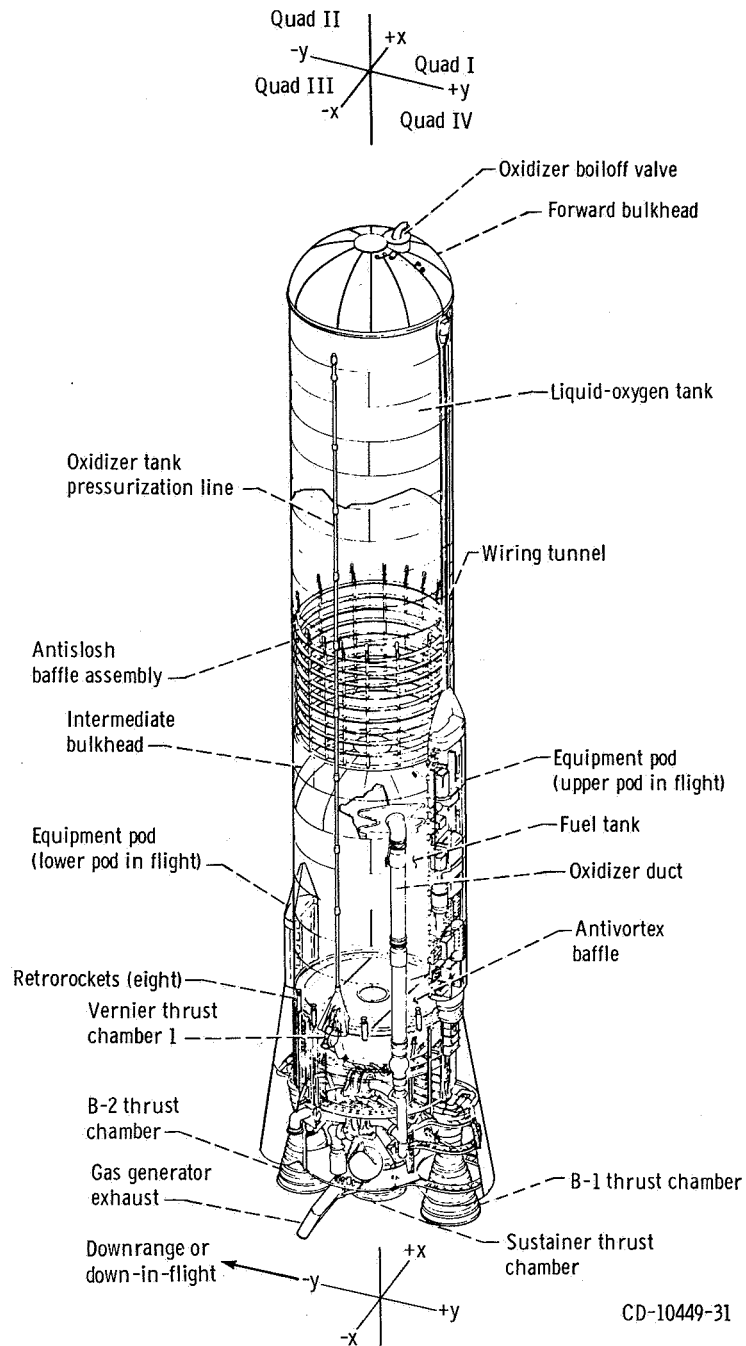


Figure III-2. - General arrangement of Atlas launch vehicle, AC-16.

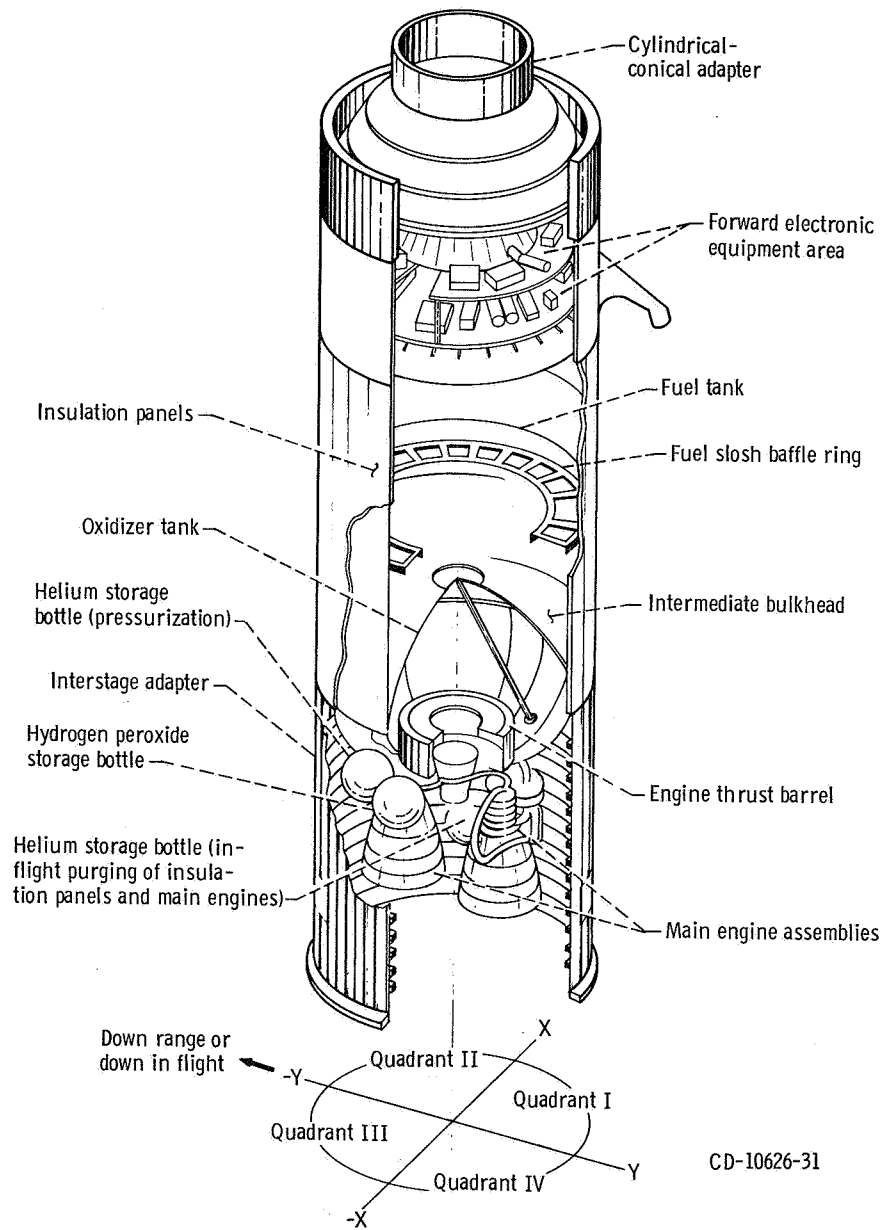


Figure III-3. - General arrangement of Centaur vehicle, AC-16.

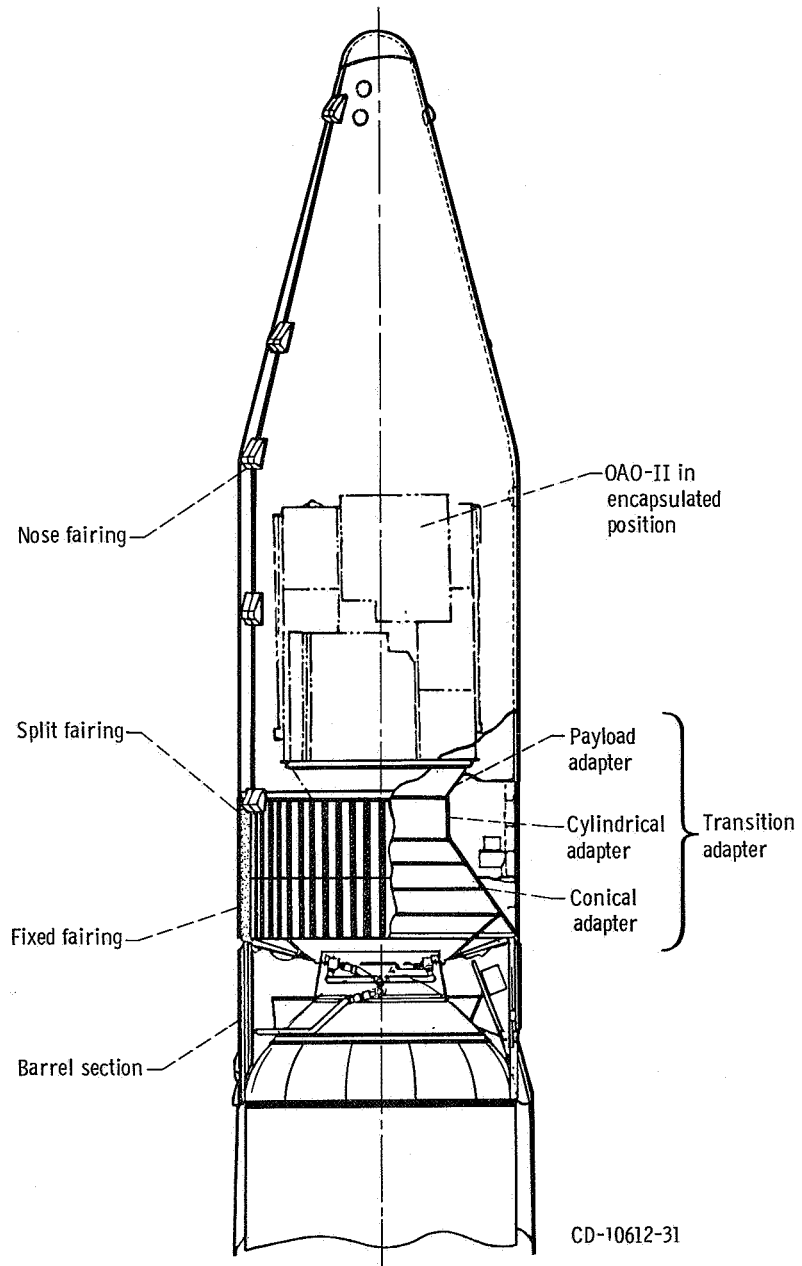


Figure III-4. - Nose fairing system, AC-16.

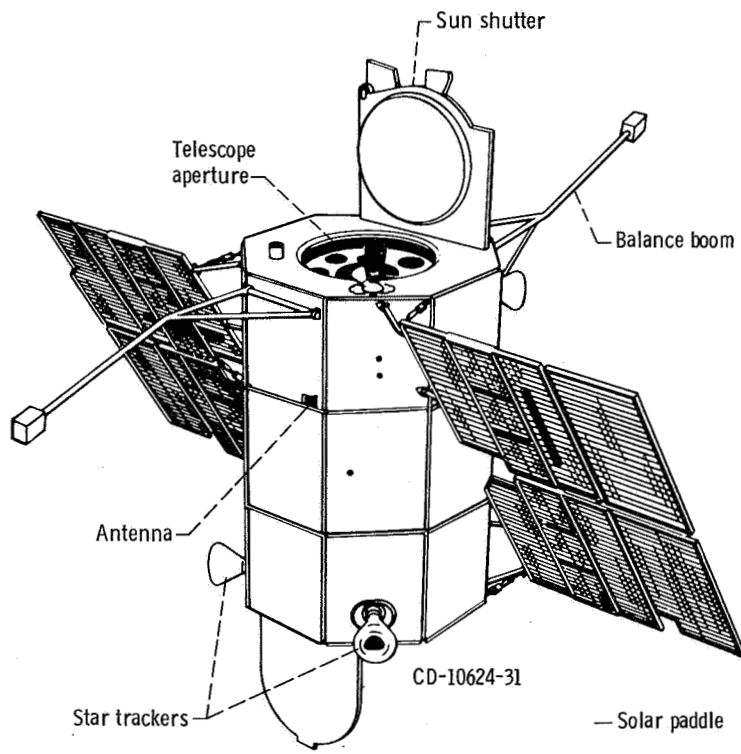


Figure III-5. - Deployed configuration of Orbiting Astronomical Observatory-II (OAO-II).

IV. MISSION PERFORMANCE

by William A. Groesbeck

The Atlas-Centaur vehicle AC-16, with the OAO-II spacecraft, was successfully launched from Eastern Test Range Complex 36B on December 7, 1968, at 0340:09 eastern Standard time. The launch vehicle used the direct (single burn) mode of ascent to place the OAO-II into a nearly circular orbit. All launch vehicle objectives were achieved, and the spacecraft was placed in Earth orbit at an altitude of about 772 kilometers (417 n mi).

The AC-16 mission profile and the OAO-II orbital trajectory are shown in figures IV-1 and IV-2. The OAO-II launch window and countdown history, as well as a summary of postflight vehicle weights, are given in appendix A.

ATLAS FLIGHT PHASE

Ignition and thrust buildup of the Atlas engines were normal. The vehicle lifted off (T + 0 sec) with a combined vehicle weight of 147 255 kg (324 656 lbm) and a thrust-to-weight ratio of 1.2. Two seconds after lift-off, the vehicle initiated a programmed roll from the launch pad azimuth of 115° to the required flight azimuth of 60° . This flight azimuth was attained at T + 20 seconds. At T + 15 seconds, the vehicle began a pre-programmed pitchover maneuver which lasted through booster engine cutoff. The Centaur inertial guidance system was functioning during this time, but steering commands were not admitted to the Atlas flight control system until after booster engine staging.

The pitch program used to command the vehicle during the booster flight was provided by the Centaur guidance system. This pitch program, one of a series selected on the basis of measured prelaunch upper-air soundings, was stored in the Centaur airborne computer. Booster engine gimbal angles for thrust vector control did not exceed 2.4° during the atmospheric ascent.

Vehicle acceleration during the boost phase was according to the mission plan. Centaur guidance issued the booster engine cutoff signal when the vehicle acceleration reached 5.74 g's (specification 5.79 ± 0.113). Three seconds later at T + 155.2 seconds, the Atlas programmer issued the staging command to separate the booster engine section from the vehicle. Staging transients were small, and the maximum vehicle angular rate in pitch, yaw, or roll did not exceed 3.11 degrees per second. Vehicle steering by the inertial guidance system was initiated about 5 seconds following Atlas booster engine staging. At the start of guidance steering, the vehicle was slightly off the required

steering vector by about 1° nose low in pitch and 1° nose right in yaw. The guidance system steered the vehicle to the proper vector and issued commands to continue the pitchover maneuver during the Atlas sustainer flight phase.

Insulation panels were jettisoned during the sustainer flight phase at $T + 196.8$ seconds. All four panels were severed by the shaped charges and fell away from the vehicle. Unlike previous Atlas-Centaur flights, the nose fairing was jettisoned after Centaur main engine start, rather than during Atlas phase of flight. Vehicle angular rates resulting from the jettisoning of the insulation panels were insignificant.

Sustainer and vernier engine system performance was satisfactory throughout the flight. Sustainer engine cutoff was initiated by liquid-oxygen depletion at $T + 234.5$ seconds. Maximum vehicle acceleration just prior to sustainer engine cutoff was 1.57 g's. Coincident with sustainer engine cutoff, the guidance steering commands to the Atlas flight control system were disabled, allowing the vehicle to coast in a free-flight mode. This guidance mode prevented gimbaling the Centaur main engines and allowed the engines to be centered to maintain clearance between the engines and the interstage adapter during Atlas-Centaur separation.

The Atlas staging command was issued by the flight programmer at $T + 236.4$ seconds. A shaped-charge firing cut the interstage adapter to separate the two stages. Eight retrorockets on the Atlas then fired to move the Atlas stage away from the Centaur. The transients during separation were small, and the maximum angular rate imparted to the vehicle did not exceed 0.5 degree per second.

CENTAUR FLIGHT PHASE

The main engine start sequence for the Centaur stage was initiated prior to sustainer engine cutoff. Propellant boost pumps were started at $T + 199.2$ seconds and allowed to come up to speed. To prevent boost pump cavitation during the near-zero-gravity period from sustainer engine cutoff until main engine start at $T + 246.0$ seconds, the required net positive suction pressure was provided by pressure pulsing the propellant tanks with helium. Eight seconds prior to main engine start, the Centaur programmer issued prestart commands for engine firing. Centaur main engines were gimballed to zero. Engine prestart valves were opened to flow liquid hydrogen through the lines to chill the engine turbopumps. Chillover of the turbopumps ensured against cavitation during pump acceleration and made possible a uniform and rapid thrust build-up after engine ignition. At $T + 246.0$ seconds, the ignition command was issued by the flight programmer and engine thrust increased to full flight levels.

Guidance steering for the Centaur stage was enabled at $T + 250$ seconds. The total residual angular rates and disturbing torques induced during the Atlas-Centaur

staging interval resulted in only a slight vehicle drift off the steering vector. This attitude drift error was corrected within 1 second after start of guidance steering.

The nose fairing was unlatched and jettisoned at T + 257.6 seconds. Disturbances due to separation caused a slight roll disturbance of 1.76 degrees per second; but this disturbance was damped out within 2 seconds. About 9 seconds after fairing jettison, the guidance system commanded a yaw maneuver (dog leg) to realign the velocity vector to meet the OAO-II orbit inclination requirement of 35° . Main engine shutdown was commanded by Centaur guidance at T + 698.2 seconds. Orbital insertion occurred approximately over Bermuda at an altitude of about 772 kilometers (417 n mi).

The Centaur engine burn time to establish the parking orbit was about 13 seconds longer than expected. The additional firing time was necessary to compensate for an apparent low thrust level. The propellant utilization system performed satisfactorily and accurately controlled the fuel and oxidizer flow rates to the engines.

SPACECRAFT SEPARATION

Coincident with the main engine cutoff, guidance steering commands were temporarily disabled, and the hydrogen peroxide vehicle rate control system was activated. Angular rates resulting from engine shutdown transients were small and were quickly damped to rates less than the control threshold of 0.2 degree per second. The residual vehicle motion below the rate threshold allowed only a negligible drift in vehicle attitude. This drift did not interfere with the subsequent spacecraft separation.

The Centaur - OAO-II coasted in a near-zero-gravity field for about 50 seconds. During this time, commands were given by the Centaur programmer to the spacecraft to deploy solar panels, to extend balance arms, and to arm the spacecraft separation pyrotechnics. All commands were properly received by the spacecraft.

At T + 748.3 seconds, the command for spacecraft separation was given. The hydrogen peroxide vehicle rate control system was commanded off, the pyrotechnically operated latches were fired, and the separation springs pushed the OAO-II away from the Centaur. The maximum angular rate of the Centaur was 0.37 degree per second just prior to, and 0.65 degree per second just following spacecraft separation. These rates are well within the maximum allowable rate of 1 degree per second for the Centaur at the time of spacecraft separation.

CENTAUR RETROMANEUVER

Following spacecraft separation, it was necessary for the Centaur stage to perform a reorientation and retrothrust maneuver in order to alter its orbit and place it beyond

the view of the OAO-II star tracker. The vehicle began to reorient to a new vector which was approximately the negative geocentric radius vector at $T + 1055$ seconds. At $T + 1149$ seconds, with the Centaur aligned to the new radius vector, two vernier engines were fired to provide 444.8 newtons (100 lbf) of thrust for 49 seconds. As these engines were commanded off, two 13.3-newton (3-lbf) thrust engines were commanded on and fired continuously for the next 350 seconds. The final part of the retromaneuver was then accomplished by opening the engine prestart valves to allow residual propellants in the tanks to "blowdown" through the main engines. The prestart valves remained open, allowing tank pressures to decrease to zero, and the vehicle continued in orbit in a nonstabilized flight mode.

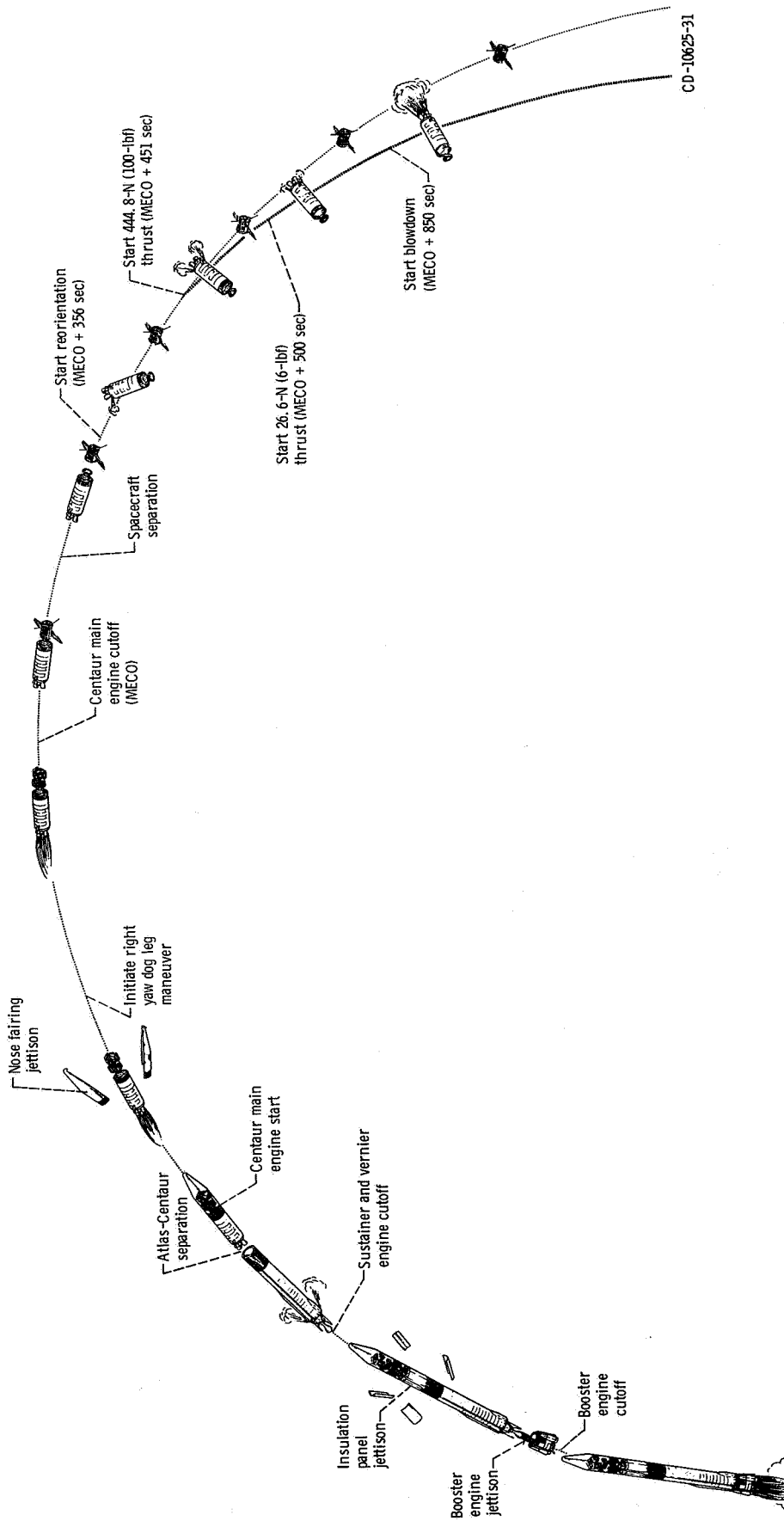
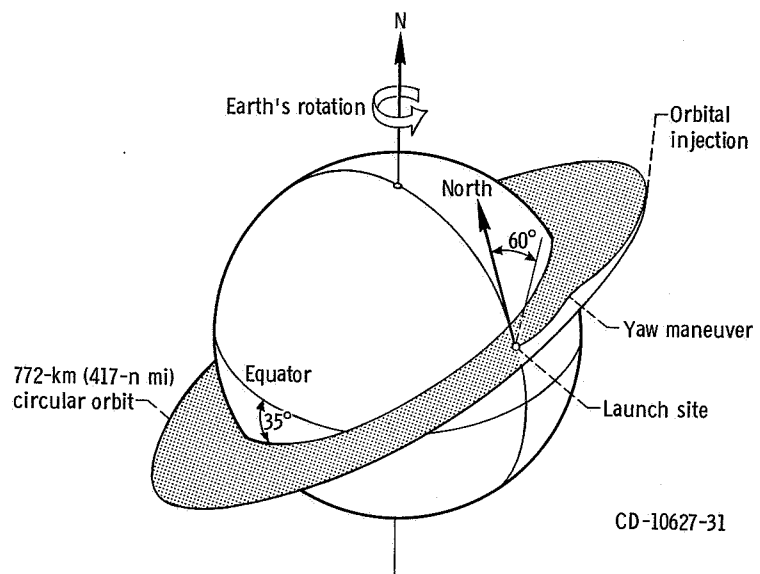


Figure IV-1. - Atlas-Centaur flight profile, AC-16.



CD-10627-31

Figure IV-2. - OAO-II orbital trajectory, AC-16. Flight azimuth, 60° .

V. TRAJECTORY AND PERFORMANCE

by John J. Nieberding

MISSION PLAN

The mission plan for AC-16 was to launch the OAO-II spacecraft into a circular Earth orbit at an altitude, measured at the equator, of 772 kilometers (417 n mi) and at an orbital inclination to the equator of 35° . Achievement of this orbit required the steepest ascent trajectory ever flown by Atlas-Centaur. The ascent mode was direct ascent (i. e. , Atlas and Centaur employed a nearly continuous powered phase, with the Centaur main engines firing only once). In order to achieve the required orbital inclination, a yaw maneuver around Bermuda was required during the Centaur firing period. Following main engine firing, the spacecraft was separated from Centaur to begin its postseparation sequence. The Centaur then performed a retromaneuver to meet a complex postseparation spacecraft viewing constraint.

TRAJECTORY RESULTS

Lift-off Through Atlas Booster Phase

Wind conditions at the launch site, based on data from a weather balloon sent aloft approximately 8 minutes after lift-off, were such that the ground wind was from the west/northwest (direction, 290°) at a speed of 11 kilometers per hour (6 knots). However, at an altitude of 12.2 kilometers (6.6 n mi), the speed had increased to a maximum of 102 kilometers per hour (89 knots) from 273° . These wind conditions required the use of pitch program 182 and yaw program 8 to minimize angle of attack through the booster phase of flight.

Radar tracking and Centaur guidance data indicated that the AC-16 flight path during the Atlas booster phase was very close to the predicted path. The transonic region, or the time span when the vehicle passes through Mach 1, occurred from about 60 to 65 seconds. During this period the axial load factor (thrust acceleration in g's) was nearly constant (fig. V-1). This is indicative of the vehicle's vibrations. Maximum dynamic pressure occurred at about $T + 80$ seconds (see fig. V-2). Atlas booster engine cutoff occurred at $T + 152.1$ seconds (see table V-I) when the vehicle axial load factor reached 5.74. (The axial load factor at booster engine cutoff is designed to be 5.7 ± 0.113 .) This cutoff was 0.8 second earlier than predicted.

At booster engine cutoff, the altitude was about 0.8 kilometer (0.4 n mi) lower than predicted, while the inertial velocity was about 96.6 kilometers per hour (88 ft/sec) lower than predicted (see figs. V-3 and V-4) (Note that fig. V-4 plots velocity relative to the atmosphere, not inertial velocity.) These deviations are well within tolerances.

Atlas Sustainer Phase

An abrupt decrease in acceleration occurred at $T + 152.1$ seconds when the booster engines cut off. This decrease is shown in figure V-1 and also in figure V-4, where a change in slope indicates a change in acceleration. A small but sudden increase in acceleration occurred at $T + 155.2$ seconds when the booster engine section, weighing 3378 kilograms (7448 lbm), was jettisoned. Following booster jettison, the constantly decreasing vehicle propellant weight caused the axial acceleration to increase smoothly until sustainer and vernier engine cutoff at $T + 234.5$ seconds, except for a small perturbation caused by jettisoning the 526-kilogram (1159-lbm) insulation panels at $T + 196.8$ seconds. This cutoff occurred at exactly the time predicted. At this time, the altitude was less than 0.30 kilometer (0.16 n mi) lower than expected; the inertial velocity was about 65.4 kilometers per hour (60 ft/sec) low. The axial acceleration at sustainer and vernier engine cutoff dropped abruptly to zero, indicating the loss of all thrust.

Centaur Main Engine Firing Phase

Atlas-Centaur separation was timed to occur 1.9 seconds after sustainer engine cutoff. Note in figure V-4 that the velocity decreased significantly between sustainer engine cutoff and Centaur main engine start. This velocity loss indicates a period of free-fall in a steep trajectory under the influence of gravity only. The increase in velocity and acceleration at Centaur main engine start ($T + 246.0$ sec) can be seen in figures V-4 and V-1, respectively.

After main engine start, the uniformly decreasing Centaur propellant weight caused the axial acceleration to increase smoothly until the 1115-kilogram (2458-lbm) split fairing - nose fairing combination was jettisoned at $T + 257.6$ seconds. The reason for jettisoning the nose fairing during the Centaur phase (as opposed to the usual jettison prior to sustainer engine cutoff) was twofold: (1) the acceleration level sensed at this time (about 0.75 g's) was nearer to the 1-g level at which the fairing had been tested than the level would have been during the late sustainer phase (about 1.5 g's), and (2) the

probability of Atlas retrorocket exhaust impingement on the spacecraft optics was precluded by delaying the time of fairing jettison.

Shortly after the fairing was jettisoned, the Centaur main engines were gimbaled in order to perform a turn (yaw maneuver) to the right. This maneuver was required to achieve a final orbit inclination of 35° . Figure V-5 illustrates the instantaneous trace of the point at which Earth impact would occur if the Atlas-Centaur vehicle would lose all thrust or jettison a piece of hardware. These traces are called instantaneous impact point (IIP) traces. The figure shows the elliptical areas of impact for the sustainer section and nose fairing for three launch azimuths of 80° , 67° , and 60° . In order to achieve 35° inclination without performing any yaw maneuver, a launch azimuth of 67° or 113° would have been required. Tracking constraints precluded a launch azimuth of 113° . With an azimuth of 67° , there was a high probability that the nose fairing would impact inside the zone around Bermuda protected by Range Safety. This same zone prevented launching at azimuths between 60° and 80° . The 60° launch azimuth was chosen because the launch vehicle had better performance capability at 60° than at 80° . This azimuth then required a yaw to the right, once past Bermuda, to essentially "parallel" the 67° IIP trace and thereby achieve the proper orbital inclination.

During the remainder of the Centaur phase, the axial acceleration and relative velocity increased uniformly until Centaur main engine cutoff. During this period, however, the acceleration was approximately 3.2 percent lower than predicted because of low Centaur thrust. This effect can be seen in figure V-4, where the velocities are lower than expected throughout the Centaur phase until the proper cutoff value had been achieved, 13.0 seconds later than predicted. Based on a trajectory reconstructed from postflight Centaur guidance data, altitude at main engine cutoff differed from the predicted value by less than 0.18 kilometer (0.10 n mi), and velocities agreed to within 1.2 kilometers per hour (1.1 ft/sec). The spacecraft separated from Centaur 50.1 seconds later. Comparisons of the spacecraft orbit actually achieved with the orbit predicted are presented in table V-II. The difference between the predicted parameters and those based on the Guidance Reconstructed Trajectory (GRT) is an indication of the errors caused by guidance equation inaccuracies and dispersions in the Centaur main engine shutdown impulse. The difference between the GRT data and those based on the Best Estimate of Trajectory (BET) is primarily due to errors in guidance hardware and BET tracking data. The difference between Goddard Space Flight Center's tracking data and the BET is primarily caused by tracking and orbit determination errors. One point is to be noted: Figure V-3 shows the altitude at main engine cutoff (and, hence, also at spacecraft separation since the orbit is nearly circular) to be 779 kilometers (420 n mi). Yet table V-II quotes a perigee altitude of only about 772 kilometers (417 n mi). The reason is that the 779 kilometers (420 n mi) is referenced to an oblate Earth. At main engine cutoff, the actual altitude above the real, oblate Earth was 779 kilo-

meters (420 n mi). However, by the time the vehicle crossed the equator, keeping a nearly constant radius, because the Earth has a greater diameter at the equator its altitude was about 772 kilometers (417 n mi). Thus, the apogee and perigee altitudes quoted in table V-II refer to the maximum and minimum altitudes respectively, when the vehicle passes over the equator.

Centaur Retromaneuver

Operation of the OAO-II spacecraft was restricted to periods when the Centaur tank is out of view of the spacecraft star sensor. Figure V-6 illustrates the pertinent geometry. When a line is drawn from the spacecraft 14° above the spacecraft horizon and then rotated about the spacecraft, maintaining the 14° angle, a conical volume is generated. If the Centaur tank, after separation from the spacecraft, is not within this volume, it is potentially in view of the spacecraft star sensor. A Centaur retromaneuver capable of assuring that the tank will be permanently out of view was not possible. The only possible maneuvers resulted in the Centaur's going out of view at some time after separation but again coming back into view at some later time. Analysis revealed that in order to minimize the probability of the Centaur staying in view for excessively long periods of time, the retromaneuver should be designed to yield a time to get out of view of 5.7 days after spacecraft separation with a corresponding return to view 64.3 days later. Centaur guidance data indicated that the Centaur went out of view in 6.5 days and returned into view 73.5 days later. Radar tracking data from the North American Air Defense Command (NORAD) showed a time to get out of view of 5.5 days, and a return to view 61.5 days later. Because of potentially large dispersions in the impulse supplied by the Centaur retromaneuver, these data are considered to be in good agreement with predicted values. (Predicted and actual Centaur postretromaneuver orbital parameters are given in table V-III.)

TABLE V-I. - FLIGHT EVENTS RECORD, AC-16

Event	Programmer time, sec	Preflight time, sec	Actual time, sec
Lift-off (2-in. (5.08-cm) motion)	T + 0	T + 0	T + 0
Start roll	T + 2.0	T + 2.0	T + 2.0
Start pitchover	T + 15.0	T + 15.0	T + 15.0
Stop roll	T + 20.0	T + 20.0	T + 20.0
Booster engine cutoff (BECO)	BECO	T + 152.9	T + 152.1
Jettison booster engines	BECO + 3.1	T + 156.0	T + 155.2
Admit guidance steering	BECO + 8.0	T + 160.9	T + 160.1
Jettison insulation panels	BECO + 45.0	T + 197.9	T + 196.8
Start Centaur booster pumps	BECO + 47.0	T + 199.9	T + 199.2
Sustainer engine cutoff (SECO); inhibit guidance steering	SECO	T + 234.6	T + 234.5
Atlas-Centaur separation	SECO + 1.9	T + 236.5	T + 236.4
Fire Atlas retrorockets	SECO + 2.0	T + 236.6	T + 236.5
Centaur prestart	SECO + 3.5	T + 238.1	T + 238.0
Centaur main engine start	SECO + 11.5	T + 246.1	T + 246.0
Readmit guidance steering	SECO + 15.5	T + 250.1	T + 250.0
Jettison nose fairing	SECO + 23.5	T + 258.1	T + 257.6
Centaur main engine cutoff (MECO)	MECO	T + 685.2	T + 698.2
Deploy solar paddles	MECO + 10.0	T + 695.2	T + 708.2
Extend balance booms	MECO + 25.0	T + 710.2	T + 723.2
Spacecraft separate	MECO + 50.0	T + 735.2	T + 748.3
Start reorientation to retrovector	MECO + 356.0	T + 1041.2	T + 1055.2
Start propellant settling engines	MECO + 451.0	T + 1136.2	T + 1149.2
Stop propellant settling engines; start propellant retention engines	MECO 500.0	T + 1185.2	T + 1198.2
Start discharge of Centaur residual propellants (blow-down)	MECO + 850.0	T + 1535.2	T + 1548.2

TABLE V-II. - OAO-II ORBIT PARAMETERS, AC-16

Parameter	Units	Predicted value	Actual value		
			GRT ^a	BET ^b	GSFC ^c
Epoch	sec from lift-off	736.0	748.3	748.3	748.3
Semimajor axis	km	7150.018	7150.885	7151.799	7151.979
	n mi	3860.701	3861.169	3861.663	3861.760
Inclination	deg	34.9982	34.9990	34.9811	34.9815
Eccentricity	----	0.000089	0.000083	0.00022	0.00030
Apogee altitude	km	772.586	773.210	775.197	775.950
	n mi	417.163	417.500	418.573	418.980
Perigee altitude	km	771.312	772.114	772.045	771.654
	n mi	416.475	416.908	416.871	416.660
Period	min	100.283	100.299	100.318	100.322

^aGuidance Reconstructed Trajectory obtained from telemetered Centaur guidance data.

^bBest Estimate of Trajectory obtained from Eastern Test Range radar tracking data.

^cGoddard Space Flight Center data obtained from Manned Space Flight Net tracking data.

TABLE V-III. - CENTAUR POSTRETROMANEUVER
ORBITAL PARAMETERS, AC-16

Parameter	Units	Predicted value	Actual value
Epoch	sec from lift-off	5485.1	7842.0
Semimajor axis	km	7152.0	7148.3
	n mi	3861.8	3859.8
Inclination	deg	35.0293	34.9908
Eccentricity	----	0.00550	0.00645
Apogee altitude	km	813.4	814.5
	n mi	439.2	439.8
Perigee altitude	km	734.7	729.3
	n mi	396.7	393.8
Period	min	100.328	100.247

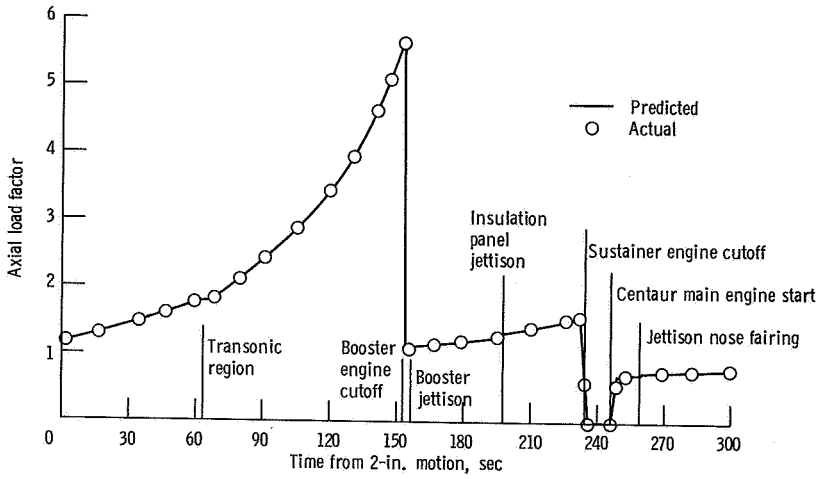


Figure V-1. - Axial load factor as function of time, AC-16.

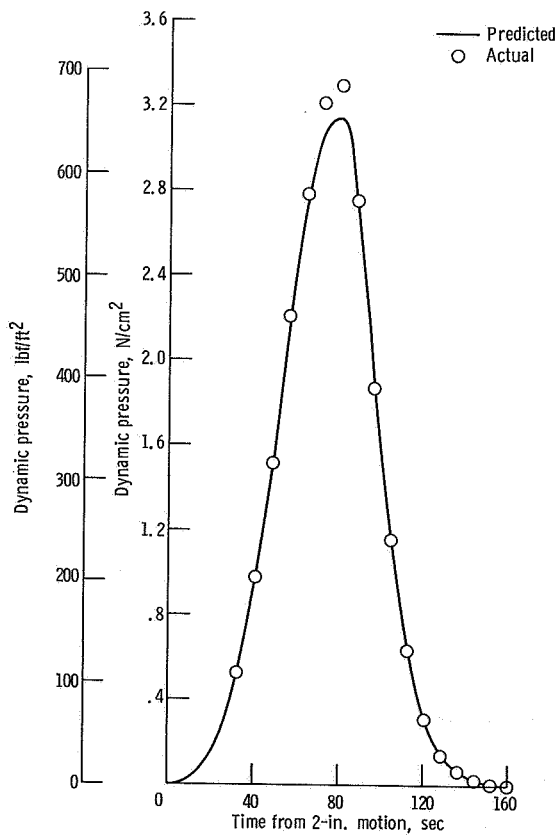


Figure V-2. - Dynamic pressure as function of time, AC-16.

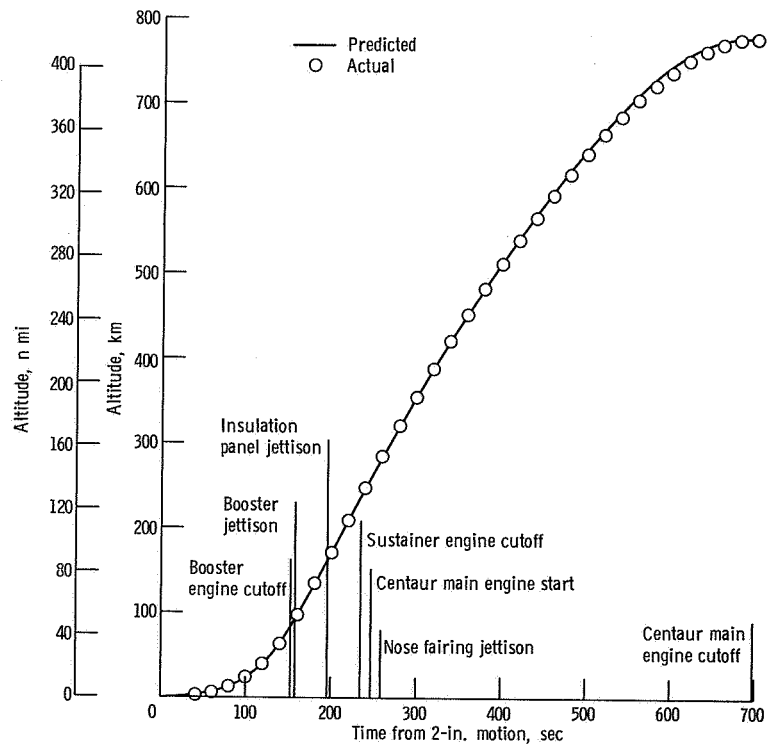


Figure V-3. - Altitude as function of time, AC-16.

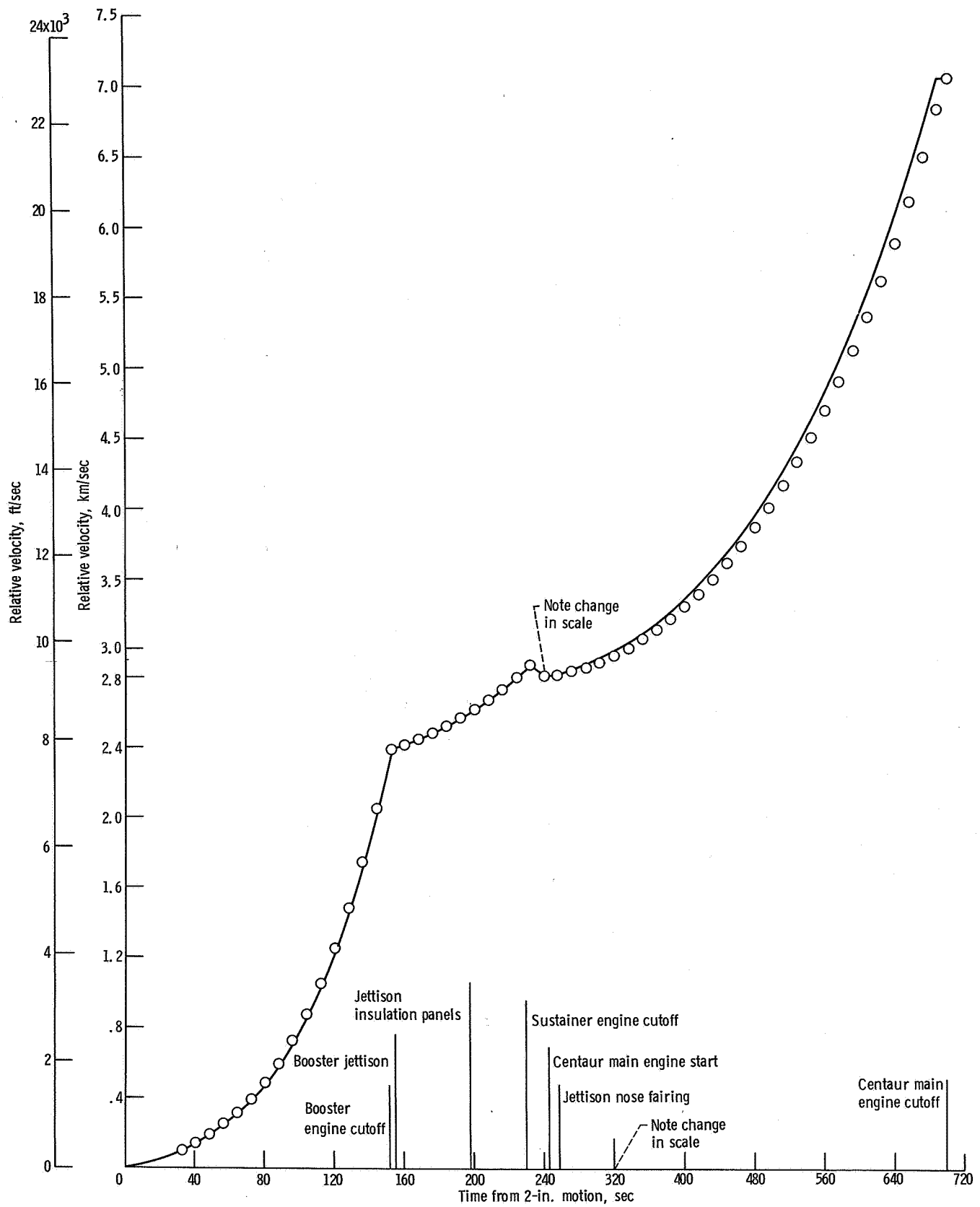


Figure V-4. - Relative velocity as function of time, AC-16.

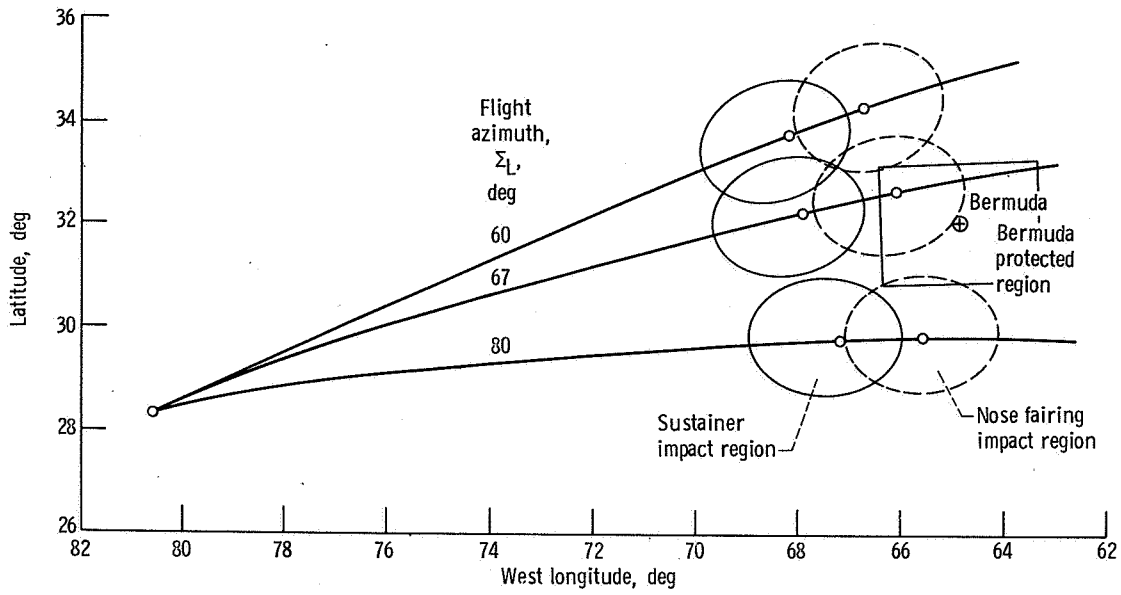


Figure V-5. - Instantaneous impact point traces for OAO-II mission.

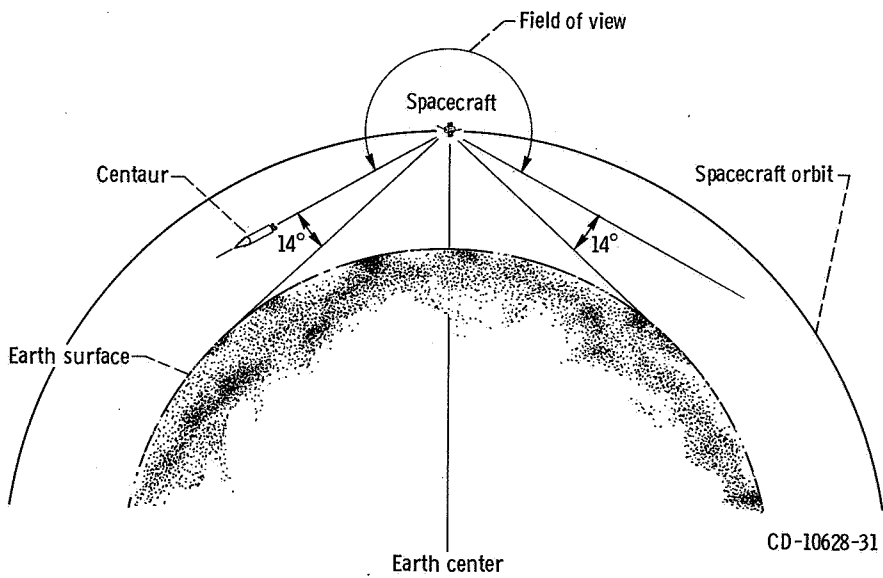


Figure V-6. - OAO-II field of view.

VI. LAUNCH VEHICLE SYSTEM ANALYSIS

PROPULSION SYSTEMS

by Kenneth W. Baud, Charles H. Kerrigan,
Ronald W. Ruedelee, and Donald B. Zelten

Atlas

System description. - The Atlas engine system (fig. VI-1) consists of a booster engine, a sustainer engine, two vernier engines, an engine start system (pressurization and auxiliary propellant), and an electrical control system. The engines are of the single-burn type. During engine start, electrically fired pyrotechnic igniters are used to ignite the gas generator propellants for driving the turbopumps, and hypergolic igniters are used to ignite the propellants in the thrust chambers of the booster, sustainer, and vernier engines. The propellants are liquid oxygen and RP-1 (kerosene).

The booster engine, rated at 1494×10^3 newtons (336×10^3 lbf) thrust at sea level, is made up of two gimbaled thrust chambers, propellant valves, two oxidizer and two fuel turbopumps driven by one gas generator, a lubricating oil system, and a heat exchanger. The sustainer engine, rated at 258×10^3 newtons (58×10^3 lbf) thrust at sea level, consists of a thrust chamber, propellant valves, one oxidizer and one fuel turbopump driven by a gas generator, and a lubricating oil system. The entire sustainer engine system gimbals. Each vernier engine is rated at 2.98×10^3 newtons (670 lbf) thrust at sea level, and propellants are supplied from the sustainer turbopump. The vernier engines gimbal for roll control.

The engine start system consists of two small propellant tanks (each ~51 cm (20 in.) in diam) and a pressurization system.

System performance. - The performance of the Atlas propulsion system for the OAO-II mission was satisfactory. During the engine start phase, valve opening times and starting sequence events were within tolerances. The flight performance of the engines was evaluated by comparing measured parameters with the expected values. The data are tabulated in table VI-I. Booster engine cutoff occurred at $T + 152.1$ seconds when the axial acceleration reached 5.74 g's. Sustainer engine cutoff and vernier engine cutoff occurred at $T + 234.5$ seconds and were due to liquid-oxygen depletion, the planned shutdown mode. Transients were normal during shutdown of all engines.

Centaur Main Engines

System description. - Two RL10A-3-3 engines (identified as C-1 and C-2) are used to provide thrust for the Centaur stage. Each engine has a thrust chamber which is regeneratively cooled and turbopump fed. Propellants are liquid oxygen and liquid hydrogen injected at an oxidizer-to-fuel mixture ratio of approximately 5 to 1. Engine rated thrust is 66 700 newtons (15 000 lbf) at an altitude of 61 000 meters (200 000 ft) and a design combustion chamber pressure of 274 newtons per square centimeter (400 psi). Thrust chamber nozzle expansion area ratio is 57 to 1, and design specific impulse is 442 seconds.

These engines use a "bootstrap" process: pumped fuel, after circulating through the thrust chamber tubes, is expanded through a turbine which drives the propellant pumps (see engine system schematic, fig. VI-2). This routing of fuel through the thrust chamber tubes serves the dual purpose of cooling the thrust chamber walls and of adding energy to the fuel prior to expansion through the turbine. After passing through the turbine, the fuel is injected into the combustion chamber. The pumped oxidizer is supplied directly to the combustion chamber after passing through the propellant utilization (mixture ratio control) valve.

The thrust level is maintained by regulating the amount of fuel bypassed around the turbine as a function of combustion chamber pressure. Ignition is accomplished by means of a spark igniter recessed in the propellant injector face. Starting and stopping are controlled by pneumatically operated valves. Helium pressure to these valves is supplied through engine mounted solenoid valves which are controlled by electrical signals from the vehicle control system.

System performance. - In-flight turbopump chilldown was commanded 8.0 seconds prior to main engine start. This chilldown was accomplished by opening both the oxidizer and the fuel pump inlet valves, allowing the propellants to flow into the engines. The oxidizer passed through the pump and into the combustion chamber; the fuel passed through the pump and overboard through two separate cooldown valves, one located downstream of each pump stage. This chilldown successfully prevented cavitation of the turbopumps during the start transient.

Main engine start was commanded at $T + 246.0$ seconds. The engine start transient was normal. Engine acceleration times to 90-percent chamber pressure were 1.48 and 1.41 seconds for the C-1 and C-2 engines, respectively. Total impulse from the main engine start command through 2.0 seconds of operation was calculated to be 43 300 and 45 900 newton-seconds (9740 and 10 360 lbf-sec) for the C-1 and the C-2 engines, respectively. The differential impulse between engines was well within the allowable of 25 000 newton-seconds (5700 lbf-sec).

The pump inlet pressures remained well above saturation at all times during engine operation. The pump inlet net positive suction pressures (i. e., total pressure minus saturation pressure) at different times throughout the engine firing period are presented in table VI-II. At no time did the levels drop below the minimum required of 2.76 and 5.52 newtons per square centimeter (4.0 and 8.0 psi) for the fuel and oxidizer pumps, respectively.

Steady-state operating conditions during the engine firing period are presented in table VI-III. The readings of chamber pressure taken while the propellant utilization valves were "nulled" (during the first 90 and last 13 seconds of main engine operation) were approximately 6.9 and 5.5 newtons per square centimeter (10 and 8 psi) less than those obtained on the final acceptance tests of the C-1 and C-2 engines, respectively. If these lower values of chamber pressure were indicative of a change in engine performance, other engine internal parameters should substantiate this change. However, the remaining engine internal parameters indicated normal levels: fuel venturi upstream pressures, fuel turbine inlet temperatures, and oxidizer pump speeds were fairly consistent with the values obtained during the final ground acceptance tests. These values do not substantiate the lower-than-expected values of chamber pressure, and the cause of the lower-than-expected chamber pressure is unknown.

Main engine performance in terms of thrust, specific impulse, and mixture ratio is presented in table VI-IV. Performance was calculated using the Pratt & Whitney characteristic velocity (C*) technique. An explanation of this technique is presented in appendix B of this report. The lower levels of thrust and higher levels of specific impulse, compared to acceptance test data, are the result of the low levels of chamber pressure previously discussed.

Main engine cutoff was commanded at $T + 698.2$ seconds, and the shutdown sequence was normal. Main engine cutoff total impulse was calculated to be 13 620 newton-seconds (3070 lbf-sec). This value compares favorably with the predicted value of $13\,550 \pm 775$ newton-seconds (3055 ± 175 lbf-sec). The main engine firing duration of 452.2 seconds was 13.1 seconds longer than predicted. No explanation is available for the long firing duration; however, there was no adverse effect on launch vehicle performance.

Retromaneuver. - A vehicle retrothrust operation ("blowdown") was started 850 seconds following main engine cutoff. The retrothrust was provided by opening the pump inlet valves and allowing the propellants in the tanks to discharge through the main engine system continuously until the loss of vehicle power, which caused the inlet valves to close, terminating this operation. Engine pump inlet pressures and temperatures responded as expected to this operation. These parameters are presented for the beginning and end of the first orbital pass in table VI-V. At the end of the first orbital pass, both Centaur propellant tanks had been depleted of their liquid supply but were still discharging gases.

Centaur Boost Pumps

System description. - A single boost pump is used in each propellant tank to supply propellants to the main engine turbopumps at the required inlet pressures. Each boost pump is a mixed-flow centrifugal type and is powered by a hot-gas-driven turbine. The hot gas consists of superheated steam and oxygen from the catalytic decomposition of 90-percent-concentration hydrogen peroxide. Constant power is maintained on each turbine by metering the hydrogen peroxide through fixed orifices upstream of the catalyst bed. An overspeed speed control system is provided on each turbine. However, on this flight they were disconnected. The complete boost pump and hydrogen peroxide supply systems are shown in figures VI-3 to VI-6.

Boost pump performance. - Performance of the boost pumps was satisfactory for the entire flight. Boost pump start was initiated at $T + 199.2$ seconds. Boost pump operation was terminated simultaneously with main engine cutoff at $T + 698.2$ seconds.

The turbine inlet pressure delay time (time from boost pump start signal to time of first indication of turbine inlet pressure rise) was 1 second for both turbines. Steady-state turbine inlet absolute pressure for the oxidizer boost pump was 65.7 newtons per square centimeter (95.4 psi). The expected value based on prelaunch ground tests was 66.1 newtons per square centimeter (96.0 psi). The average steady-state turbine inlet absolute pressure for the fuel boost pump was 67.9 newtons per square centimeter (98.6 psi) with peak-to-peak pressure oscillations of 17.2 newtons per square centimeter (25 psi) superimposed. The expected value based on prelaunch test data was 70.3 newtons per square centimeter (102 psi). The pressure oscillations were noted during the prelaunch testing on this particular turbine, and have also been noted on several other turbines during both ground testing and flights. There was no detrimental effect on the turbine speed.

Fuel boost pump turbine speed is shown in figure VI-7. The steady-state speed was approximately 1300 rpm higher than the prelaunch test value of 39 900 rpm. Oxidizer boost pump turbine speed is shown in figure VI-8. The steady-state speed was approximately 1500 rpm higher than the prelaunch test value of 32 900 rpm. Boost pump turbine speeds have been consistently higher than the acceptance test values on virtually all previous Centaur flights. These differences are due to the inability to accurately simulate the flight conditions during prelaunch ground tests.

Turbine bearing temperatures for the fuel and oxidizer boost pumps are shown in figures VI-9 and VI-10, respectively. The maximum values were comparable to values recorded on previous single-burn flights.

Liquid-oxygen temperature at the boost pump inlet is shown in figure VI-11. The temperature rise between boost pump start and main engine start was a result of warm fluid being returned to the sump area through small bleed holes in the pump volute

casting. The temperature dropped shortly after main engine start, when the flow to the main engines began and the warm liquid was removed from the sump. Since there was no pressurization of the tank after main engine start, the tank pressure decreased as the liquid oxygen was drained from the tank. There was a corresponding decrease in the liquid-oxygen bulk temperature as liquid continually evaporated to maintain the liquid saturated at the ullage pressure.

Liquid-hydrogen temperature at the boost pump inlet is shown in figure VI-12. The rise in temperature between $T - 0.5$ minutes and $T + 1.5$ minutes was caused by lockup of the hydrogen tank primary (lower range) vent valve. Heat input to the liquid during this time resulted in a tank pressure increase and a corresponding bulk temperature increase. When the vent valve was unlocked, the liquid hydrogen resaturated at the primary vent valve pressure setting, and a sharp drop in temperature resulted. The continued decrease in temperature after main engine start was a result of propellant outflow. As the pressure in the tank decreased, the liquid hydrogen resaturated at the reduced pressures.

Hydrogen Peroxide Engine and Supply System

System description. - The hydrogen peroxide system (figs. VI-4 and VI-13) consists of 14 thruster engines, a supply bottle, and interconnecting tubing to the engines and boost pump turbines. The engines are used after main engine cutoff. Four 222.4-newton- (50-lbf-) thrust engines and four 13.3-newton- (3-lbf-) thrust engines are used primarily for propellant settling and retention and for retromaneuver. Two clusters, each of which consists of two 15.6-newton- (3.5-lbf-) thrust engines and one 26.7-newton- (6-lbf-) thrust engine, are used for attitude control (see table VI-XIII, GUIDANCE AND FLIGHT CONTROL SYSTEMS, for mode of operation). Propellant is supplied to the engines from a positive-expulsion, bladder-type storage tank which is pressurized with helium to an absolute pressure of about 210 newtons per square centimeter (305 psi) by the pneumatic system. The hydrogen peroxide is decomposed in the engine catalyst beds, and the hot decomposition products are expanded through converging-diverging nozzles to provide thrust. Hydrogen peroxide is also provided to drive the boost pump turbines. All the hydrogen peroxide supply lines, except for one short line, are equipped with heaters. However, on AC-16 and all other single-burn vehicles, the heaters are not required on the boost pump feedlines, and they are electrically disconnected.

Configuration changes were made on AC-16 as a result of suspected cryogenic leakage during the AC-17 flight. All of the openings in the liquid-oxygen-tank radiation shield were covered in the vicinity of the hydrogen peroxide bottle to shield the hydrogen peroxide system from any leakage from the liquid-oxygen tank. A fiber glass shield was

also installed on the hydrogen-peroxide-bottle support yoke to protect the system from possible leakage from the liquid-oxygen-tank sump flanges and the liquid-oxygen supply ducting. Instrumentation was added to assist in the detection of any cryogenic leakage and to obtain temperature data for the boost pump hydrogen peroxide supply lines.

System performance. - The supply bottle was tanked with 106.5 kilograms (234.9 lbm) of hydrogen peroxide. The bottle absolute pressure at lift-off was 224 newtons per square centimeter (325 psi). The pressure decreased to about 214 newtons per square centimeter (310 psi) by $T + 180$ seconds and then remained constant throughout the flight. The decrease in pressure is normal because the pneumatic regulator is referenced to ambient pressure, which becomes essentially zero when the vehicle leaves the atmosphere.

Four of the engine chamber surfaces were instrumented for temperature measurement (fig. VI-14): two 15.6-newton- (3.5-lbf-) thrust engines (A-1 and A-2), one 13.3-newton- (3-lbf-) thrust engine (S-1), and one 222.4-newton- (50-lbf-) thrust engine (V-1). All engine temperature data indicated normal performance. Temperature changes verified engine firing as programmed and as required to maintain vehicle control. The data showed that at $T + 1492$ seconds, during the S-half-on mode of firing (see table VI-XIII, GUIDANCE AND FLIGHT CONTROL SYSTEMS), a large disturbing torque on the vehicle exceeded the control capability of the S-engines. A rise in the V-1 engine chamber temperature at this time verified that the 222.4-newton- (50-lbf-) thrust engine fired to maintain vehicle control. The disturbing torque was caused by venting of the liquid-hydrogen tank. On previous flights, the vent stack was jettisoned as a part of the nose fairing, and venting was accomplished through balanced thrust vent ducting. However, on AC-16, because of the configuration of the nose fairing, the stack was not jettisoned, and this disturbing torque was expected when venting occurred.

The A-1 and A-2 engine chamber temperatures, during the second orbital pass ($T + 7370$ to $T + 8230$ sec over the Canary telemetry station) showed that these engines were still firing and maintaining vehicle control.

Boost pump hydrogen peroxide supply line temperature evaluation. - Several transducers were installed on AC-16 to determine in-flight temperatures of the hydrogen peroxide supply lines for the boost pumps. Location and identification of the transducers are shown in figure VI-14. The temperature data obtained from the AC-16 flight are shown in figure VI-15.

In general, the supply line temperature data indicated no abnormal conditions throughout the flight. At $T - 180$ seconds, the temperature measurement CP346T, between the bottle and boost pump feed valve, showed a sharp temperature rise. This rise was a result of warm hydrogen peroxide being forced from the bottle and into the line at the time of bottle pressurization. Immediately after lift-off, all temperatures decreased

due to termination of the warm gas conditioning supply to the Centaur thrust section. Venting of the conditioning gas from the thrust section during the boost phase also contributed to the temperature decreases after lift-off.

The radiation shield temperature measurement (CP350T) started to rise at $T + 100$ seconds due to thermal radiation from the Atlas-Centaur interstage adapter. The interstage adapter temperature increased during the boost phase as a result of aerodynamic heating. An increase in the radiation shield temperature rise rate occurred at boost pump start ($T + 199.2$ sec) because the liquid-oxygen boost pump turbine exhaust discharges into the enclosed Centaur thrust section. The radiation shield temperature then decreased abruptly at $T + 236.4$ seconds, when Atlas-Centaur separation occurred. A steady decrease in the radiation shield temperature then occurred until $T + 1052$ seconds. At this time, the temperature began to rise again, reflecting an increase in the solar radiation on the aft end of the Centaur when the reorientation maneuver was started. The radiation shield temperature appeared to reach a maximum at approximately $T + 2100$ seconds, and then began a slow decrease which continued through $T + 8230$ seconds.

At boost pump start, all hydrogen peroxide supply line temperatures rose abruptly as the warm peroxide from the supply bottle flowed through the lines. During boost pump operation, all line temperatures, except CP352T, stabilized at values near the temperature of the hydrogen peroxide in the bottle, which was 302 K (544° R). However, CP352T, which was located less than 5 centimeters (2 in.) from the face of the hot turbine, continued to rise slowly throughout the boost pump operating period, and was 321 K (578° R) at main engine and boost pump cutoff.

In the space environment, the unheated lines remote from the turbines cool due to radiation. The lines near the turbines are heated by radiation and conduction from the hot turbine housing. Temperature measurements (CP344T, CP345T, CP346T, CP347T, and CP351T) on the lines remote from the turbines showed a gradual cooling trend after main engine cutoff, as was expected. The temperature measurements (CP348T, CP349T, and CP352T) which were located near the hot turbines showed a definite warming trend after main engine cutoff, as was expected. Shortly after main engine and boost pump cutoff, essentially all of the supply line temperatures began to exhibit rather abrupt changes which continued throughout the coast until loss of telemetry data at $T + 8230$ seconds. These abrupt changes were caused by "slugging" of residual hydrogen peroxide remaining in the lines downstream of the feed valve after boost pump cutoff. As small pockets or "slugs" of residual hydrogen peroxide moved past a transducer on a relatively cool line, a temperature increase occurred. Conversely, as small pockets or "slugs" of residual hydrogen peroxide moved past a transducer on a relatively hot line, a temperature decrease occurred.

A long time period was required to empty the residual hydrogen peroxide from the lines because of the combined effect of the low-gravity environment and the small flow-restricting orifices located near the turbines (see fig. VI-4). At T + 6800 seconds, measurement CP348T began to rise sharply, indicating that the random outflow (slugging) of residual hydrogen peroxide through the hydrogen boost pump supply line had ceased and that the short section of line between the speed limiting valve and catalyst bed was empty. The temperature at this location increased to a maximum value of 373 K (670⁰ R), and then began to decrease slowly as the turbine cooled. The "slugging" was still evident in the liquid-oxygen boost pump turbine supply lines until loss of data at T + 8230 seconds. However, the gradual warming trend shown by measurement CP352T from T + 7600 to T + 8230 seconds indicated that the liquid-oxygen boost pump turbine supply lines were also nearly empty.

A simultaneous change in several of the supply line temperatures occurred at T + 1492 seconds. This change was the result of residual hydrogen peroxide movement in the lines when a large vehicle disturbance occurred. Pressure rise in the hydrogen tank caused the secondary (upper range) vent valve to relieve, and gaseous hydrogen was vented overboard at T + 1492 seconds. The venting imparted a large disturbing torque on the vehicle.

Based on the hydrogen peroxide supply line temperature data, it was concluded that there were no cryogenic leaks near the hydrogen peroxide system on AC-16. It was also concluded that small quantities of residual hydrogen peroxide were retained in the boost pump supply lines (downstream of the feed valve) until loss of telemetry data at T + 8230 seconds. The liquid-hydrogen boost pump supply line between the speed limiting valve and catalyst bed became dry at T + 6800 seconds, resulting in a maximum line temperature of 373 K (670⁰ R) at measurement CP348T.

Comparison of AC-16 and AC-17 temperature data. - Two of the AC-16 temperature measurements (CP344T and CP345T) were of particular interest because of a flight failure of AC-17. The boost pumps failed to operate for the second burn of the AC-17 flight; this failure was attributed to blockage of the hydrogen peroxide flow to the boost pump turbines. Cryogenic leakage and subsequent freezing of the hydrogen peroxide within the boost pump turbine supply lines was a primary suspect. Only two temperature measurements were installed on the hydrogen peroxide supply lines to the turbines for AC-17. These two measurements were CP344T and CP345T (also installed on AC-16).

Comparison of the temperature data from measurements CP344T and CP345T for both AC-16 and AC-17 revealed the same abrupt temperature changes after main engine cutoff on both flights. Two significant differences were noted: (1) on AC-17, CP344T showed a sharp temperature rise for 76 seconds after main engine cutoff that was not evident on AC-16, and (2) both CP344T and CP345T reached much lower temperatures on AC-16 than on AC-17. On AC-17, both CP344T and CP345T stayed within a tem-

perature band between 302 and 316 K (545^o and 570^o R) during the entire coast period of 61 minutes. On AC-16, these same two measurements decreased steadily to values of 242 and 255 K (436^o and 460^o R) after 61 minutes of coast. These two differences noted in the temperature data were due to configuration differences between the two vehicles. On AC-17, 222.4-newton- (50-lbf-) thrust engines were fired for 76 seconds immediately after main engine cutoff to settle propellants; on AC-16, these engines were not programmed to fire during this time period. Convective heating due to impingement of the engine exhaust plumes on the supply line caused the temperature to rise on AC-17. Measurements CP344T and CP345T showed lower temperatures on AC-16 because the boost pump turbine supply line heaters were electrically connected on AC-17, but were disconnected on AC-16.

TABLE VI-I. - ATLAS PROPULSION SYSTEM PERFORMANCE, AC-16

Performance parameter	Unit	Expected operating range	Flight values at -		
			T + 10 sec	Booster engine cutoff, T + 152.1 sec	Sustainer and vernier engine cutoff, T + 234.5 sec
Booster engine:					
Thrust chamber 1:					
Pressure, absolute	N/cm ²	386 to 410	398	401	(a)
	psi	560 to 595	577	581	(a)
Turbopump speed	rpm	6225 to 6405	6369	6393	(a)
Thrust chamber 2:					
Pressure, absolute	N/cm ²	386 to 410	400	403	(a)
	psi	560 to 595	580	584	(a)
Turbopump speed	rpm	6165 to 6345	6319	6334	(a)
Gas generator chamber pressure, absolute	N/cm ²	351 to 382	373	373	(a)
	psi	510 to 555	540	540	(a)
Sustainer engine:					
Thrust chamber pressure, absolute	N/cm ²	469 to 493	486	476	476
	psi	680 to 715	705	690	690
Gas generator discharge pressure, absolute	N/cm ²	407 to 473	441	441	441
	psi	620 to 680	640	640	640
Engine turbopump speed	rpm	10 025 to 10 445	10 287	10 196	10 301
Vernier engine thrust chamber absolute pressure:					
Engine 1	N/cm ²	172 to 183	181	178	181
	psi	250 to 265	262	258	262
Engine 2	N/cm ²	172 to 183	181	178	182
	psi	250 to 265	262	258	264

^aNot applicable.

TABLE VI-II. - CENTAUR MAIN ENGINE PUMP INLET
NET POSITIVE SUCTION HEAD, AC-16

Time from main engine start, sec	Location							
	C-1 fuel pump		C-2 fuel pump		C-1 oxidizer pump		C-2 oxidizer pump	
	Net positive suction head							
	N/cm ²	psi	N/cm ²	psi	N/cm ²	psi	N/cm ²	psi
0	12.9	18.7	12.4	18.0	55.7	80.7	55.4	80.4
^a ~1.2	6.4	9.2	5.7	8.2	27.5	39.9	33.2	48.1
10	5.4	7.9	6.4	9.3	19.1	27.7	19.7	28.6
^b 90	7.1	10.3	6.6	9.5	19.9	28.8	20.4	29.6
^c 100	7.8	11.1	7.3	10.6	18.3	26.5	18.7	27.1
^d 112	6.9	10.0	5.5	7.9	21.4	31.0	21.9	31.7
^d 353	8.3	12.1	7.9	11.5	20.0	29.0	20.2	29.3
^b 450	5.6	8.2	6.7	9.9	20.5	29.7	20.7	30.0

^aMinimum dip during start transient.

^bThis time was selected as being representative while the propellant utilization valves were nulled.

^cThis time was selected as being representative of when the propellant utilization valves were commanded to the oxidizer rich stop.

^dThis time was selected as representing the minimum and the maximum mixture ratio conditions the engines experienced during the portion of flight that the propellant utilization valves were controlling.

TABLE VI-III. - CENTAUR MAIN ENGINE OPERATING DATA, AC-16

Parameter	Units	Expected value	Time from main engine start ^a , sec											
			90		100		112		353		450			
			C-1	C-2	C-1	C-2	C-1	C-2	C-1	C-2	C-1	C-2		
Fuel pump inlet total pressure, absolute	N/cm ² psi	16.2 to 24.1 23.5 to 33.9	20.6 29.9	20.7 30.1	21.2 30.8	21.5 31.2	20.2 29.4	19.4 28.2	19.1 27.7	16.2 23.5	16.7 24.2			
Fuel pump inlet temperature	K °R	20.1 to 21.6 36.1 to 38.8	21.2 38.2	21.5 38.6	21.3 38.3	21.2 38.2	21.4 38.5	21.4 38.5	20.4 36.8	20.4 36.7	20.2 36.4			
Oxidizer pump inlet total pressure, absolute	N/cm ² psi	31.8 to 47.3 46.2 to 68.7	41.8 60.8	42.5 61.6	40.3 58.5	43.3 62.9	43.9 63.6	40.4 58.6	39.7 57.6	38.8 56.3	39.0 56.6			
Oxidizer pump inlet temperature	K °R	95.3 to 98.3 171.5 to 176.9	98.1 176.6	98.1 176.6	98.1 176.6	98.1 176.6	98.0 176.5	98.0 176.5	97.0 174.8	96.1 173.0	96.1 173.0			
Oxidizer pump speed	rpm	12 163 ± 347	12 100.0	12 380.0	11 920.0	12 260.0	12 620.0	11 840.0	12 100.0	12 040.0	12 300.0			
Fuel venturi upstream pressure, absolute	N/cm ² psi	b ⁵ 508 ± 17 b ⁷ 737 ± 25	505.0 732.0	515.0 748.0	494.0 716.0	515.0 749.0	540.0 784.0	491.0 714.0	508.0 737.0	505.0 734.0	516.0 750.0			
Fuel turbine inlet temperature	K °R	b ² 207 ± 12 b ³ 372 ± 22	208.0 374.0	220.0 394.0	228.0 410.0	185.0 332.0	200.0 359.0	221.0 398.0	231.0 416.0	204.0 368.0	215.0 388.0			
Oxidizer injector differential pressure	N/cm ² psi	b ³ 1.7 ± 6.9 b ⁴ 6 ± 10	29.4 42.7	30.4 44.1	32.3 46.9	26.2 38.2	27.7 40.2	30.9 44.8	32.5 47.1	29.3 42.5	30.2 43.7			
Engine chamber pressure, absolute	N/cm ² psi	b ² 70.8 ± 3.7 b ³ 92.4 ± 5.4	263.0 381.0	263.0 382.0	264.0 383.0	261.0 379.0	263.0 382.0	263.0 382.0	263.0 382.0	263.0 381.0	263.0 382.0			

^aSee footnotes to table VI-II for explanation of time sample selection.

^bExpected value with nominal inlet conditions and nulled propellant utilization valve angle.

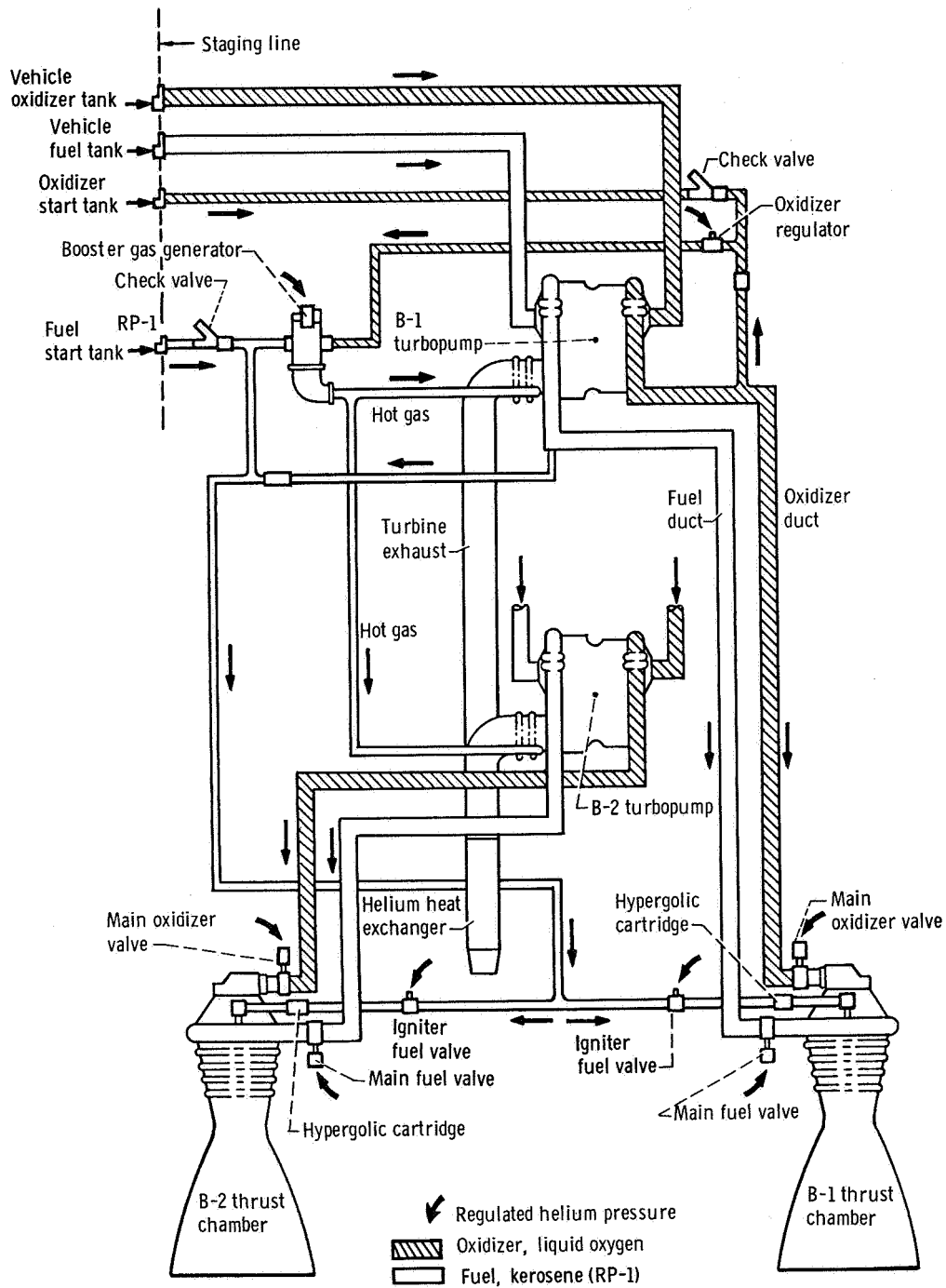
TABLE VI-IV. - CENTAUR MAIN ENGINE PERFORMANCE, AC-16

Performance parameter	Units	Acceptance value	Time from main engine start ^a , sec											
			90		100		112		353		450			
			C-1	C-2	C-1	C-2	C-1	C-2	C-1	C-2	C-1	C-2		
Thrust	N lbf	66 400.0 14 930.0	65 160.0 14 650.0	65 910.0 14 820.0	66 320.0 14 910.0	63 720.0 14 330.0	64 380.0 14 470.0	65 570.0 14 740.0	66 040.0 14 850.0	64 560.0 14 510.0	65 010.0 14 610.0			
Specific impulse	sec	444.8	445.2	445.7	443.7	447.9	447.8	443.7	444.7	445.3	445.8			
Mixture ratio	---	5.032	4.865	4.925	5.420	4.292	4.293	5.303	5.259	4.789	4.833			

^aSee footnotes to table VI-II for explanation of time sample selection.

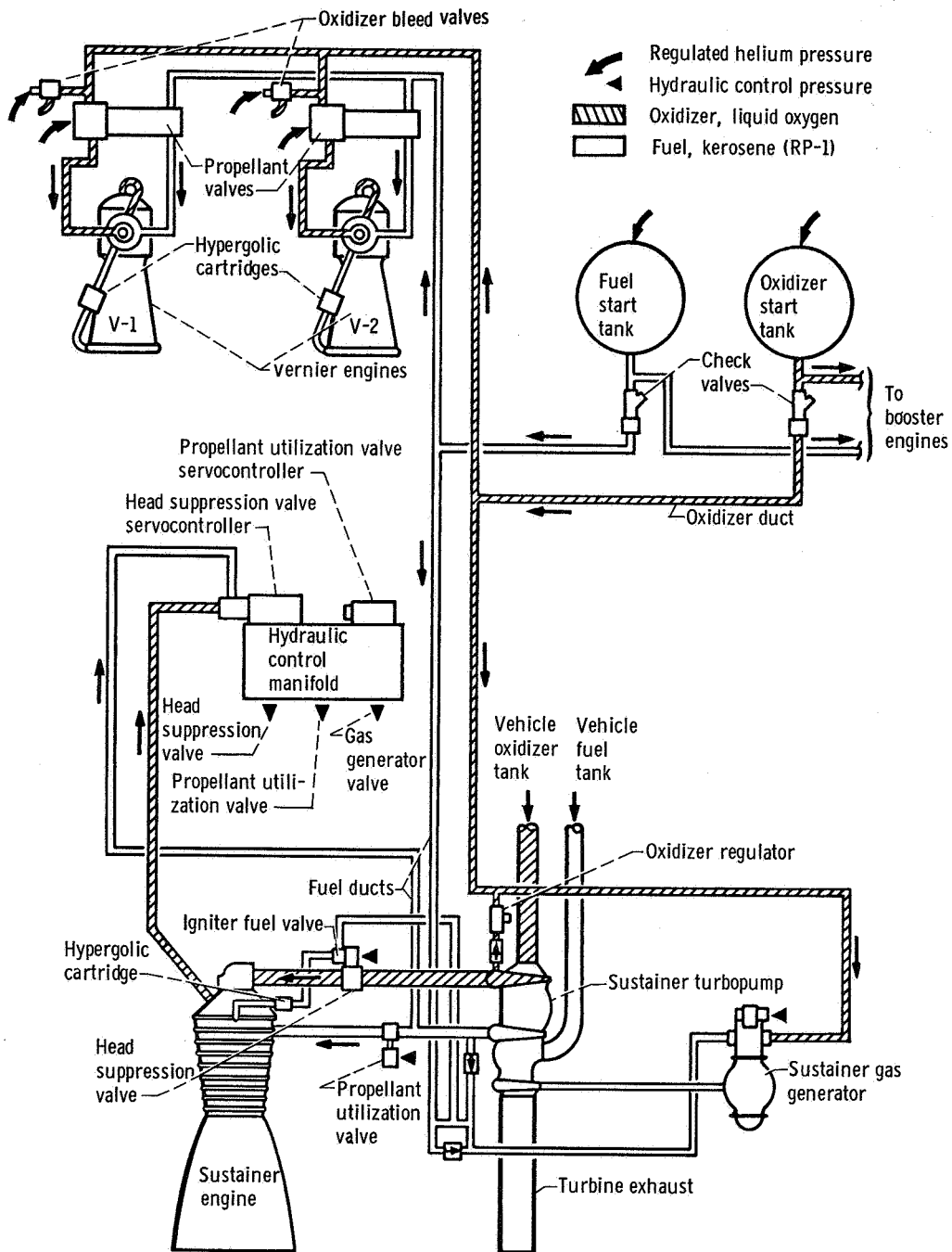
TABLE VI-V. - CENTAUR MAIN ENGINE PUMP INLET PRESSURES AND
TEMPERATURES DURING RETROTHRUST, AC-16

Parameter	Units	Time from start of retrothrust, sec							
		-5		5		300		6480	
		C-1	C-2	C-1	C-2	C-1	C-2	C-1	C-2
Fuel pump inlet	N/cm ²	0	0	19.3	18.7	11.2	10.7	1.0	1.0
pressure, absolute	psi	0	0	27.9	27.1	16.3	15.5	1.6	1.6
Fuel pump inlet	K	>24.7	>24.8	21.7	21.8	>24.7	>24.8	>24.7	>24.8
temperature	°R	>44.4	>44.6	39.1	39.5	>44.4	>44.6	>44.4	>44.6
Oxidizer pump inlet	N/cm ²	0	0	21.4	21.2	20.8	20.6	1.9	2.4
pressure, absolute	psi	0	0	31.0	30.7	30.2	29.9	2.7	3.4
Oxidizer pump inlet	K	97.0	97.2	96.9	97.0	97.0	97.0	>102.0	>102.0
temperature	°R	174.8	175.0	174.6	174.8	174.8	174.8	>183.3	>183.3



(a) Atlas vehicle booster engine.

Figure VI-1. - Atlas propulsion system, AC-16.



(b) Atlas vehicle sustainer and vernier engines.

Figure VI-1. - Concluded.

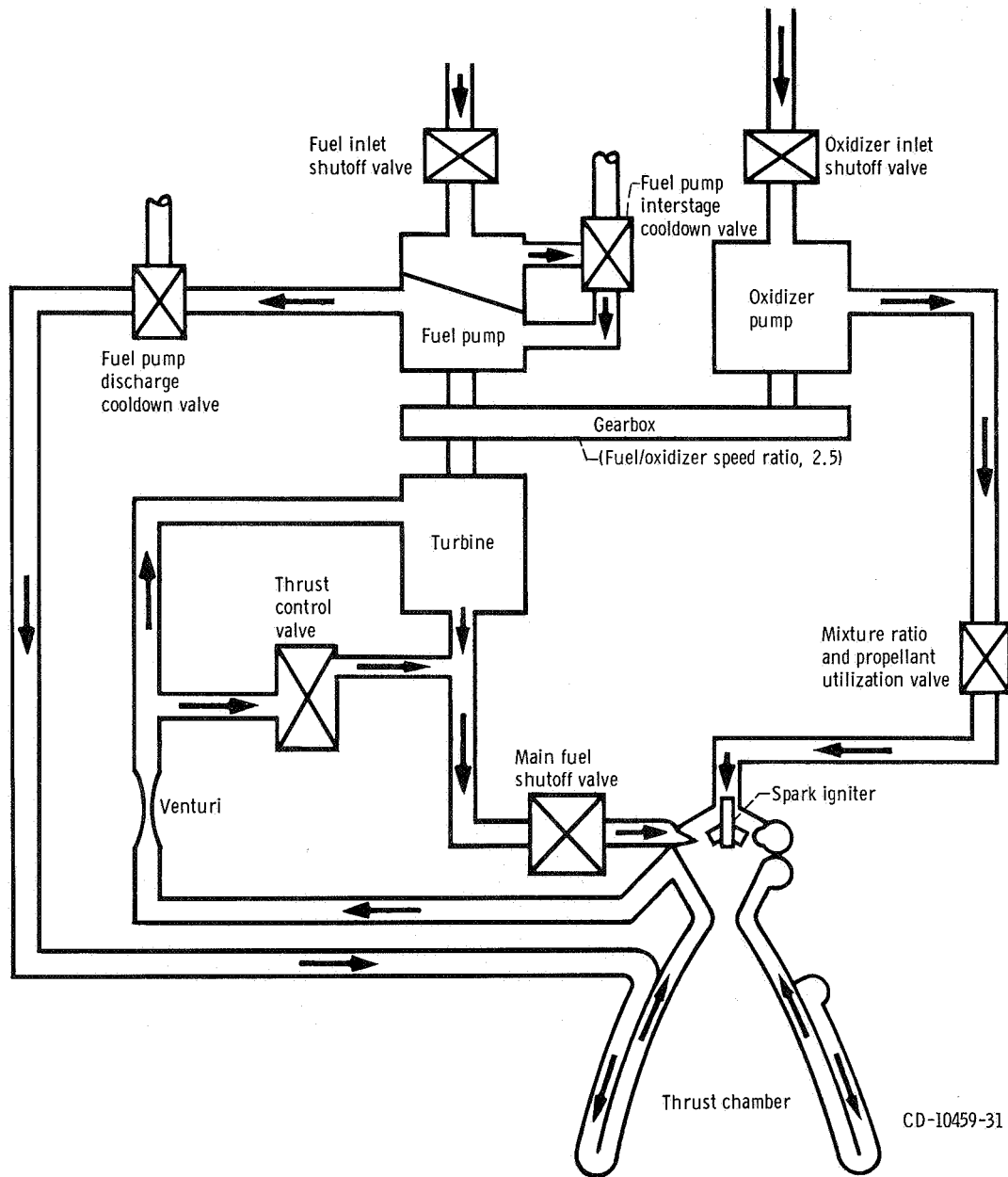


Figure VI-2. - Centaur propulsion system, AC-16.

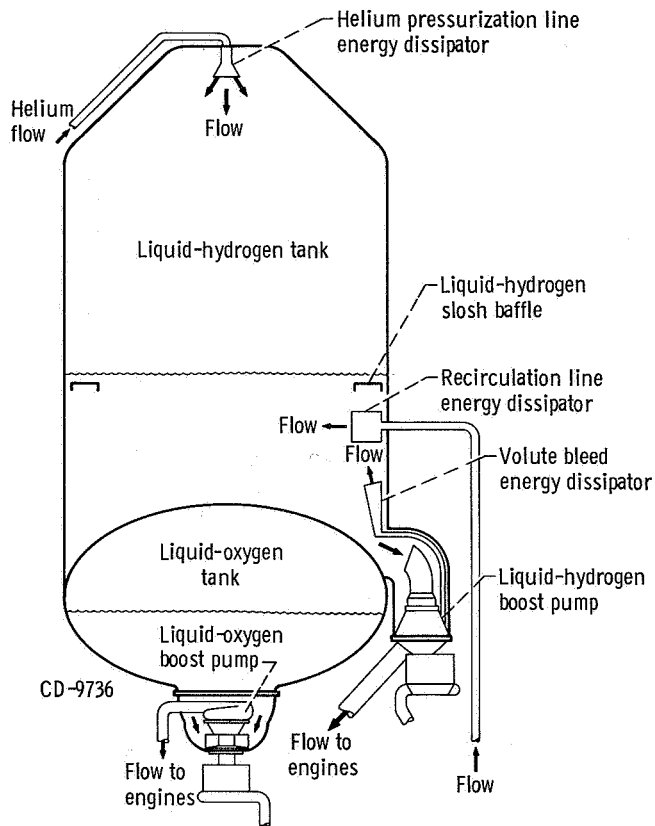


Figure VI-3. - Location of Centaur liquid-hydrogen and liquid-oxygen boost pumps, AC-16.

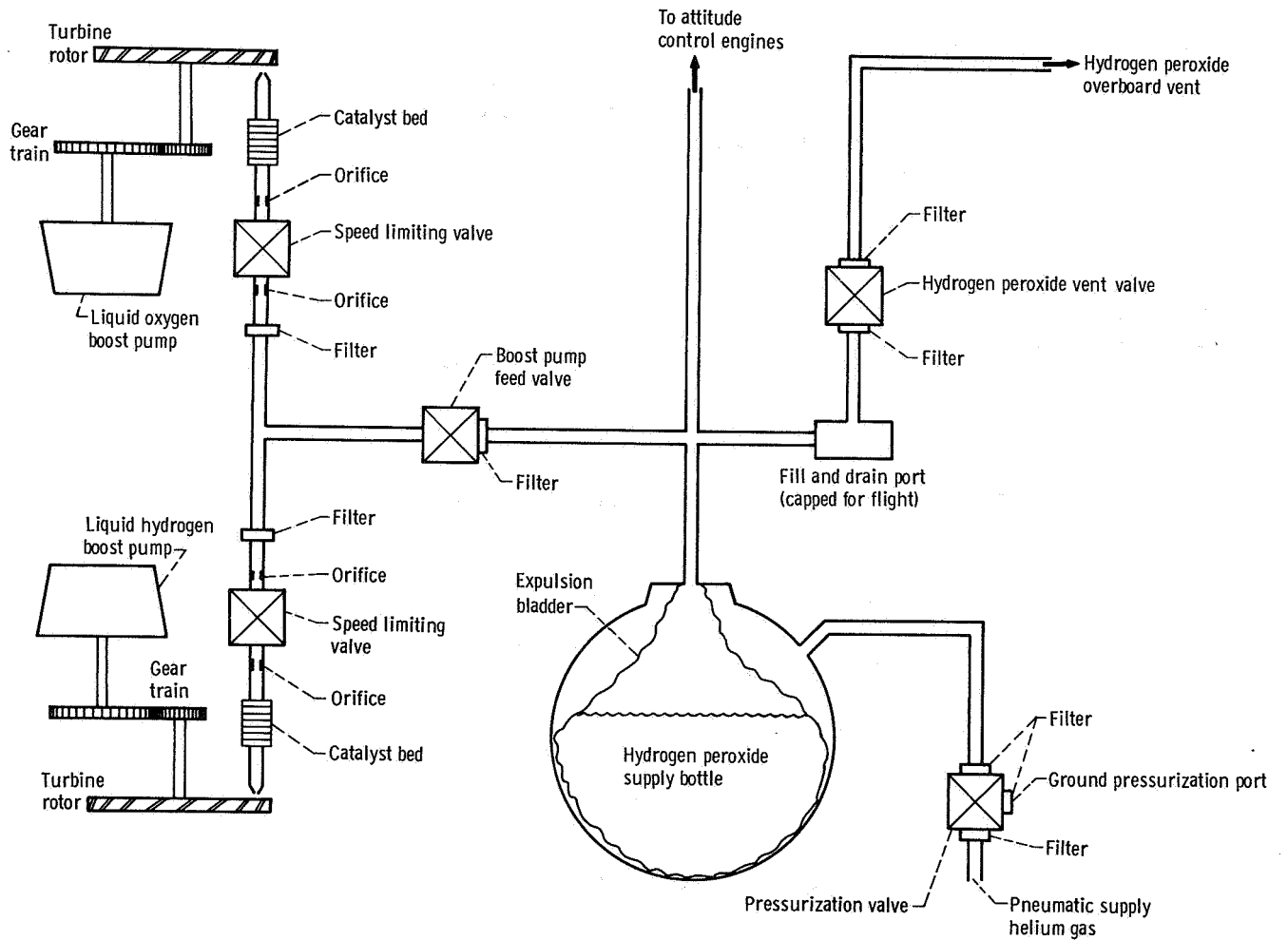


Figure VI-4. - Schematic drawing of Centaur boost pump hydrogen peroxide supply, AC-16.

CD-9515

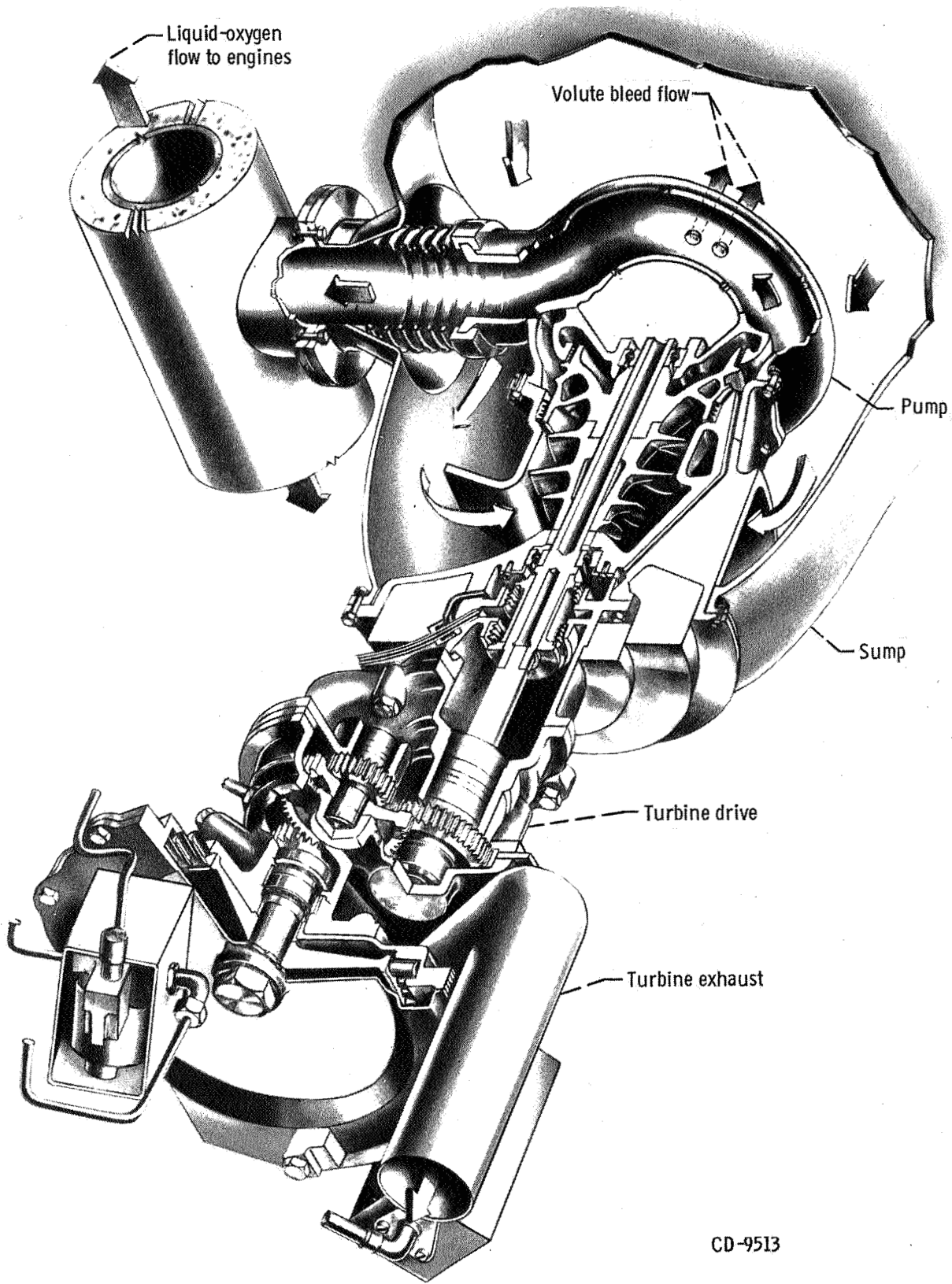


Figure VI-5. - Centaur liquid-oxygen boost pump and turbine cutaway, AC-16.

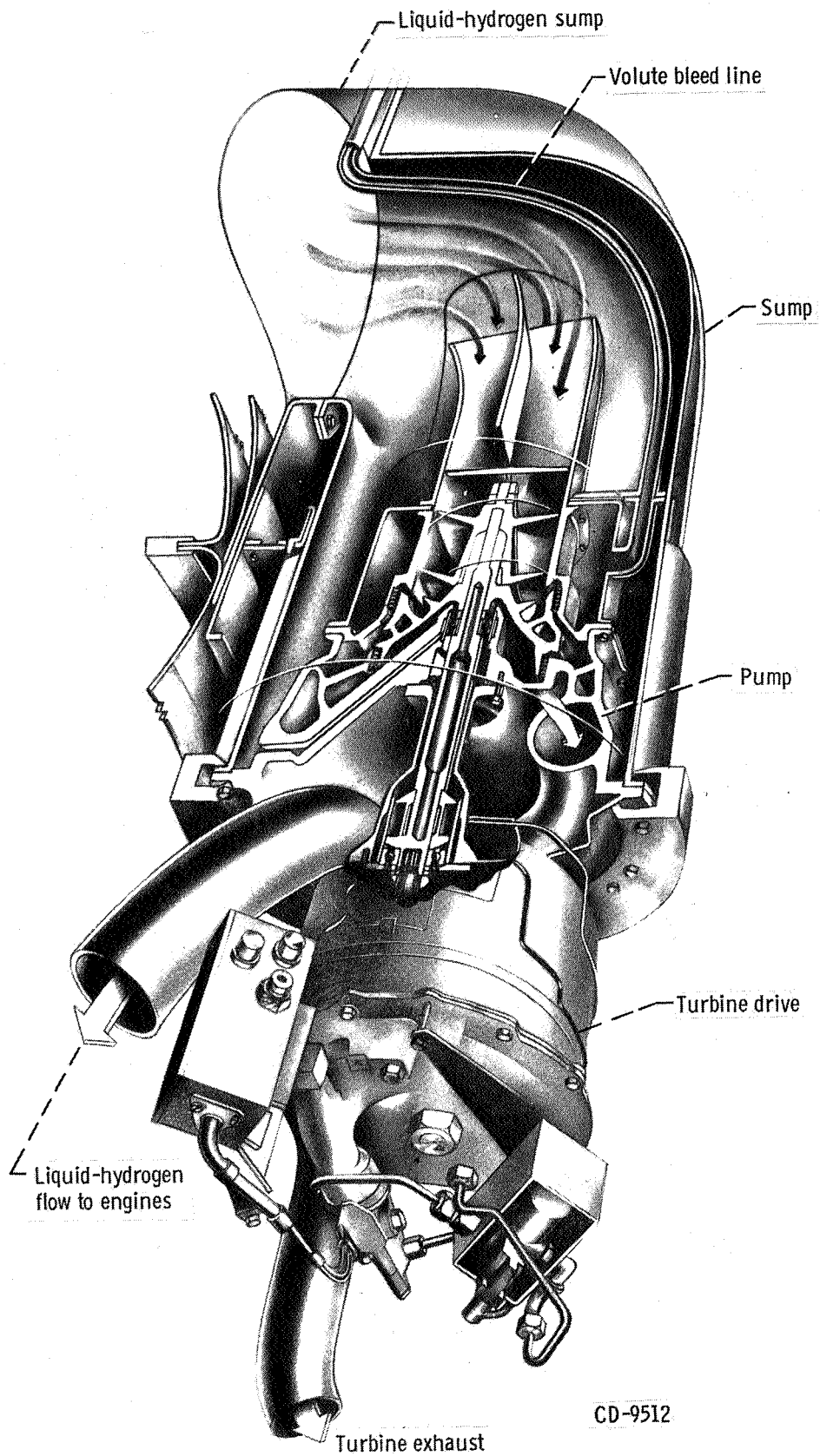


Figure VI-6. - Centaur liquid-hydrogen boost pump and turbine cutaway, AC-16.

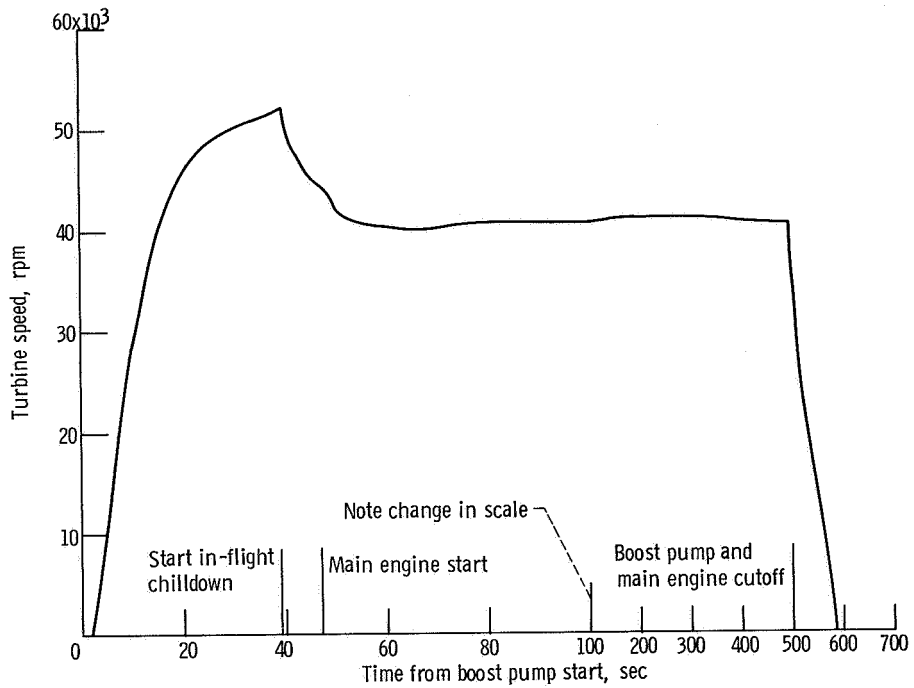


Figure VI-7. - Centaur fuel boost pump turbine speed, AC-16.

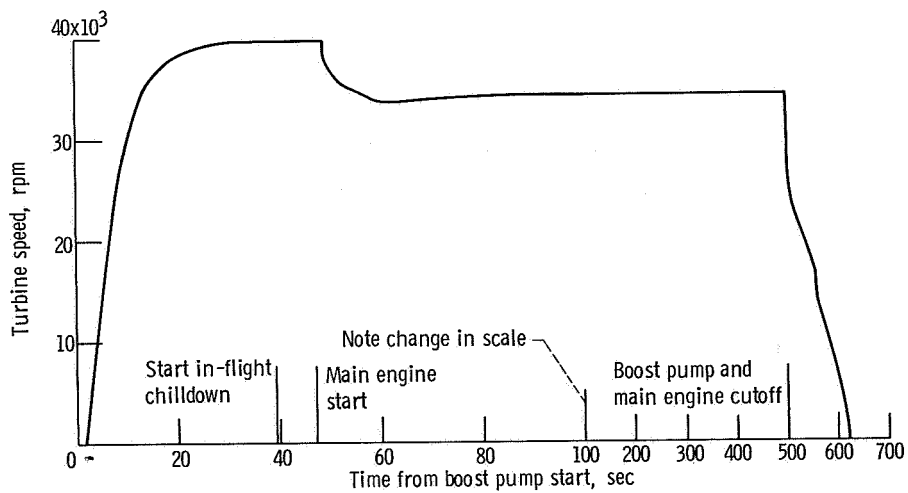


Figure VI-8. - Centaur oxidizer boost pump turbine speed, AC-16.

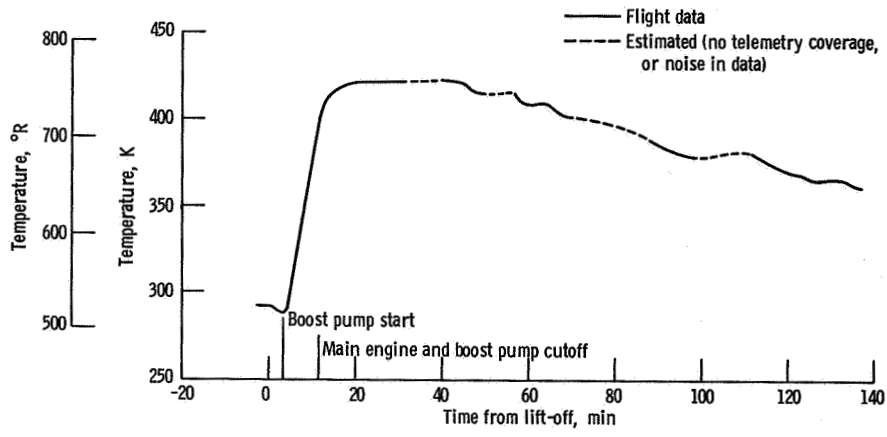


Figure VI-9. - Centaur fuel boost pump turbine bearing temperature, AC-16.

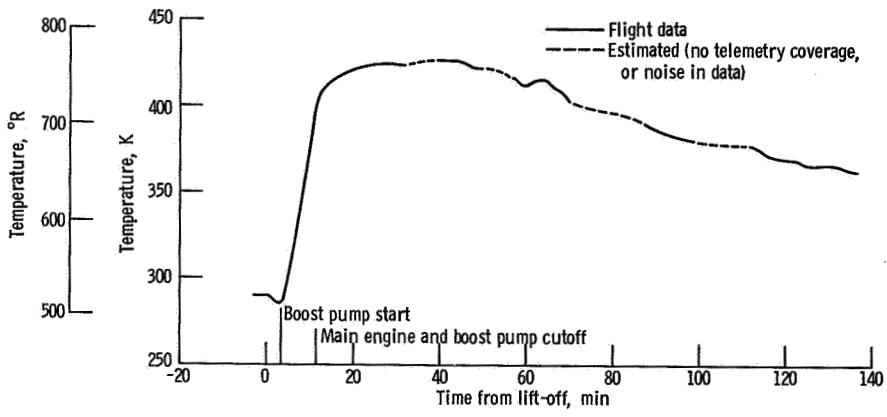


Figure VI-10. - Centaur oxidizer boost pump turbine bearing temperature, AC-16.

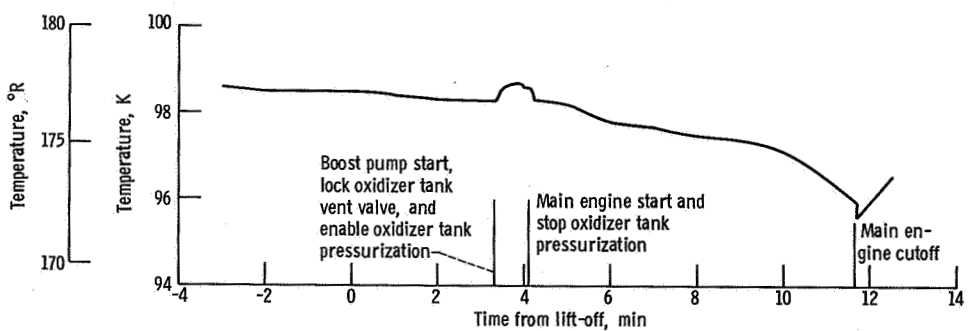


Figure VI-11. - Centaur liquid-oxygen temperature at boost pump inlet, AC-16.

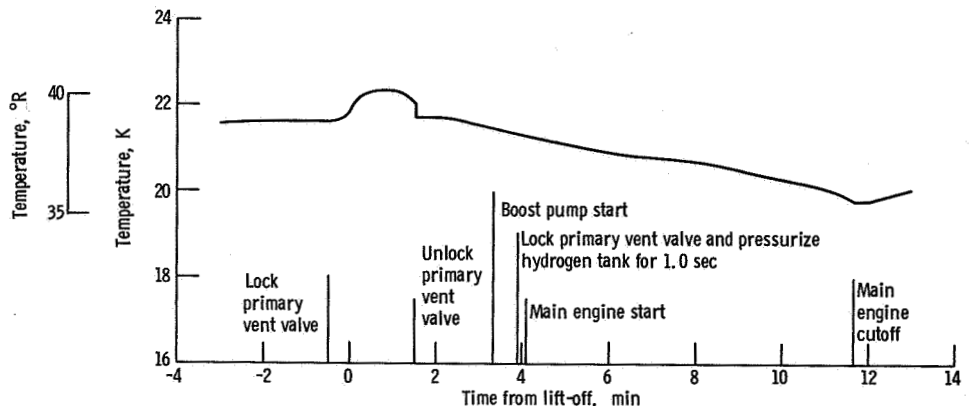
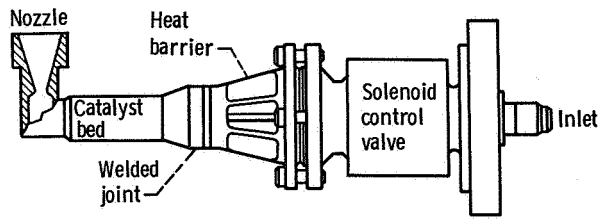
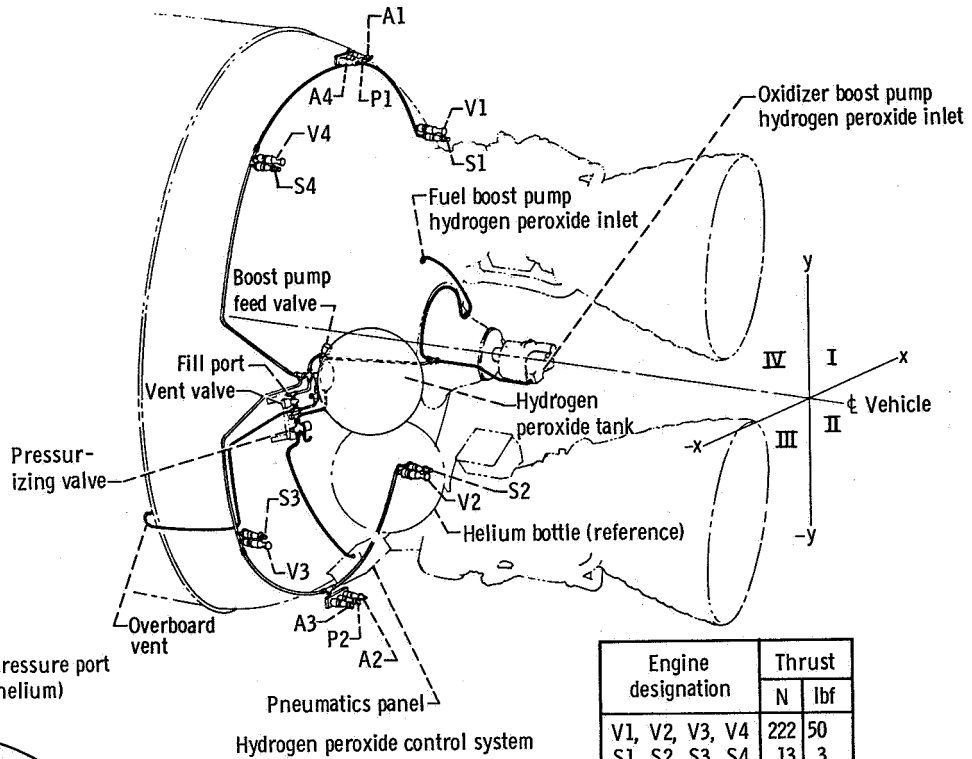


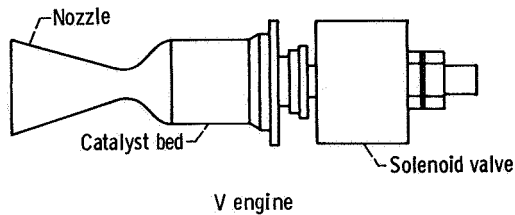
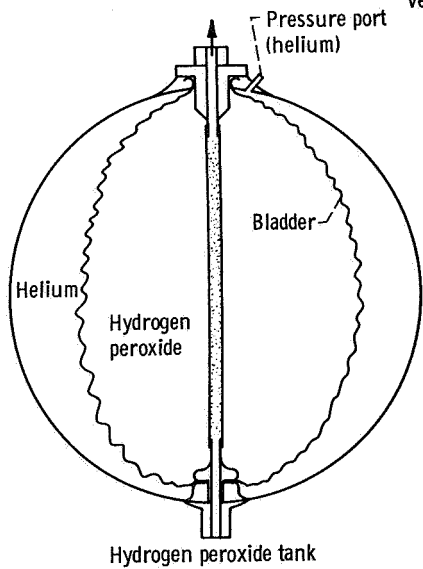
Figure VI-12. - Centaur liquid-hydrogen temperature at boost pump inlet, AC-16.



Typical A, P, and S engine, except S engine has straight nozzle



Engine designation	Thrust	
	N	lbf
V1, V2, V3, V4	222	50
S1, S2, S3, S4	13	3
A1, A2, A3, A4	16	3.5
P1, P2	27	6



CD-9781-31

Figure VI-13. - Hydrogen peroxide system isometric, AC-16.

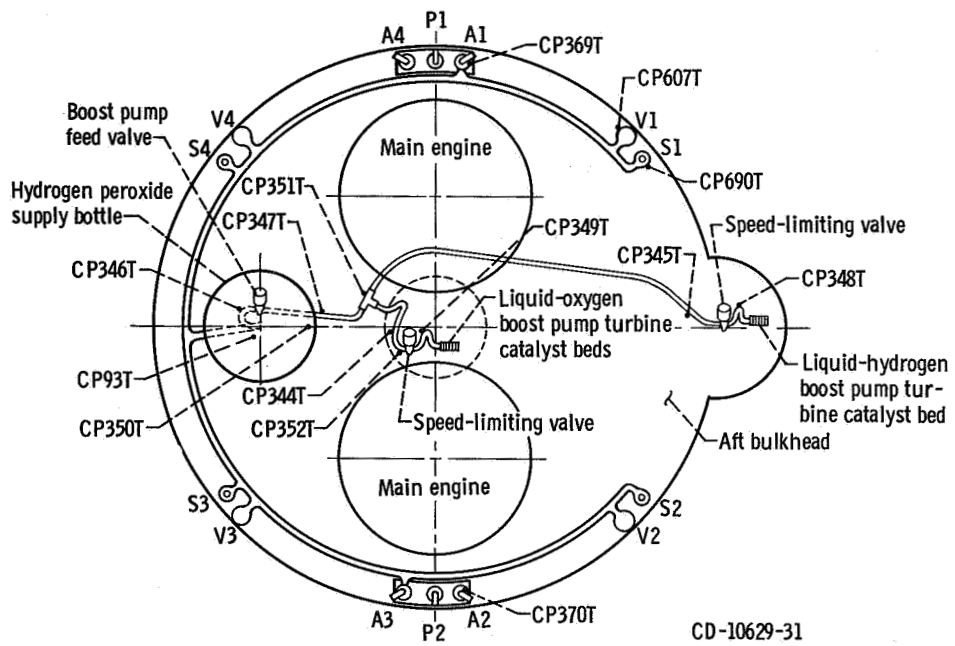


Figure VI-14. - Hydrogen peroxide system instrumentation, AC-16.
View looking forward; the A engines are positioned approximately 25° outboard from horizontal plane.

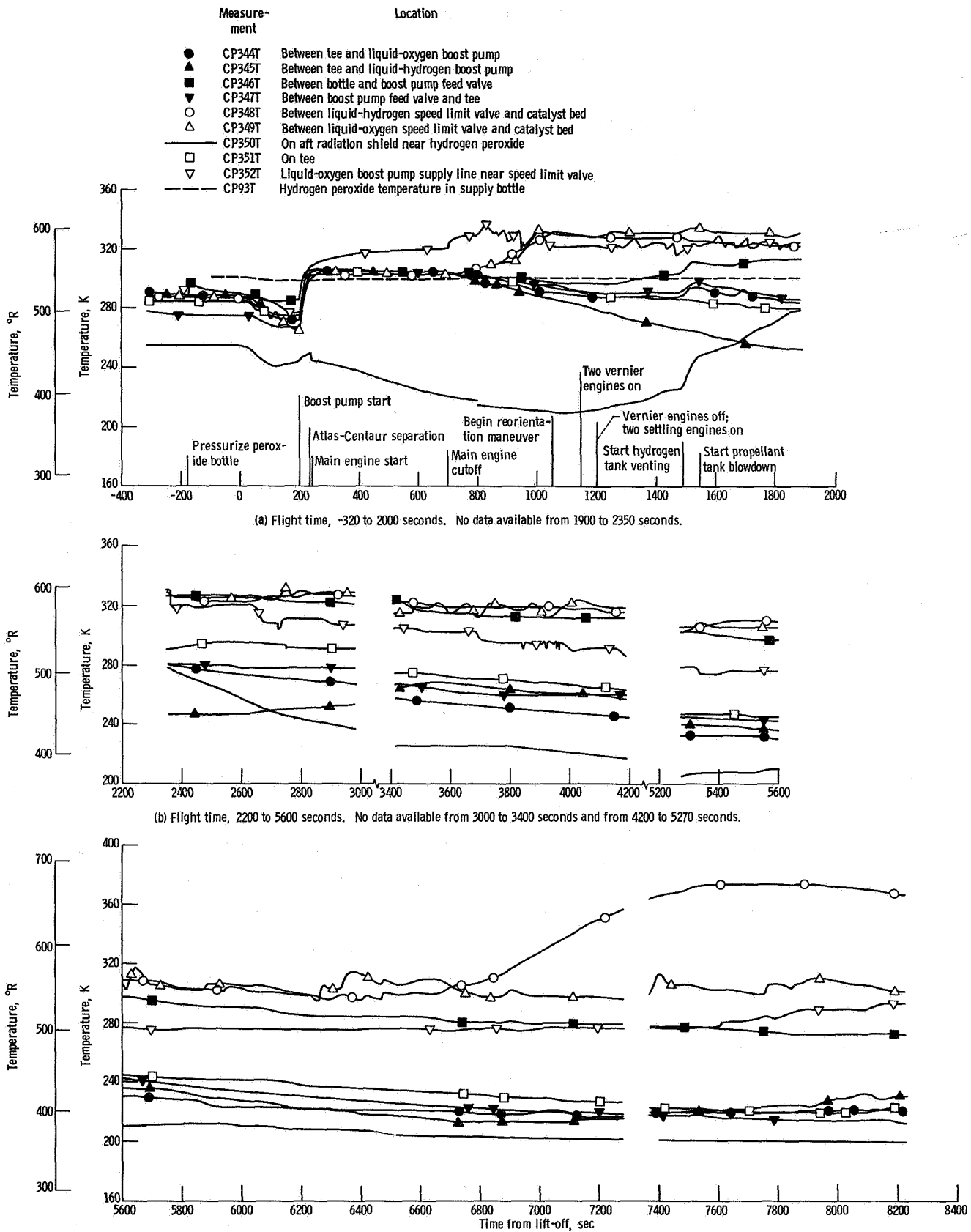


Figure VI-15. - Centaur boost pump hydrogen peroxide supply line temperatures, AC-16.

PROPELLANT LOADING AND PROPELLANT UTILIZATION

by Richard C. Kalo

Level Indicating System for Propellant Loading

System description. - The Atlas propellant level indicating system consists of a portable sight gage assembly for RP-1 fuel (kerosene) loading and platinum hot-wire-type sensors for oxidizer (liquid oxygen) loading.

The fuel loading levels are determined by visual observation of the sight gage assembly, which is connected to the fuel probe by two temporary sense lines. After tanking, the fuel sight gage assembly and sense lines are removed, and the connecting points on the vehicle are secured for flight.

The liquid-oxygen loading levels are determined from liquid sensors located at discrete points in the oxidizer (liquid oxygen) tank. The sensing elements are the hot-wire type made with platinum wire (0.0025-cm (0.001-in.) diam), which has a linear resistance-temperature coefficient. The sensors are supplied with a nearly constant current of approximately 200 milliamperes; the voltage drop across a sensor reflects the resistance value of the sensor. When uncovered, the wire has a high resistance and therefore a high voltage drop. When covered (immersed in a cryogenic fluid), it has a low resistance and low voltage drop. The control unit amplifies a change in voltage level and applies this signal to an electronic trigger circuit. When a sensor is wetted, a control relay is deenergized, and a signal is sent to the propellant loading operator.

The Centaur propellant level indicating system (fig. VI-16) utilizes platinum hot-wire level sensors in both the liquid-oxygen and liquid-hydrogen tanks. These sensors are similar in operation to those used in the Atlas liquid-oxygen tank.

System performance. - Atlas and Centaur propellant loading was satisfactorily accomplished. The weight of the Atlas fuel (RP-1) tanked was calculated to be 37 885 kilograms (83 457 lbm) based on a density of 800 kilograms per cubic meter (49 lb/ft³). The weight of the Atlas liquid oxygen tanked was calculated to be 85 586 kilograms (188 687 lbm) based on a density of 1100 kilogram per cubic meter (69.29 lb/ft³).

The calculated Centaur propellant weights at lift-off were 2374 kilograms (5242 lbm) \pm 3 percent of liquid hydrogen and 11 540 kilograms (25 476 lbm) \pm 1.5 percent of liquid oxygen. Data used to calculate these propellant weights are presented in table VI-VI.

Atlas Propellant Utilization System

System description. - The Atlas propellant utilization system (fig. VI-17) consists of two mercury manometer assemblies, a computer-comparator, a hydraulically actua-

ted propellant utilization fuel valve, sense lines, and associated electrical harnessing. The system is used to ensure nearly simultaneous depletion of the propellants and minimum propellant residuals at sustainer engine cutoff. This is accomplished by controlling the propellant mixture ratio (oxidizer flowrate to fuel flowrate) to the sustainer engine. During flight, the manometers sense propellant head pressures which are indicative of propellant mass. The mass ratio is then compared to a reference ratio (at lift-off the ratio is 2.27) in the computer-comparator. If needed, a correction signal is sent to the propellant utilization valve controlling the main fuel flow to the sustainer engine. The oxidizer flow is regulated by the head suppression valve. This valve senses propellant utilization valve movement and moves in a direction opposite to that of the propellant utilization valve. This opposite movement thus alters propellant mixture ratio to maintain constant propellant mass flow to the engine.

System performance. - The Atlas propellant utilization system operation was satisfactory. The propellant utilization system fuel valve angles during flight and the predicted valve angles are shown in figure VI-18. The valve operates at the center position for the first 13 seconds of flight because the error signal to the valve is grounded during this period to eliminate abnormal system behavior. The valve was in the fuel rich position from $T + 13$ seconds to approximately $T + 67$ seconds, and then operated in the oxygen rich position reaching the oxidizer rich stop by $T + 140$ seconds. The valve remained at the oxidizer rich stop until $T + 169$ seconds, and then operated alternately in fuel rich and oxidizer rich positions. After $T + 215$ seconds the valve was on the oxidizer rich stop and remained there to ensure sustainer engine cutoff by usable-liquid-oxygen depletion.

Atlas propellant residuals. - The residual propellants above the sustainer engine pump inlets at sustainer engine cutoff were calculated to be 236 kilograms (520 lbm) of liquid oxygen and 151 kilograms (336 lbm) of RP-1. These residuals were calculated by using the time the head sensing port uncovers as a reference. Calculation of the propellants consumed, from the time the port uncovers to sustainer engine cutoff, considered the effect of flow-rate decay for a liquid-oxygen depletion.

Centaur Propellant Utilization System

System description. - The Centaur propellant utilization system (fig. VI-19) is used during flight to control the ratio of propellants consumed by the main engines and to provide minimum deviation from calculated weights of usable propellant residuals. The probes (sensors) of the propellant utilization system are also used during tanking to indicate propellant levels within the range of these probes. In flight, the mass of propellant in each tank is sensed by a capacitance probe and compared in a bridge balancing

circuit. If the mass ratio of propellants remaining in the tanks varies from the pre-determined value (oxidizer to fuel ratio, 5 to 1), an error signal is sent to the proportional servopositioners which control the liquid-oxygen flow control valves (one on each engine). When the mass ratio is greater than 5 to 1, the liquid-oxygen flow is increased to return the ratio to 5 to 1. When the ratio is less than 5 to 1, the liquid-oxygen flow is decreased. The sensing probes do not extend to the top of the tanks, and therefore are not used for control until after the probes are uncovered, at approximately 90 seconds after Centaur main engine start. For this 90 seconds the liquid-oxygen flow control valves are maintained at a propellant mixture ratio of approximately 5 to 1. The valves are also commanded to the null position at an approximate 5 to 1 propellant mixture ratio 15 seconds before Centaur main engine cutoff because the probes do not extend to the bottom of the tanks, and system control is lost when the liquid level depletes below the bottom of the probe.

System performance. - All prelaunch checks and calibrations of the propellant utilization system were within specifications. The in-flight operation of the system was satisfactory during Centaur main engine firing. The liquid-oxygen flow control valve angles during the engine firings are shown in figures VI-20 and VI-21.

The liquid-oxygen probe uncovered at main engine start plus 96.5 seconds. The liquid-hydrogen probe also uncovered 8.5 seconds later. The vehicle programmer commanded the valves to begin controlling at main engine start plus 89.6 seconds. The valves then moved to the oxygen rich stop and remained there for approximately 7.5 seconds. During this time, the system compensated for an excess of 40.4 kilograms (89 lbm) of liquid oxygen. The system had been programmed to compensate for 46.7 kilograms (103 lbm) of excess liquid oxygen by the propellant utilization system bias to ensure liquid-oxygen depletion. The difference between the actual correction made and the programmed value can be attributed to the following:

- (1) Engine consumption rate error accumulated during the first 90 seconds of engine firing
- (2) Propellant loading tolerance

Propellant residuals. - The propellant residuals were calculated by using data obtained from the propellant utilization system. The propellant residuals remaining at Centaur main engine cutoff were calculated by using the times that the propellant levels passed the bottoms of the probes as reference points. The residuals are listed in the following table:

	Units	Liquid propellant	
		Hydrogen	Oxygen
Total propellants	kg	86.3	265
	lbm	190.0	584
Usable propellants	kg	54.0	234
	lbm	119.0	515
Firing time remaining to depletion	sec	10.6	9.15

TABLE VI-VI. - CENTAUR PROPELLANT LOADING, AC-16

Quantity or event	Units	Propellant tank	
		Hydrogen	Oxygen
Amount of sensor required to be wet:			
At T - 90 seconds	percent	99.8	-----
At T - 75 seconds	percent	-----	100.2
Sensor location (vehicle station number)	-----	174.99	373.16
Tank volume at sensor ^a	m ³	35.6	12.9
	ft ³	1256.69	370.94
Ullage volume at sensor	m ³	0.32	0.23
	ft ³	11.22	6.58
Liquid-hydrogen sensor 99.8 percent uncovered at -	sec	T - 82	-----
Liquid-oxygen sensor 100.2 percent uncovered at -	sec	-----	T - 0
Ullage pressure at time sensors uncovered, absolute	N/cm ²	15.3	21.3
	psi	22.3	30.9
Density at time sensors uncovered ^b	kg/m ³	66.96	1099
	lbm/ft ³	4.185	68.68
Propellant weight in tank when sensor uncovered	kg	2382	11 540
	lbm	5259	25 476
Liquid-hydrogen boiloff prior to vent valve close ^c	kg	7.95	-----
	lbm	17.49	-----
Liquid-oxygen boiloff prior to lift-off ^c	kg	-----	0
	lbm	-----	0
Ullage volume at lift-off	m ³	0.374	0.23
	ft ³	13.2	6.58
Weight at lift-off ^d	kg	2374	11 540
	lbm	5242	25 476

^aVolumes include 0.05-m³ (1.85-ft³) liquid oxygen and 0.72-m³ (2.53-ft³) liquid hydrogen for lines from boost pumps to engine turbopump inlet valves.

^bLiquid-hydrogen density taken from ref. 2. Liquid-oxygen density taken from ref. 3.

^cBoiloff rates determined from tanking test to be 0.015 kg/sec (0.33 lbm/sec) for liquid hydrogen and 0.14 kg/sec (0.29 lbm/sec) for liquid oxygen.

^dPropellant loading accuracy: hydrogen, ±3.2 percent; oxygen, ±1.5 percent.

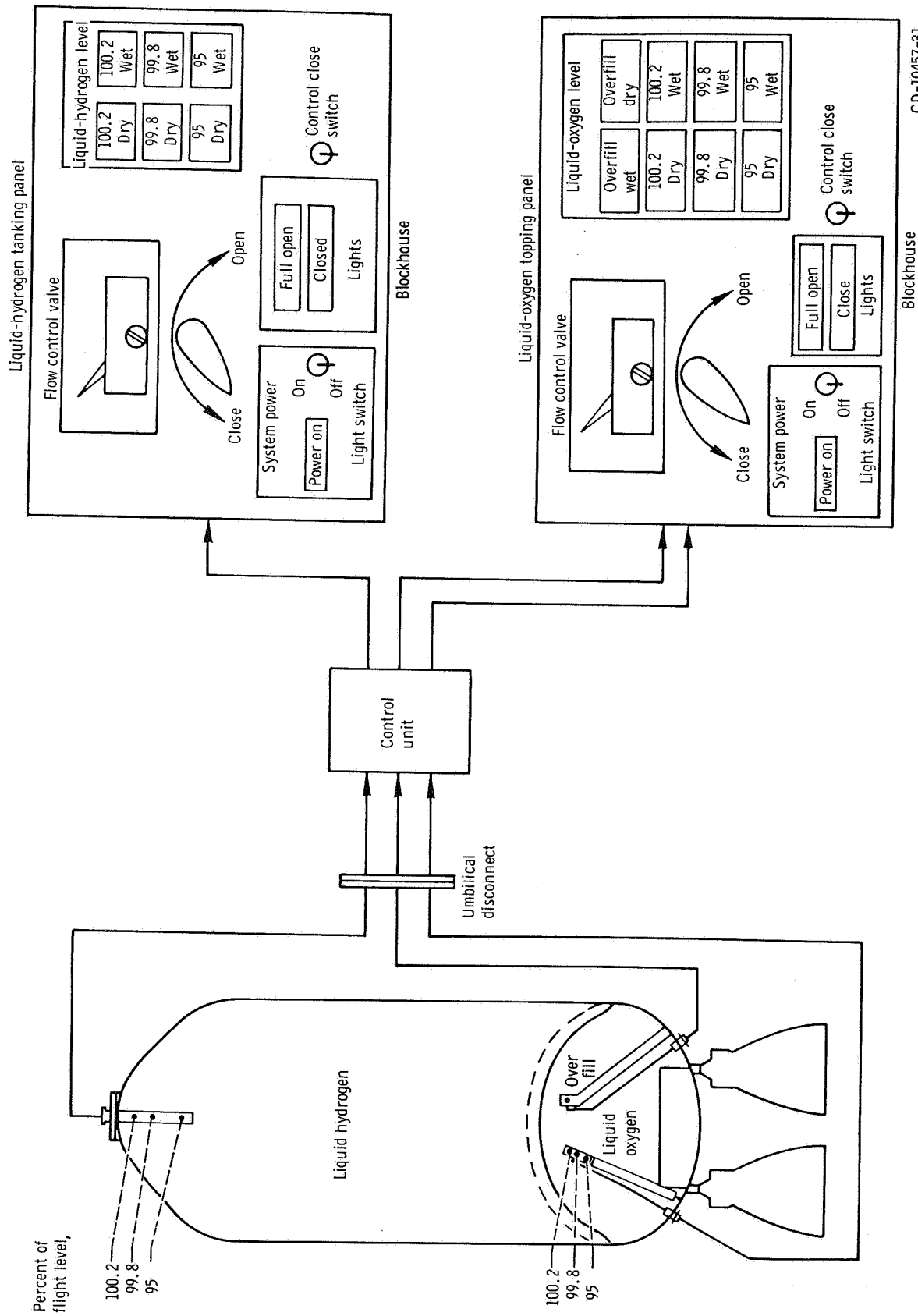
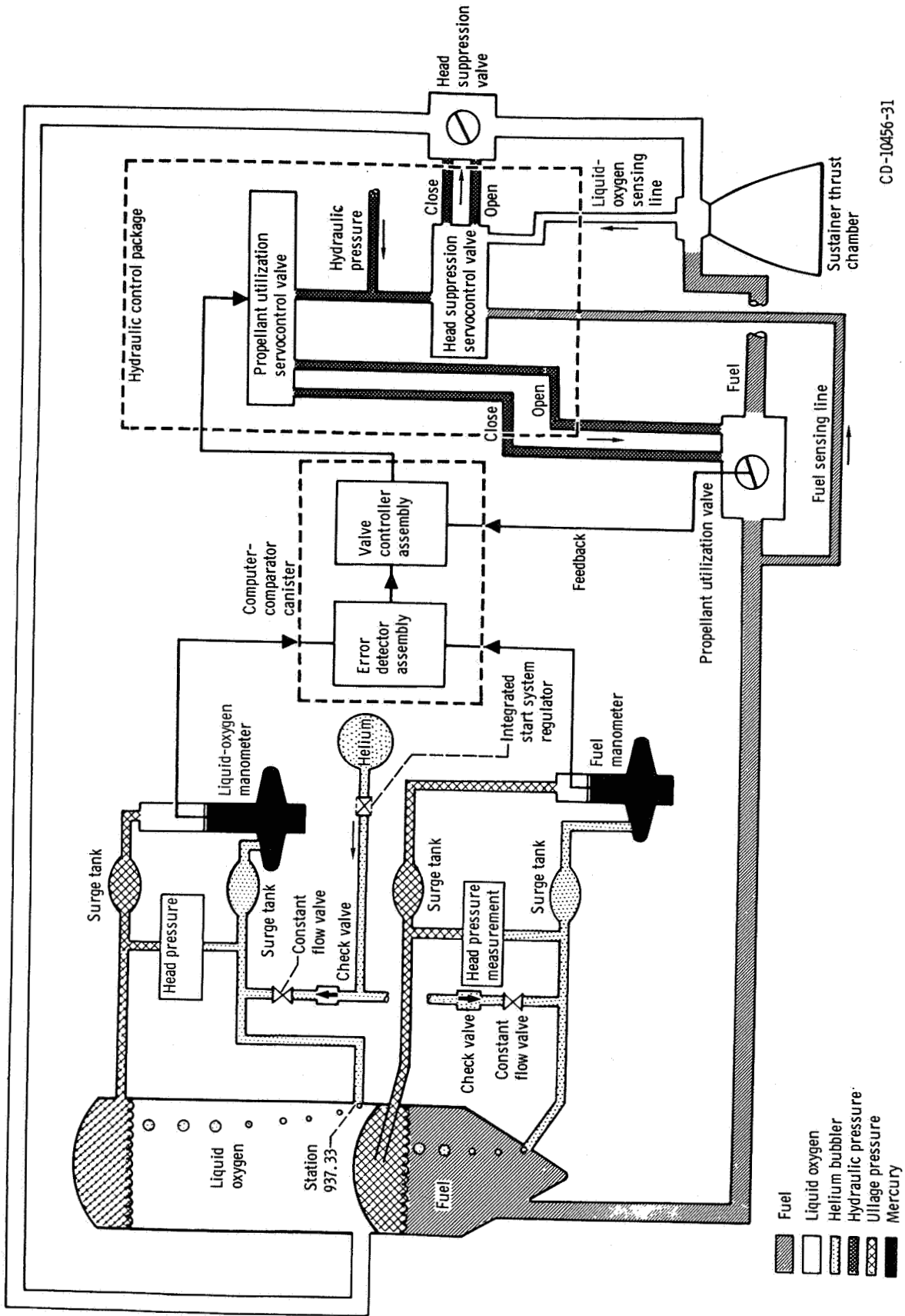


Figure VI-16. - Propellant level indicating system for Centaur propellant loading, AC-16.

CD-10457-31

Blockhouse



CD-10456-31

Figure VI-17. - Atlas propellant utilization system, AC-16.

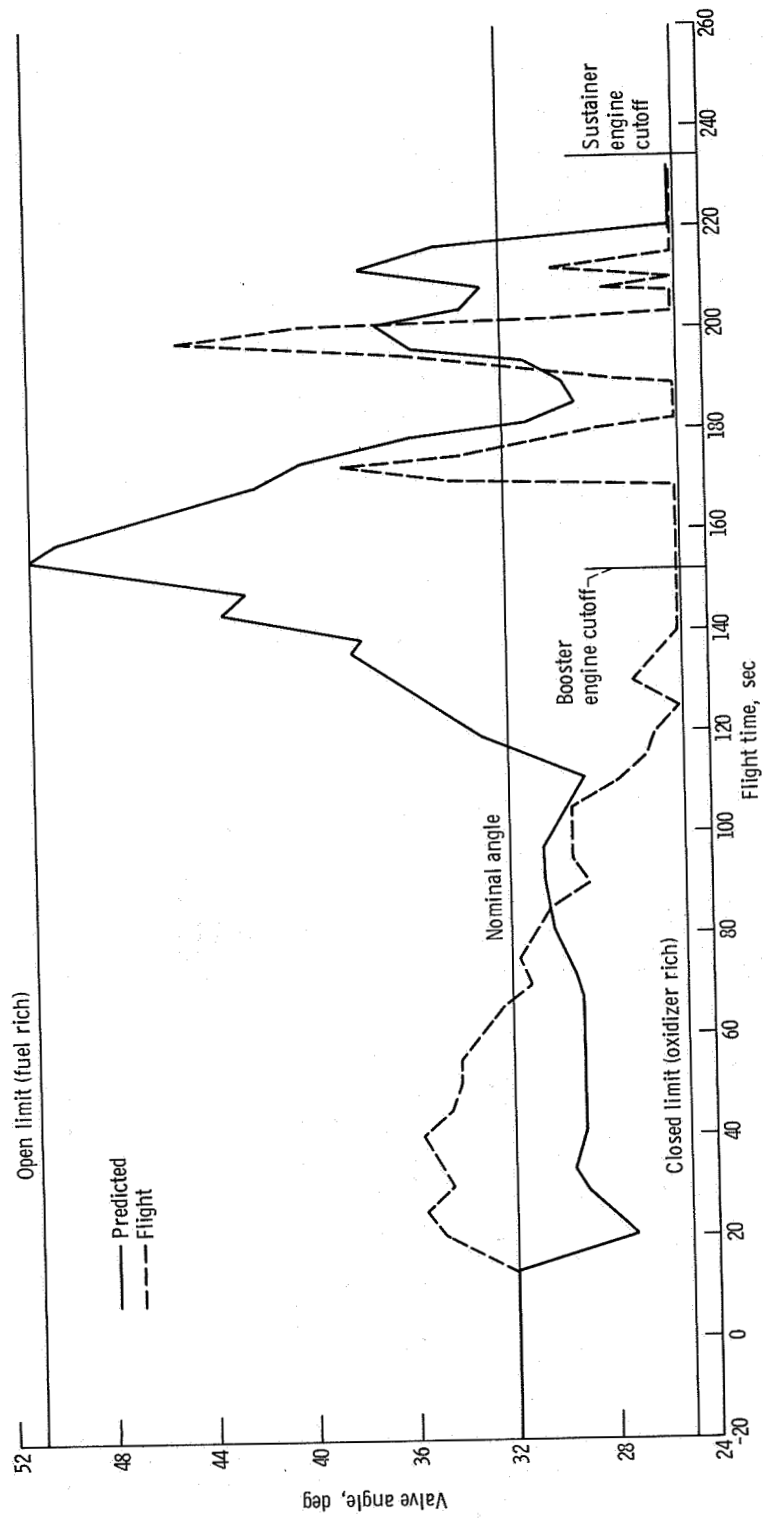
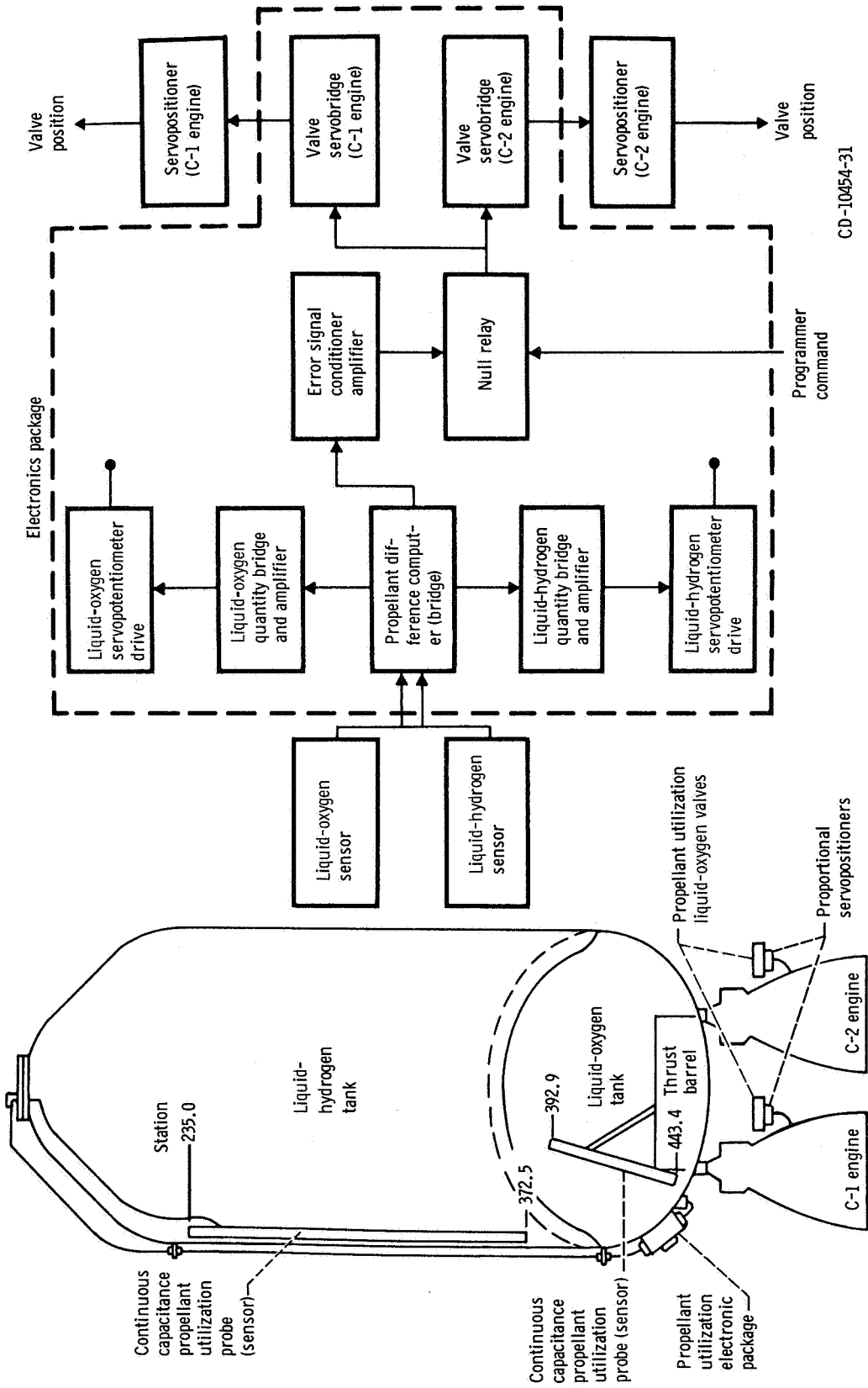


Figure VI-18. - Atlas propellant utilization fuel valve angles, predicted and flight data, AC-16. Valve angle limits: +15 percent O/F ratio, 25.1°; nominal O/F ratio, 32.1°; -15 percent O/F ratio, 50.9°.



CD-10454-31

Figure VI-19. - Centaur propellant utilization system, AC-16.

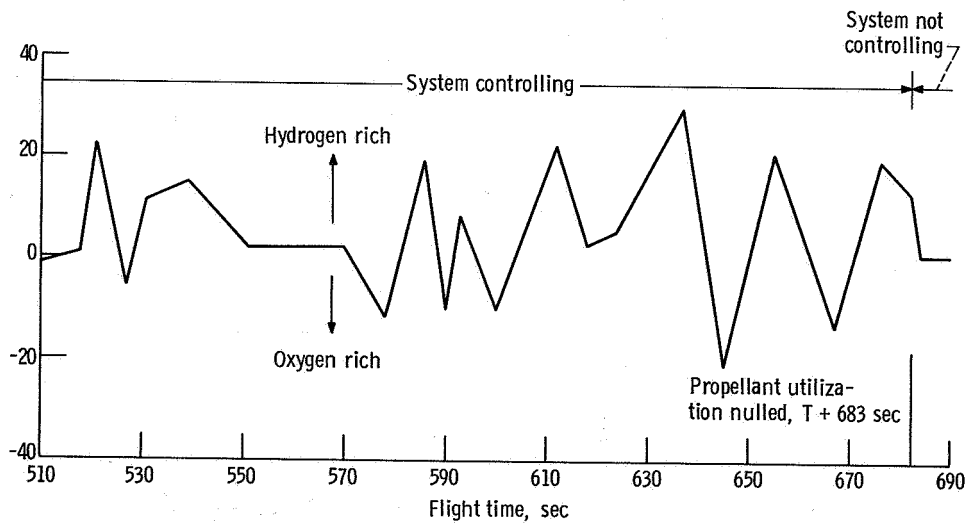
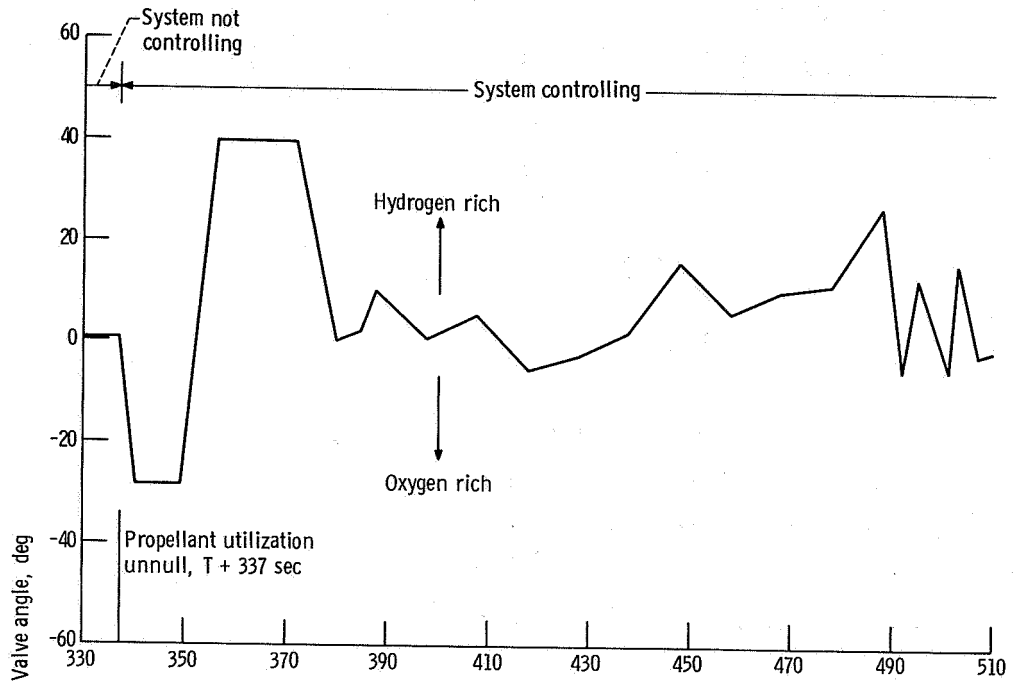


Figure VI-20. - Centaur propellant utilization valve angles for C-1 engine, AC-16. Main engine start, T + 247.5 seconds; main engine cutoff, T + 698 seconds.

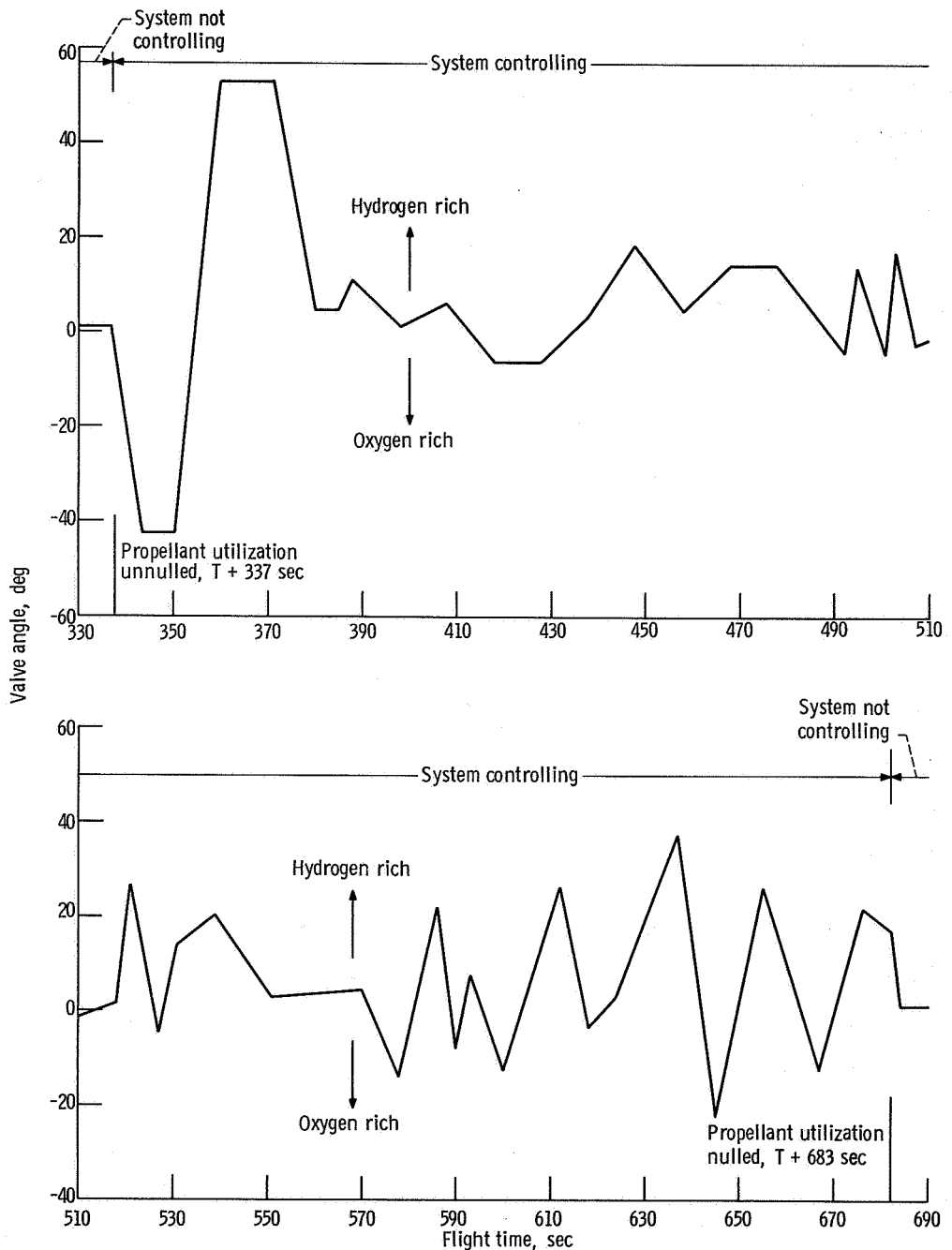


Figure VI-21. - Centaur propellant utilization valve angles for C-2 engine, AC-16. Main engine start, T + 247.5 seconds; main engine cutoff, T + 698 seconds.

PNEUMATIC SYSTEMS

by Eugene J. Fourney and Merle L. Jones

Atlas

System description. - The Atlas pneumatic system (fig. VI-22) supplies helium gas for tank pressurization and for various vehicle functions. The system is comprised of three independent subsystems: propellant tank pressurization, engine control, and booster section jettison.

Propellant tank pressurization subsystem: This subsystem is used to maintain propellant tank pressures at required levels to support the pressure-stabilized tank structure, and to satisfy the inlet pressure requirements of the engine turbopumps. In addition helium gas is supplied from the fuel tank pressurization line to pressurize the hydraulic reservoirs and turbopump lubricant storage tanks. The subsystem consists of eight shrouded helium storage bottles, a heat exchanger, and fuel and oxidizer tank pressure regulators and relief valves.

The eight shrouded helium storage bottles with a total capacity of 967 000 cubic centimeters (59 000 in.³) are mounted in the jettisonable booster engine section. The bottle shrouds are filled with liquid nitrogen during prelaunch operations to chill the helium and thus provide a maximum storage capacity at about 2070 newtons per square centimeter (3000 psi). The liquid nitrogen drains from the shrouds at lift-off. During flight the cold helium passes through a heat exchanger located in the booster engine turbine exhaust duct and is heated before being supplied to the tank pressure regulators. The propellant tank pressurization subsystem pressurization control is switched from the ground to the airborne system at about T - 60 seconds. Airborne regulators are set to control fuel tank gage pressure between 44.1 and 46.2 newtons per square centimeter (64 and 67 psi) and the oxidizer tank pressure between 19.58 and 24.13 newtons per square centimeter (28.4 and 35.0 psi). From approximately T - 60 seconds to T + 20 seconds, the liquid-oxygen regulator sense line is biased by a helium "bleed" flow into the liquid-oxygen tank regulator sensing line which senses ullage pressure. The bias causes the regulator to control tank pressure at a lower level than the normal regulator setting. Depressing the liquid-oxygen tank pressure increases the differential pressure across the bulkhead between the propellant tanks to counteract the launch transient loads that act in a direction to cause bulkhead reversal. At T + 20 seconds the bias is removed by closing explosively actuated valves, and the ullage pressure in the liquid-oxygen tank increases to the normal regulator control range. The increased pressure then provides sufficient vehicle structural stiffness to withstand bending loads during the remainder of the ascent.

Pneumatic regulation of tank pressure is terminated at booster engine staging. Thereafter, the fuel tank pressure decays slowly, but the oxidizer tank pressure decay is less than the fuel tank pressure decay since it is partially sustained by liquid-oxygen boiloff.

Engine controls subsystem: The engine controls subsystem supplies helium pressure for actuation of engine control valves, for pressurization of the engine start tanks, for purging booster engine turbopump seals, and for the reference pressure to the regulators which control oxidizer flow to the gas generator. Pressure control in the system is maintained through Atlas-Centaur separation. These pneumatic requirements are supplied from a single 76 000-cubic centimeter (4650-in.³) storage bottle pressurized to a gage pressure of about 2070 newtons per square centimeter (3000 psi) at lift-off.

Booster engine jettison subsystem: The booster engine jettison subsystem supplies pressure for release of the pneumatic staging latches to separate the booster engine package. A command from the Atlas flight control system opens two explosively actuated valves to supply helium pressure to the 10 piston-operated staging latches. Helium for the system is supplied by a single 14 260-cubic-centimeter (870-in.³) bottle charged to a gage pressure of 2070 newtons per square centimeter (3000 psi).

System performance. - Atlas pneumatic system performance data are presented in table VI-VII. Individual subsystem performance during flight was as follows:

Propellant tank pressurization subsystem: Control of the propellant tank pressures was switched from the ground pressurization control unit to the airborne regulators at approximately T - 63 seconds. Ullage pressures were properly controlled throughout the flight.

The fuel tank pressure regulator controlled at a gage pressure of about 45.75 newtons per square centimeter (66.5 psi) until termination of pneumatic control at booster engine staging. During the sustainer phase, the fuel tank ullage pressure decreased normally and was 38.87 newtons per square centimeter (56.14 psi) at sustainer engine cutoff.

The oxidizer tank ullage pressure was steady at 21.24 newtons per square centimeter (30.8 psi) after switching from the pressurization control unit to "pneumatics internal" at approximately T - 63 seconds. The pressure decreased to 20.75 newtons per square centimeter (30.1 psi) at engine start and decreased slightly until T + 20 seconds. At T + 20 seconds the oxidizer ullage tank pressure was 20.62 newtons per square centimeter (29.9 psi). At this time the regulator sense line bias was terminated, and the pneumatic regulator increased the liquid-oxygen tank ullage pressure to 23.20 newtons per square centimeter (33.8 psi). Three seconds were required for the ullage pressure to stabilize. The liquid-oxygen tank pressure remained within the required limits until termination of pneumatic regulation at booster engine staging. After booster

engine staging, the ullage pressure decreased from 23.05 to 21.51 newtons per square centimeter (33.45 to 31.19 psi) at sustainer engine cutoff.

Engine control subsystem: The booster and sustainer engine control regulators provided the required helium pressure for engine control throughout the flight.

Booster section jettison subsystem: Booster section jettison subsystem performance was satisfactory. The explosively actuated valve was opened on command, allowing high-pressure helium to actuate the 10 booster staging latches.

Centaur

System description. - The Centaur pneumatic system, which is shown schematically in figure VI-23, consists of four subsystems: propellant tank venting, propellant tank pressurization, propulsion pneumatics, and helium purge pneumatics.

Propellant tank venting subsystem: The structural stability of the propellant tanks is maintained throughout the flight by the propellant boiloff gas pressures. These pressures are controlled by a vent system on each propellant tank. Two pilot-controlled, pressure-actuated vent valves and ducting comprise the hydrogen tank vent system. The primary vent valve is fitted with a continuous-duty solenoid valve which, when energized, prevents the vent valve from relieving. The secondary hydrogen vent valve does not have the control solenoid and is always in the "unlocked" mode. The relief range of the secondary valve is above that of the primary valve, preventing overpressurization of the hydrogen tank when the primary vent valve is locked. The vented hydrogen gas is ducted overboard through a single vent. The oxygen tank vent system uses a single vent valve which is fitted with the control solenoid valve. The vented oxygen gas is ducted overboard through the interstage adapter. The duct, which remains with the Centaur after separation from the interstage adapter, is oriented to approximately align the venting thrust vector with the vehicle center of gravity.

The vent valves are commanded to the locked mode at specific times (1) to satisfy the structural requirements of the pressure-stabilized tank, (2) to permit controlled pressure increases in the tanks to satisfy the boost pump pressure requirements, (3) to restrict venting during nonpowered flight to avoid vehicle disturbing torques, and (4) to restrict hydrogen venting to nonhazardous times. (A fire could conceivably occur during the early part of the atmospheric ascent if a plume of vented hydrogen washed back over the vehicle and if it were exposed to an ignition source. A similar hazard could occur at Atlas booster engine staging when residual oxygen envelops a large portion of the vehicle.)

Propellant tank pressurization subsystem: The propellant tank pressurization subsystem supplies helium gas in controlled quantities for in-flight pressurization, in addi-

tion to that provided by the propellant boiloff gases. It consists of a helium storage bottle, two normally closed solenoid valves and orifices, and a pressure switch assembly which senses oxygen tank pressure. The solenoid valves and orifices provide metered flow of helium to both propellant tanks for step pressurization during the main engine start sequence and to the oxygen tank at main engine cutoff. The pressure-sensing switch controls the pressurization of the oxygen tank during the main engine start sequence.

Propulsion pneumatics subsystem: The propulsion pneumatics subsystem supplies helium gas from the helium storage bottle at regulated pressures for actuation of main engine control valves and pressurization of the hydrogen peroxide storage bottle. It consists of two pressure regulators, which are referenced to ambient pressure, and two relief valves. Pneumatic pressure supplied through the engine controls regulator is used for actuation of the engine inlet valves, the engine cooldown valves, and the main fuel shutoff valve. The second regulator, located downstream of the engine controls regulator, further reduces the pressure to provide expulsion pressurization for the hydrogen peroxide storage bottle. A relief valve downstream of each regulator prevents overpressurization.

Helium purge pneumatics subsystem: A ground-airborne helium purge subsystem is used to prevent cryopumping and icing under the insulation panels and in propulsion system components. A common airborne distribution system is used for prelaunch purging from a ground helium source and postlaunch purging from an airborne helium storage bottle. This subsystem distributes helium gas for purging the cavity between the hydrogen tank and the insulation panels, the seal between the barrel section and the forward bulkhead, the propellant feedline insulation, the boost pump seal vents, the engine gearbox seal vents, the engine chilldown vent-ducts, the engine thrust chambers, and the hydraulic power packages. The umbilical charging connection for the airborne bottle can also be used to supply the purge from the ground source should an abort occur after ejection of the ground purge supply line.

System performance. - The pneumatic system performance during the flight was as follows:

Propellant tank pressurization and venting subsystems: The ullage pressures for the hydrogen and oxygen tanks during the flight are shown in figure VI-24. The hydrogen tank absolute pressure was 14.5 newtons per square centimeter (21.0 psi) at T - 28.8 seconds when the primary hydrogen vent valve was locked. The valve was locked earlier than normal on this flight to provide a greater structural capability at lift-off through an increased hydrogen tank pressure. (On most Atlas-Centaur flights the vent valve is locked at T - 8 sec.) The need for greater strength at lift-off is discussed in the section VEHICLE STRUCTURES. After vent valve lockup, the tank ullage absolute pressure increased, at an average rate of 3.51 newtons per square centimeter

per minute (5.09 psi/min), to 18.0 newtons per square centimeter (26.1 psi) at T + 31 seconds. At this time the secondary vent valve relieved and regulated tank pressure until T + 90 seconds, when the primary vent valve was enabled. The tank pressure was then reduced and was regulated by the primary vent valve.

At T + 152.1 seconds the primary hydrogen vent valve was locked for 7.1 seconds during Atlas booster engine staging. Following booster engine staging the primary vent valve was enabled and allowed to regulate tank pressure. At T + 234.1 seconds the primary hydrogen vent valve was again locked, and the tank was pressurized with helium for 1 second. The tank absolute pressure increased from 13.7 to 14.7 newtons per square centimeter (19.9 to 21.3 psi). As the warm helium in the tank cooled, the absolute pressure decreased to 13.9 newtons per square centimeter (20.2 psi) at T + 246.0 seconds (Centaur main engine start). The absolute pressure at engine prestart (T + 238.0 sec) was 14.5 newtons per square centimeter (21.0 psi) (figs. VI-24(a) and (b)).

The ullage absolute pressure in the oxygen tank was 20.6 newtons per square centimeter (29.9 psi) at lift-off. After lift-off the pressure began to decrease with the increasing vehicle acceleration which suppressed the propellant boiling. At T + 90 seconds the vent valve reseated and venting ceased. The pressure then began to increase and decrease alternately with vent valve operation until Atlas booster engine cutoff. At this time the sudden reduction in the acceleration caused an increase in the liquid-oxygen boiloff and an ullage pressure rise. As thermal equilibrium was reestablished in the tank, the ullage pressure decreased.

At T + 199.2 seconds the oxygen tank vent valve was locked, and the helium pressurization of the tank began. The tank ullage absolute pressure increased to 27.4 newtons per square centimeter (39.7 psi), which was the upper limit of the pressure switch. As the warm helium gas cooled in the tank, the absolute pressure decreased to 26.2 newtons per square centimeter (38.0 psi), when the pressure switch closed, and additional helium was injected into the tank. After the second cycle, the heat input from the boost pump recirculation flow increased the boiloff and caused the pressure to increase before it reached the lower limit of the pressure switch. At engine prestart the absolute pressure was 28.4 newtons per square centimeter (41.2 psi). After engine prestart the absolute pressure decreased to 27.5 newtons per square centimeter (39.9 psi) at main engine start and decreased thereafter to the saturation value of the oxygen gas (figs. VI-24(a) and (b)).

The ullage pressures in both propellant tanks decreased normally during main engine firing. At engine cutoff the ullage absolute pressures in the hydrogen and oxygen tanks were 9.1 and 16.5 newtons per square centimeter (13.2 and 23.9 psi), respectively. At engine cutoff the oxygen tank was pressurized with helium for 90 seconds in order to preclude the possibility of the hydrogen tank pressure exceeding the oxygen tank pressure and reversing the intermediate bulkhead. During this period the oxygen tank abso-

lute pressure increased to 19.6 newtons per square centimeter (28.4 psi). The pressure continued to increase to 20 newtons per square centimeter (29.0 psia) at T + 900 seconds and remained constant through start of retrothrust. The hydrogen tank absolute pressure increased to 18.0 newtons per square centimeter (26.1 psi) during the period between main engine cutoff and T + 1491 seconds. The secondary hydrogen vent valve then relieved and regulated tank pressure (figs. VI-24(c) and (d)).

After the start of retrothrust the hydrogen tank ullage pressure remained constant for approximately 70 seconds, indicating liquid outflow. The pressure then began to decrease, indicating either gaseous or two-phase outflow. The oxygen tank ullage pressure remained constant to loss of signal (T + 1890 sec), indicating liquid outflow (fig. VI-24(d)). At acquisition of signal (T + 2350 sec) the pressure was decreasing, indicating gaseous or two-phase outflow.

Propulsion pneumatics subsystem: The engine controls regulator and the hydrogen peroxide bottle pressure regulator maintained proper system pressure levels throughout the flight. The engine controls regulator output absolute pressure was 326 newtons per square centimeter (473 psi) at T - 0 seconds, while that of the hydrogen peroxide bottle pressure regulator was 224 newtons per square centimeter (325 psi). After lift-off both regulator output pressures decreased corresponding to the decrease in ambient pressure and remained relatively constant after the ambient pressure had decreased to zero.

Helium purge subsystem: The total helium purge flow rate to the vehicle at T - 14 seconds was 86 kilograms per hour (190 lbm/hr). The differential pressure across the insulation panels after hydrogen tanking was 0.15 newton per square centimeter (0.22 psi). The minimum allowable differential pressure required to prevent cryopumping and icing is 0.02 newton per square centimeter (0.03 psi). At T - 13.6 seconds the airborne purge system was activated, and at T - 4 seconds the ground purge was terminated. The supply of helium in the purge bottle lasted through most of the atmospheric ascent.

TABLE VI-VII. - ATLAS PNEUMATIC SYSTEM PERFORMANCE, AC-16

Parameter	Measurement number	Units	Design range	Flight values at -					
				T - 10 sec	T - 0 sec	T + 20 sec	T + 23 sec	Booster engine cutoff	Sustainer or vernier engine cutoff
Oxidizer tank ullage pressure, gage	AF1P	N/cm ² psi	(a)	21.24 30.8	20.75 30.1	^b 20.62 29.9	^c 23.20 33.8	23.05 33.45	^d 21.51 31.19
Fuel tank ullage pressure, gage	AF3P	N/cm ² psi	44.13 to 46.19 64.0 to 67.0	45.85 66.5	45.16 65.5	45.75 66.5	46.06 66.8	45.57 66.1	^d 38.87 56.14
Intermediate bulkhead differential pressure ^e	AF116P	N/cm ² psi	0.345 (min.) 0.5 (min.)	14.03 20.5	14.62 21.2	12.6 18.25	9.48 13.75	17.24 25.0	17.24 25.0
Sustainer controls helium bottle pressure, absolute	AF291	N/cm ² psi	2344 (max.) 3400 (max.)	2275 3300	2179 3160	2131 3090	2131 3090	1934 2805	1862 2700
Booster helium bottle pressure, absolute	AF246P	N/cm ² psi	2344 (max.) 3400 (max.)	2310 3350	2186 3170	1700 2465	1634 2370	438 635	(d)
Booster helium bottle temperature	AF247T	^o R ^o F	154.67 to 139.67 (-305 to -320) prior to engine start	140.57 -319.2	139.07 -320.6	125.07 -334.6	123.67 -336.0	82.67 -377	(d)

^aPrior to T - 0 sec, 19.58 to 22.17 N/cm² (28.4 to 32.3 psi); after T + 23 sec, 22.06 to 24.13 N/cm² (32.0 to 35.0 psi).

^bSignal from programmer to fire programmed pressure conax valves.

^cOxidizer tank pressure at termination of programmed pressure.

^dHelium supply bottles jettisoned with booster at booster engine cutoff plus 3 sec.

^eLowest valve was 13 psi at T + 1 sec.

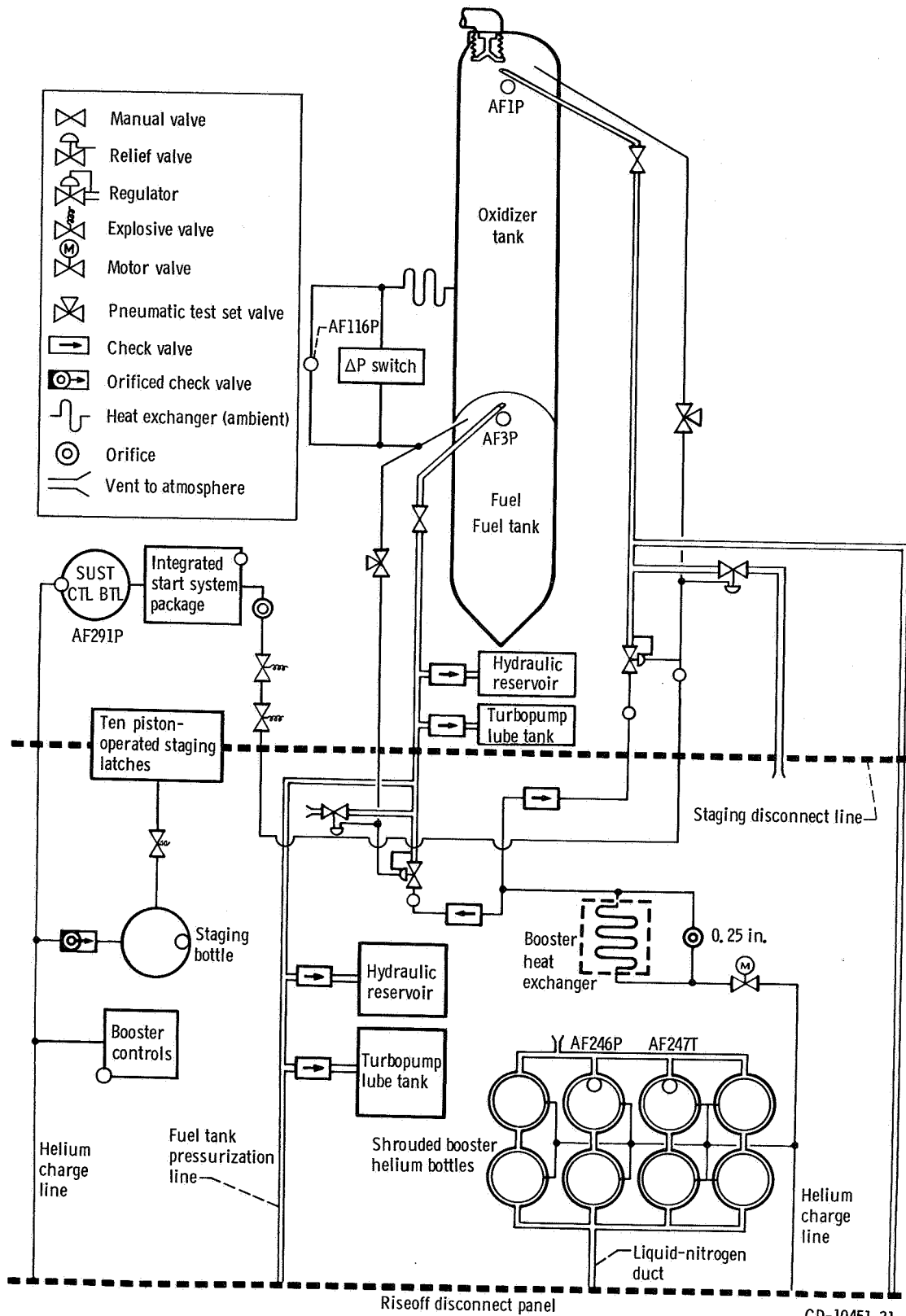
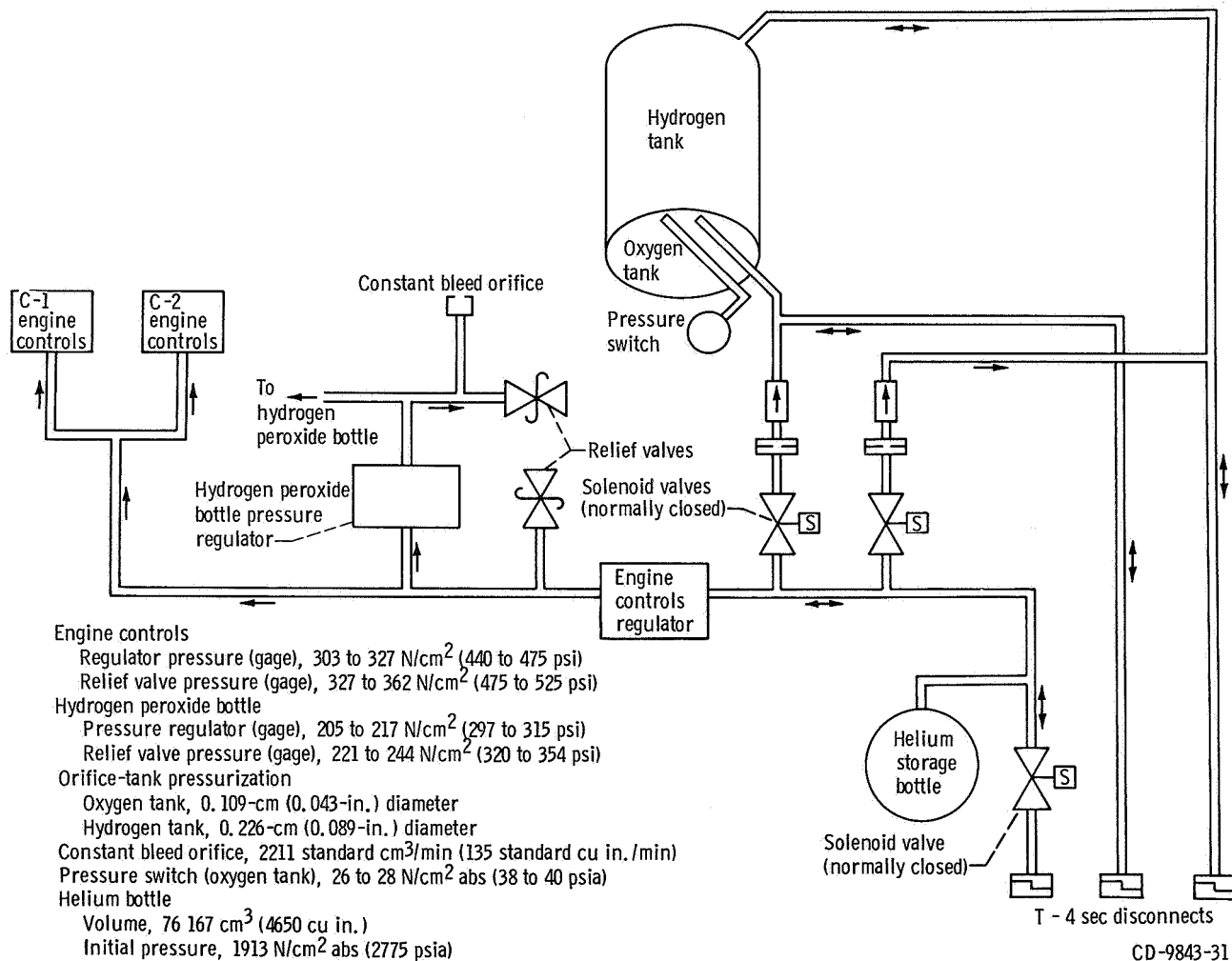
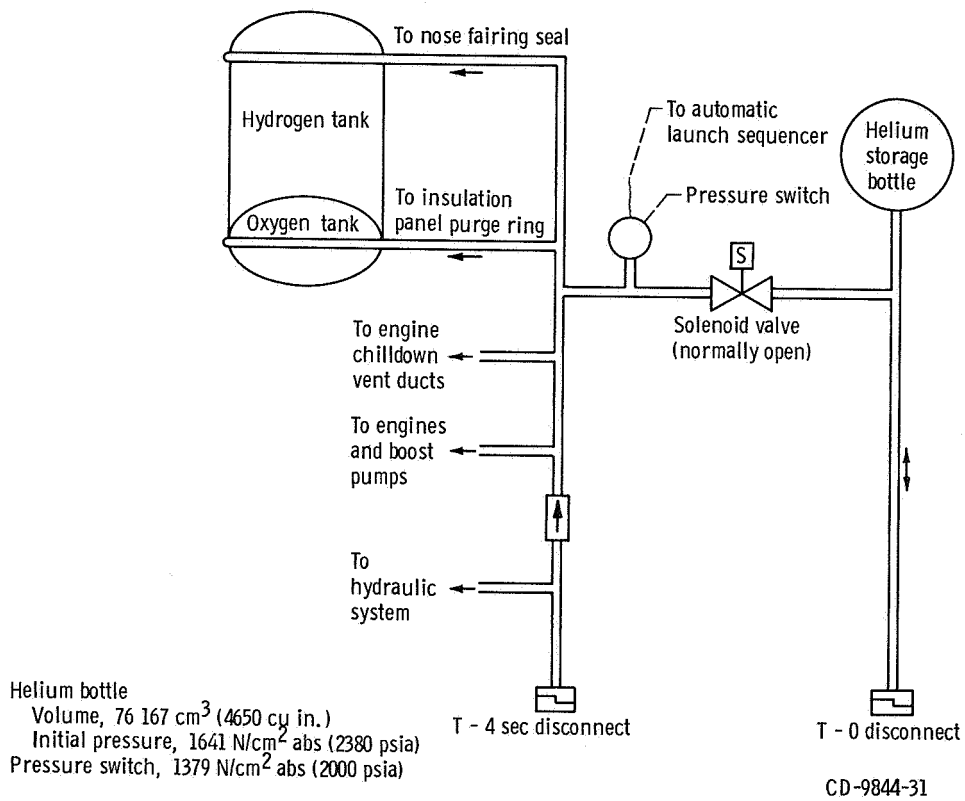


Figure VI-22. - Atlas vehicle pneumatic system, AC-16.



(a) Tank pressurization and propulsion pneumatics subsystems.

Figure VI-23. - Centaur pneumatics system, AC-16.



(b) Helium purge subsystem.

Figure VI-23. - Concluded.

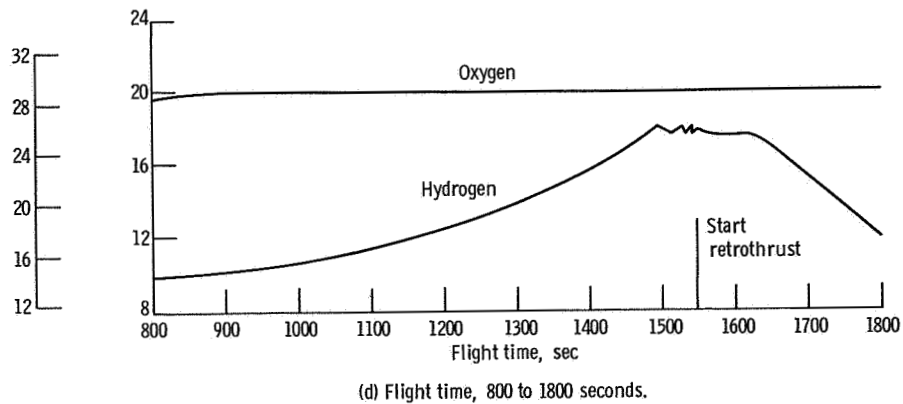
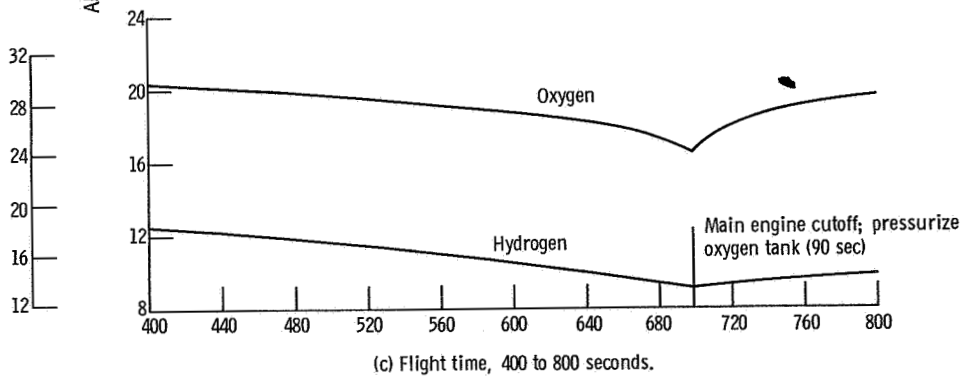
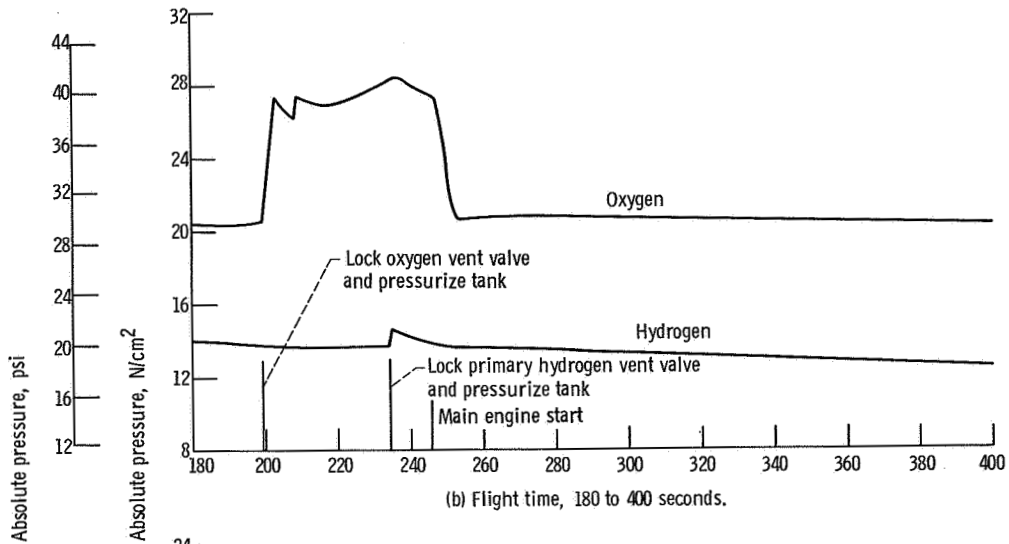
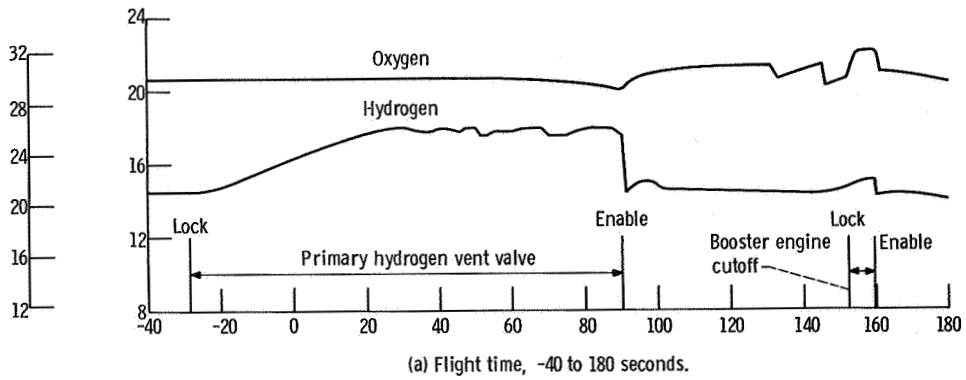


Figure VI-24. - Centaur tank pressure history, AC-16.

HYDRAULIC SYSTEMS

by Eugene J. Cieslewicz and Eugene J. Fourney

Atlas

System description. - Two hydraulic systems (figs. VI-25 and VI-26) are used on the Atlas vehicle to supply fluid power for operation of sustainer engine control valves and for thrust vector control of all engines. One system is used for the booster engines and the other for the sustainer engine.

The booster hydraulic system provides power solely for gimbaling the two thrust chambers. System pressure is supplied by a single, pressure-compensated, variable-displacement pump driven by the engine turbopump accessory drive. Additional components of the system include four servocylinders, a high-pressure relief valve, an accumulator, and a reservoir. Engine gimbaling in response to flight control commands is accomplished by the servocylinders, which provide separate pitch, yaw, and roll control during the booster engine phase of flight. The maximum booster engine gimbal angle capability is $\pm 5^{\circ}$ in the pitch and yaw planes.

The sustainer stage uses a system similar to that of the booster but, in addition, provides hydraulic power for sustainer engine control valves for gimbaling of the two vernier engines. Vehicle roll control is accomplished during the sustainer phase by differential gimbaling of the vernier engines. Actuator limit travel for the vernier engines is $\pm 70^{\circ}$ and for the sustainer engine is $\pm 3^{\circ}$.

System performance. - Hydraulic system pressure data for both the booster and sustainer circuits was normal. Pressures were stable throughout the boost flight phase. The transfer of fluid power from ground to airborne hydraulics systems was normal. Pump discharge absolute pressures increased from 1290 newtons per square centimeter (1870 psi) at T - 2 seconds to flight levels of 2100 newtons per square centimeter (3050 psi) in less than 2 seconds. Starting transients produced a normal overshoot of about 10 percent in the pump discharge pressure. Absolute pressure in the sustainer hydraulic and booster circuits stabilized at 2100 and 2171 newtons per square centimeter (3050 and 3150 psi), respectively.

During the booster phase of flight the sustainer pump return pressure transducer measurement (AH601P) indicated return pressure transients. Some transients as high as 295 newtons per square centimeter (430 psi) gage were recorded. Normal sustainer pump return pressure is approximately 44.8 newtons per square centimeter (65 psi) gage. This condition has been noted on most SLV-3C Atlas boosters. The cause of this anomaly is unknown at this time; however, it had no adverse effects on the performance of the hydraulic system.

Centaur

System description. - Two separate but identical hydraulic systems (fig. VI-27) are used on the Centaur stage. Each system gimbals one engine for pitch, yaw, and roll control. Each system consists of two servocylinders and a power package coupled to the engine. The power package contains high- and low-pressure pumps, reservoir, accumulator, pressure-intensifying bootstrap piston, and relief valves for pressure regulation. High-pressure power is provided by a constant-displacement vane-type pump driven by the liquid-oxygen turbopump accessory drive shaft. An electrically powered recirculation pump is used to provide low pressure for engine gimbaling requirements during prelaunch checkout, and during flight to align the engines prior to main engine start. It is also used for limited thrust vector control during the propellant tank discharge for the Centaur retrothrust operation. Maximum engine gimbal capability is $\pm 3^{\circ}$.

System performance. - The hydraulic system properly performed all guidance and flight control commands throughout the flight. System pressures and temperatures as a function of flight time are shown in figures VI-28 and VI-29.

Activation of the low-pressure recirculation pumps provided absolute hydraulic pressures of 71.8 newtons per square centimeter (104.1 psi) for the C-1 engine and 70.3 newtons per square centimeter (102.0 psi) for the C-2 engine system. These pumps provided pressure and flow for centering the engines prior to main engine start. Main system absolute pressure in the C-1 and C-2 systems reached 750.6 and 754.2 newtons per square centimeter (1088.6 and 1093.8 psi), respectively, at main engine start. Manifold temperatures rose from 282.9 and 283.5 K (49.8° and 50.9° F), respectively, for C-1 and C-2 at main engine start to 347.1 and 349.0 K (165.4° and 168.8° F) at main engine cutoff. After cutoff the temperatures slowly decreased to steady values of 334.3 K (142.3° F) on C-1 and 332.9 K (139.8° F) on C-2.

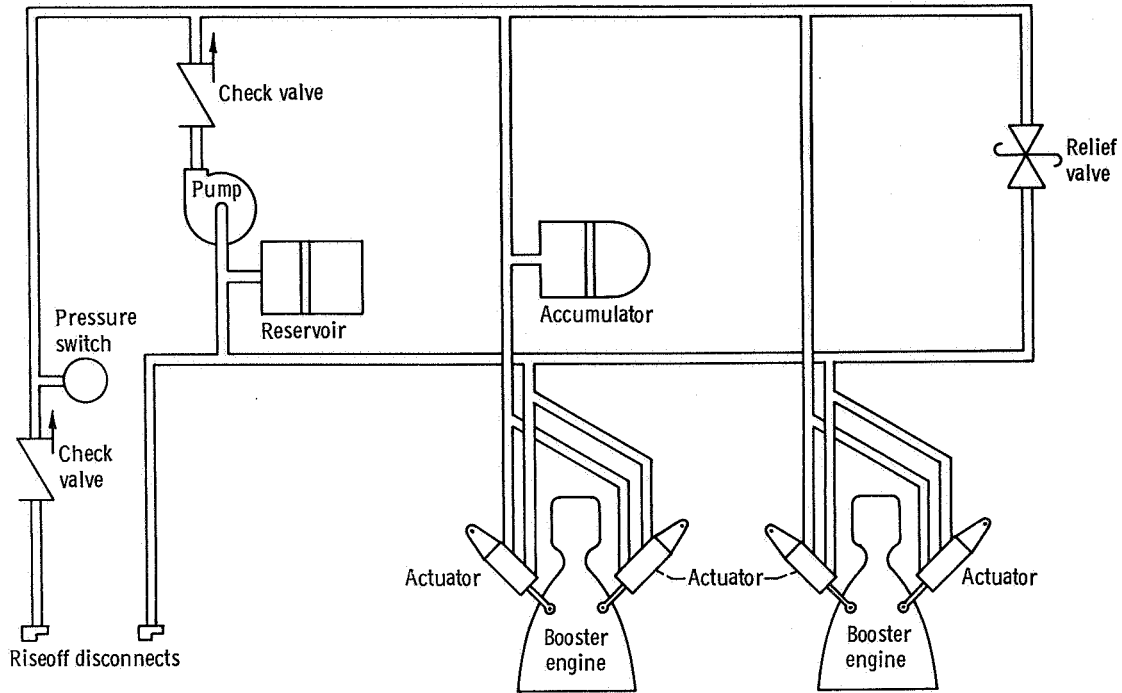


Figure V-25. - Atlas booster hydraulic system, AC-16.

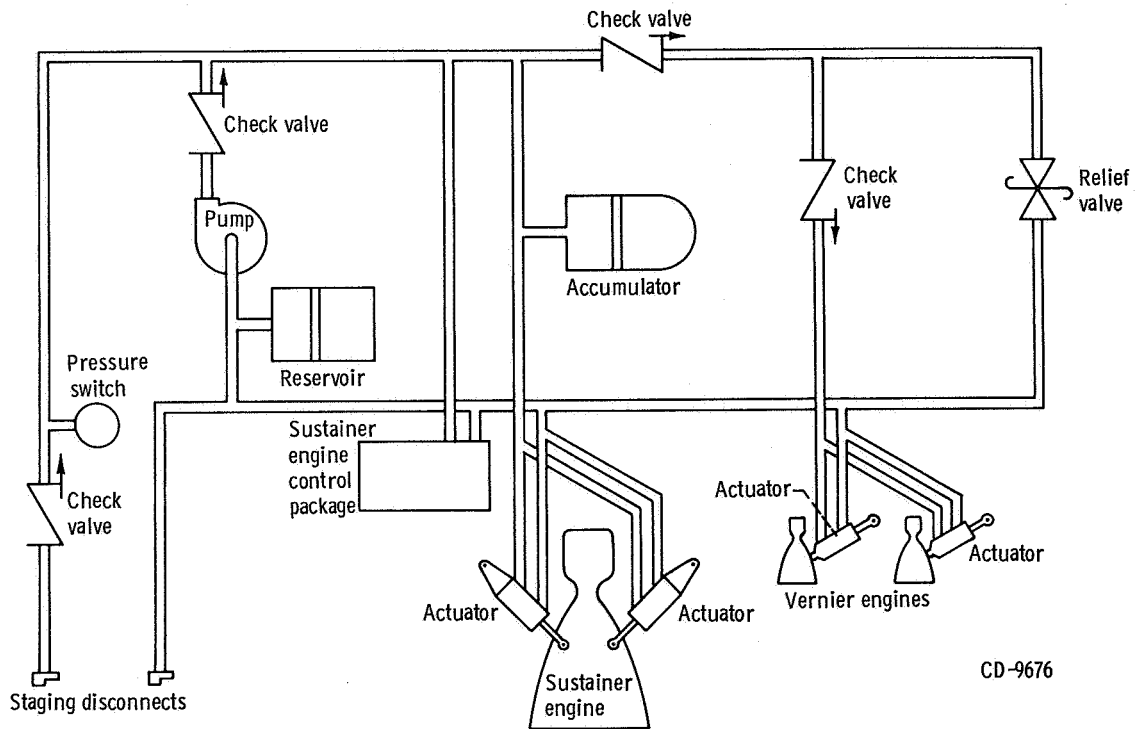


Figure VI-26. - Atlas sustainer hydraulic system, AC-16.

CD-9676

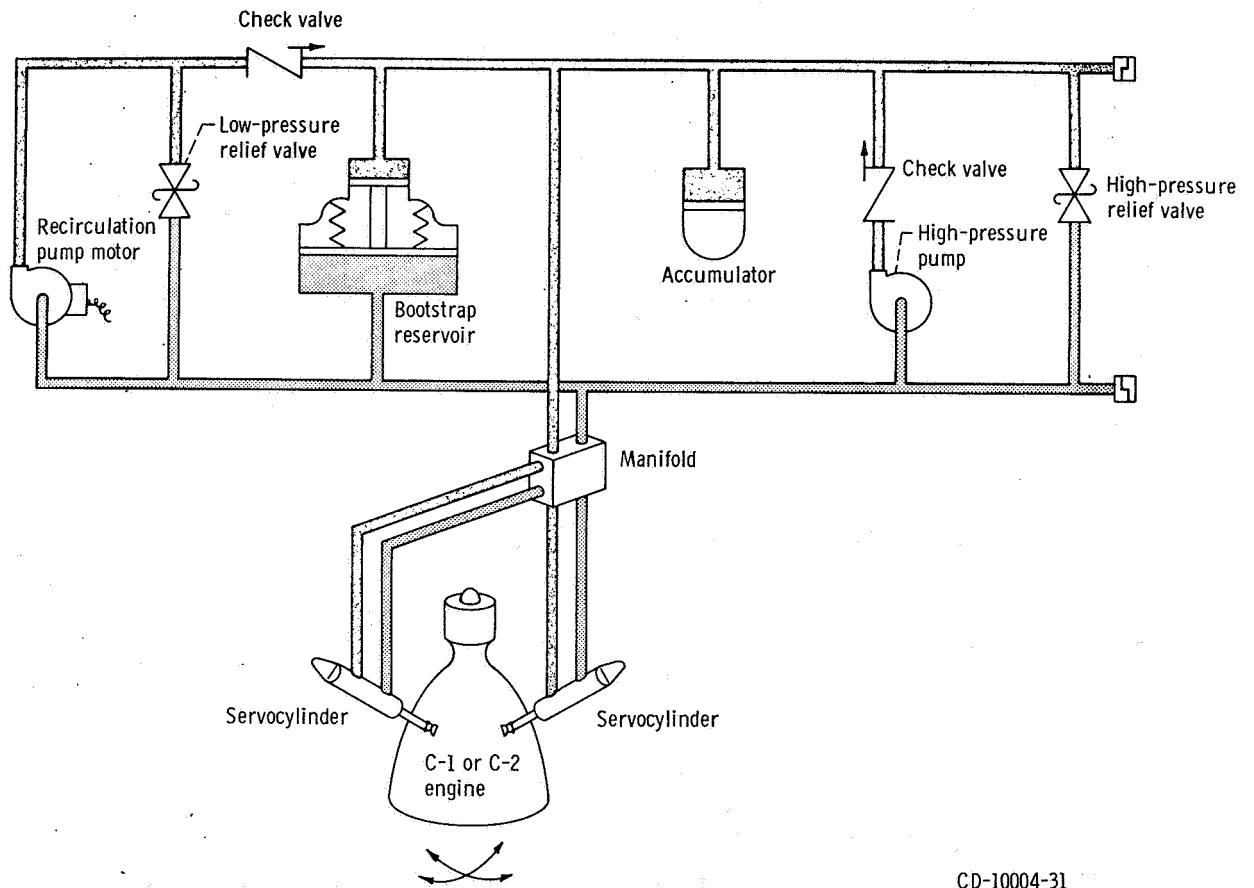
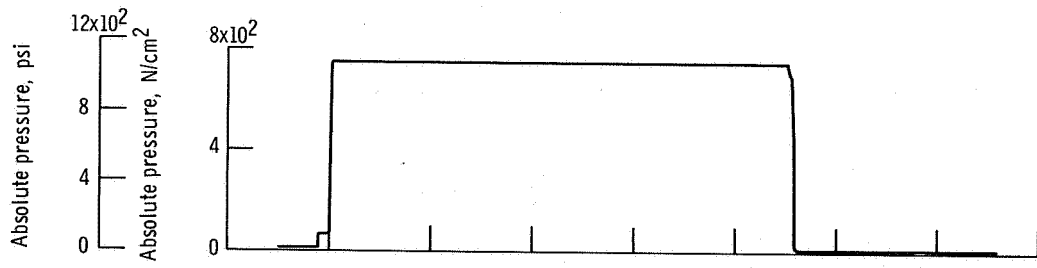
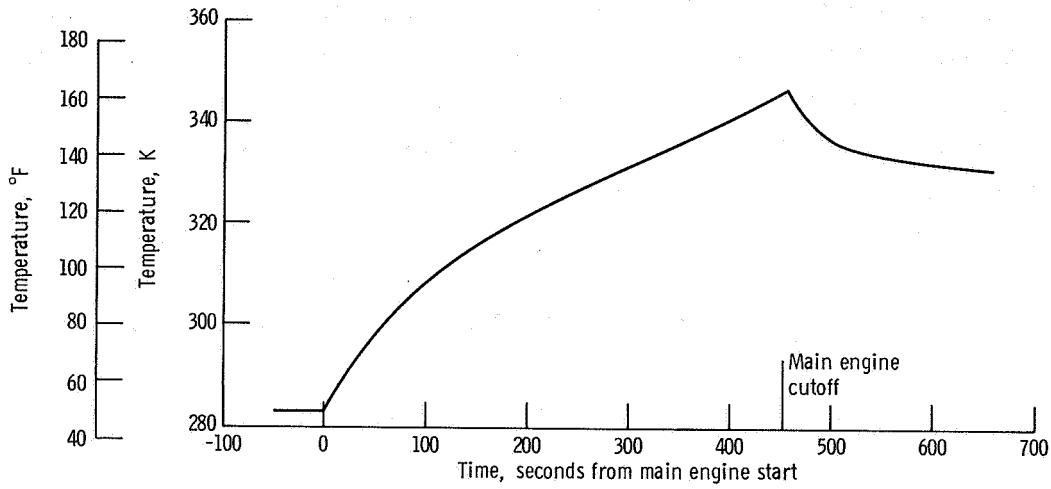


Figure VI-27. - Centaur hydraulic system, AC-16.

CD-10004-31

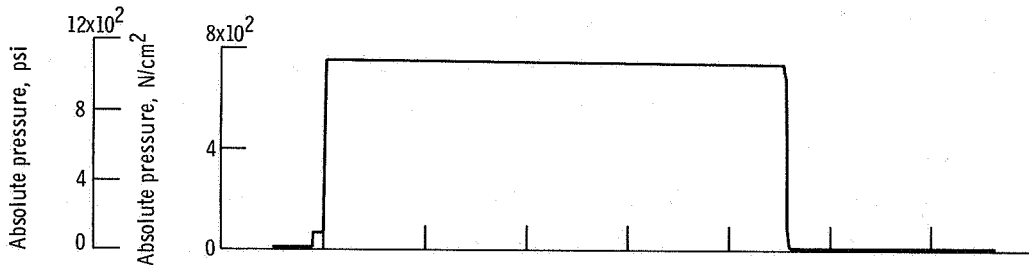


(a) Pressure.

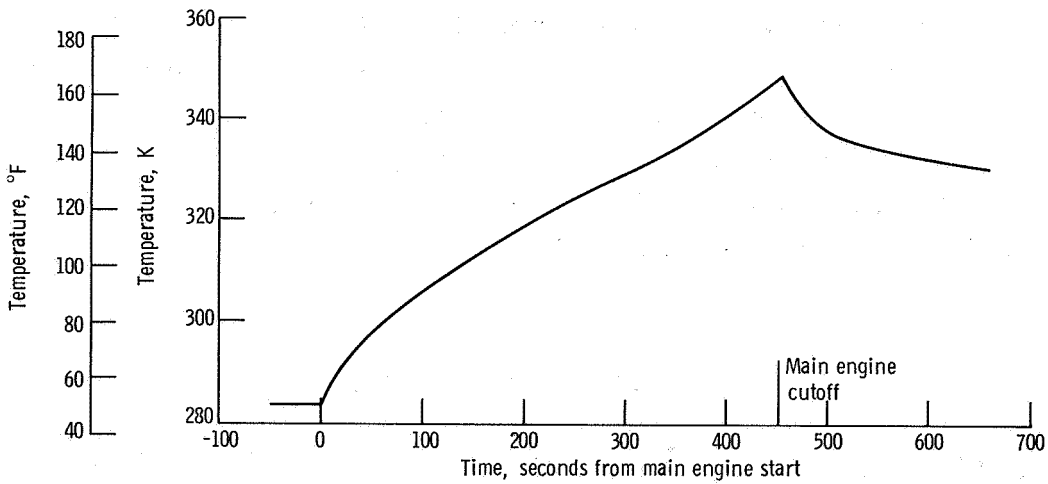


(b) Temperature.

Figure VI-28. - Hydraulic system pressure and temperature for C-1 engine, AC-16.



(a) Pressure.



(b) Temperature.

Figure VI-29. - Hydraulic system pressure and temperature for C-2 engine, AC-16.

VEHICLE STRUCTURES

by James F. Harrington, Robert C. Edwards, and Dana H. Benjamin

Atlas Structures

System description. - The primary Atlas vehicle structure is provided by the propellant tanks. These tanks are thin-walled, pressure-stabilized, monocoque sections of welded stainless-steel construction (fig. VI-30). They require internal pressure in order to maintain structural stability. The tensile strength of the tank material determines the maximum allowable pressure in the propellant tanks.

The maximum allowable and minimum required tank pressures presented in figure VI-31 are computed by using maximum design loads (as opposed to actual flight loads) with appropriate factors of safety. These required tank pressures are not constant because of varying aerodynamic loads, inertial loads, and ambient pressure during flight.

The Atlas vehicle is subjected to its highest design bending load between T + 40 and T + 100 seconds. The bending, inertia, and aerodynamic drag create compressive loads in the fuel and oxidizer tank skin. These loads are resisted by internal pressure to prevent buckling of the skin.

The maximum allowable differential pressure between the oxidizer and fuel tanks is limited by the strength of the Atlas intermediate bulkhead. The fuel tank pressure must always be greater than the oxidizer tank pressure to stabilize the intermediate bulkhead (prevent bulkhead reversal).

System performance. - The Atlas oxidizer and fuel tank ullage pressures did not approach the maximum allowable pressure during flight. The oxidizer and fuel tank ullage pressures were greater than the minimum required to resist the combined bending and axial design loads between T + 40 and T + 100 seconds (fig. VI-31). The bulkhead differential pressure was within the maximum allowable and minimum required pressure limits for all periods of flight (fig. VI-31).

The increase of longitudinal inertia force was as expected. A maximum value of 5.74 g's was reached at booster engine cutoff (T + 152.1 sec). This value was within the specified limits of 5.587 to 5.813 g's.

Centaur Structures

System description. - The primary Centaur vehicle structure is provided by the propellant tanks. These tanks are thin-walled, pressure-stabilized, monocoque sections of welded stainless-steel construction (fig. VI-32). They require internal pressure in

order to maintain structural stability. The tensile strength of the tank material determines the maximum allowable pressure in the propellant tanks.

The maximum allowable and minimum required tank pressures presented in figures VI-33(a) to (c) are computed by using maximum design loads (as opposed to actual flight loads) with appropriate factors of safety. The maximum allowable and minimum required tank pressures are not constant because of varying loads and varying ambient pressure during flight. The tank locations and criteria which determine the maximum allowable and minimum required tank pressures during different phases of flight are described in figure VI-34.

The oxidizer tank pressure most closely approaches the maximum allowable pressure at booster engine cutoff ($T + 152.1$ sec), when the high inertial load causes maximum tension stresses on the aft bulkhead (fig. VI-33(a)). The minimum required oxidizer tank pressure for aft bulkhead stability is not pertinent because this required pressure is always less than the pressure required for intermediate bulkhead stability.

The strength of the fuel tank is governed by the capability of the conical section of the forward bulkhead to resist hoop stress. Thus, the differential pressure across the forward bulkhead determines the maximum allowable fuel tank pressure.

The minimum required fuel tank pressure was higher for AC-16 than for previous flights because of the heavier and longer nose fairing and payload. However, the only required adjustment to the fuel tank pressure from previous flights was an increase during the launch phase from $T + 0$ to $T + 5$ seconds (fig. VI-33(a)).

The margin between fuel tank ullage pressure and the minimum required pressure was least during the following events:

(1) Prior to launch, the payload and nose fairing impose compression loads on the cylindrical skin at station 409.6 due to gravity and ground winds.

(2) During the launch phase from $T + 0$ to $T + 5$ seconds, the payload and nose fairing impose compression loads on the cylindrical skin at station 409.6 due to longitudinal and lateral inertia and vibration.

(3) From $T + 40$ to $T + 100$ seconds, the Centaur was subjected to maximum design bending moments. The combined loads due to inertia, aerodynamic drag, and bending impose compression on the cylindrical skin at station 409.6.

The maximum allowable differential pressure between the oxidizer and fuel tanks was limited by the strength of the Centaur intermediate bulkhead. The maximum design allowable differential pressure was 15.9 newtons per square centimeter (23.0 psi). The oxidizer tank pressure must always be greater than the combined fuel tank pressure and hydrostatic pressure of the hydrogen fuel; this is necessary to stabilize the intermediate bulkhead (prevent bulkhead reversal).

System performance. - The Centaur fuel and oxidizer tank ullage pressure profiles are compared with the design limits in figures VI-33(a) to (c).

The oxidizer tank pressure was less than the maximum allowable at booster engine cutoff (T + 152.1 sec) and all other periods of flight. The oxidizer tank pressure was maintained above the minimum required for aft bulkhead stability during all periods of flight. At no time during the flight did the fuel tank ullage pressure exceed the maximum allowable pressure. The fuel tank ullage pressure was safely above the minimum required pressure at all times. The differential pressure was less than the maximum allowable 15.9 newtons per square centimeter (23.0 psi) for all periods of flight. The oxidizer tank pressure was always greater than the combined fuel tank ullage pressure and hydrostatic pressure of hydrogen fuel.

Vehicle bending loads. - Flight bending loads were determined at station 125 on the Centaur fixed fairing. The purpose of this measurement was to ascertain the effect of the longer nose fairing on vehicle bending loads; no unexpected bending loads were measured. The maximum bending moment during flight was 16.0×10^6 centimeter-newtons (1.4×10^6 in.-lbf) at T + 70 seconds (fig. VI-35). This was well within the design limit bending moment of 32.0×10^6 centimeter-newtons (2.8×10^6 in.-lbf).

Vehicle Dynamic Loads

The Atlas-Centaur launch vehicle receives dynamic loading from three major sources: (1) external loads from aerodynamic and acoustic sources; (2) transients from engines starting and stopping and from the separation systems; and (3) loads due to dynamic coupling between major systems.

Research and development flights of the Atlas-Centaur have shown that these loads are within the structural limits established by ground test and model analysis. For operational flights such as AC-16, the number of dynamic flight measurements is limited by telemetry capacity. The instruments used and the parameters measured are given in the following table:

Instruments	Corresponding parameters
Low-frequency-range accelerometer	Vehicle longitudinal vibration
Centaur pitch rate gyro	Vehicle pitch plane vibration
Centaur yaw rate gyro	Vehicle yaw plane vibration
Angle-of-attack sensor	Vehicle aerodynamic loads
High-frequency-range accelerometer	Local spacecraft vibration

Launch vehicle longitudinal vibrations measured on the Centaur forward bulkhead are presented in figure VI-36, which depicts the presence of specific responses at the times noted. The frequency and amplitude of the vibration data measured on this flight are shown together with similar data from other flights.

During launcher release, longitudinal vibrations were excited. The amplitude and frequency of these vibrations were similar to those observed on vehicles prior to AC-16. Atlas intermediate bulkhead pressure fluctuations were the most significant effects produced by the launcher-induced longitudinal vibrations. The peak pressure fluctuations computed from these vibrations were 1.2 newtons per square centimeter (1.7 psi). Since the minimum bulkhead differential pressure measured during this time was 8.9 newtons per square centimeter (13 psi) (fig. VI-31), the calculated minimum differential pressure was 7.7 newtons per square centimeter (11 psi). The minimum design allowable differential pressure across the bulkhead is 1.4 newtons per square centimeter (2.0 psi).

During Atlas flight between T + 82 and T + 154 seconds, intermittent longitudinal vibrations of 0.10 g, 12 hertz were observed on the forward bulkhead. These vibrations are believed to be caused by dynamic coupling between structure, engines, and propellant lines (commonly referred to as POGO). The AC-16 vehicle was flown with a longer cylindrical section added to the nose fairing. As a result, AC-16 vehicle length was 17.9 feet (5.45 m) longer than AC-13, AC-14, and AC-15 vehicles and 22.2 feet (6.77 m) longer than AC-10, AC-12, and AC-11 vehicles. As a result, the parameters controlling the frequency and amplitude of these vibrations were changed slightly, but not significantly. For a detailed discussion of this low-frequency longitudinal vibration see reference 1.

During the booster engine thrust decay, short-duration longitudinal vibrations of 0.6 g, 12 hertz were observed. The analytical models did not indicate significant structural loading due to these transients.

During the booster phase of flight, the vehicle vibrates in the pitch plane and the yaw plane as an integral body at all of its natural frequencies. Previous analyses and tests have defined these natural frequencies or modes and the shapes which the vehicle assumes when the modes are excited. The rate gyros on the Centaur provide data for determining the deflection of these modes. The maximum first-mode deflection was seen in the pitch plane at T + 132 seconds (fig. VI-37). The deflection was less than 4 percent of the allowable deflection. The maximum second-mode deflection was seen in the pitch plane at T + 42 seconds (fig. VI-38). The deflection was less than 13 percent of the allowable deflection.

Predicted angles of attack were based upon upper-wind data obtained from weather balloons released before the time of launch. Vehicle bending moments were calculated by using predicted angles of attack, booster engine gimbal angle data, vehicle weights,

and vehicle stiffnesses. These moments were added to axial load equivalent moments and to moments resulting from random dispersions. The most significant dispersions considered were uncertainties in launch vehicle performance, vehicle center-of-gravity offset, and upper-atmosphere wind.

The total equivalent predicted bending moment (based upon wind data) was divided by the design bending moment allowable to obtain the predicted structural capability ratio shown in figure VI-39. This ratio is expected to be greatest between T + 60 and T + 88 seconds because of the high aerodynamic loads during this period. The maximum structural capability ratio predicted for this period was 0.87.

Transducers located on the nose fairing cap provided differential pressure measurements in the pitch plane and the yaw plane. Total pressure was computed from a trajectory reconstruction. Predicted angles of attack are shown in figures VI-40 and VI-41. The angles of attack derived from in-flight pressure data were not available for the total flight at the time of publication. However, a spot check showed that the predicted and actual angles of attack were within the expected dispersion during the most critical flight times. It follows, therefore, that the maximum predicted capability ratio of 0.87 was not exceeded.

Local shock and vibration were measured continuously by three piezoelectric accelerometers in the spacecraft area. The accelerometers were located on the forward end of the payload adapter (Centaur station 68). These accelerometers together with their amplifiers had a frequency response of 2100 hertz, and in all cases the telemetry channel Interrange Instrumentation Group (IRIG) filter frequency was less than this value. Therefore, the frequency range over which one could expect to obtain unattenuated data was limited by the standard IRIG filter frequency for that channel. In addition to the three high-frequency accelerometers, there were six low-frequency accelerometers on the payload adapter (Centaur station 85) located on the x and y axes. These accelerometers were sensitive in the tangential and longitudinal directions.

A summary of the most significant shock and vibrations levels measured continuously by the three high-frequency and six low-frequency accelerometers on AC-16 together with similar data from AC-10, AC-12, AC-11, AC-13, AC-14, and AC-15 are shown in table VI-VIII. The major reason for the apparent discrepancy between the vibration data obtained from the AC-16 vehicle and that obtained from the AC-10, AC-12, and AC-11 vehicles is that the locations of the three high-frequency vibration accelerometers on the two vehicle configurations were different. On AC-10, AC-12, and AC-11, the one continuous accelerometer was installed on one of the retromotor attach points of the Surveyor spacecraft; whereas on AC-13, AC-14, AC-15, and AC-16 the high-frequency accelerometers were installed on the forward end of the payload adapter. From the data it can be seen that the payload adapter receives more vibration (especially during launch transient) than the spacecraft structure. The steady-state vibration levels were highest near lift-off, as

expected. The maximum level of the shock loads (24 g's) on AC-16 occurred at nose fairing jettison. These shock levels were of short duration (~0.025 sec) and did not provide significant loads. An analysis of the data indicates that the levels were well within spacecraft qualification levels.

TABLE VI-VIII. - COMPARISON OF MAXIMUM SHOCK AND VIBRATION LEVELS AT MARK EVENTS^a

(a) Previous Atlas-Centaur flights

Flight event	Flight								
	AC-10	AC-12	AC-11	AC-13	AC-14	AC-15	AC-13	AC-14	AC-15
	Accelerometer location								
	Retromotor attachment 1, station 125; quadrant I-IV; longitudinally sensitive; analysis band, 10 to 790 Hz			Payload adapter, station 129; quadrant III; longitudinally sensitive; analysis band, 10 to 790 Hz			Payload adapter, station 129; quadrant I-IV; radially sensitive ^b		
Launch:									
Acceleration, g's (rms)	0.68	0.65	0.53	1.5	1.4	1.2	2.5	2.9	2.1
Frequency, Hz	165	165	160 to 170	150, 300	163, 296, 397	225, 296, 389, 425	470	485	462, 478, 525
Booster engine cutoff:									
Acceleration, g's	0.8	1.2	0.7	1.2	0.96	1.7	0.83	0.38	0.6
Frequency, Hz	11	17	12	13	14	13	4.5	4.7	4.5
Booster jettison:									
Acceleration, g's	0.5	0.46	0.3	<1/2	<1/2	<1/2	<1/2	<1/2	<1/2
Frequency, Hz	16	16	23	-----	-----	14	-----	-----	6
Insulation panel jettison:									
Acceleration, g's	10	10.1	12	~14	~13	~14	~12	~12	~9
Frequency, Hz	700	600 to 700	600 to 700	500 to 600	500 to 600	500 to 600	500 to 600	500 to 600	500 to 600
Nose fairing jettison:									
Acceleration, g's	1.4	0.49	1.1	2.1	2.7	3.2	2.0	1.6	2.0
Frequency, Hz	32	20	32	400 to 500	400 to 500	400 to 500	400 to 500	400 to 500	400 to 500
Atlas-Centaur separation:									
Acceleration, g's	12	13	12	~14	~13	~14	~12	~12	~9.5
Frequency, Hz	600	600 to 700	700	500 to 600	500 to 600	500 to 600	500 to 600	500 to 600	500 to 600
Main engine first start:									
Acceleration, g's	0.38	0.5	0.4	0.5	0.6	0.5	(c)	(c)	(c)
Frequency, Hz	20	20 to 21	19 to 20	22	20	22	(c)	(c)	(c)
Main engine first cutoff:									
Acceleration, g's	1.14	0.95	2.0	1.6	0.9	0.9	0.9	0.7	0.7
Frequency, Hz	33	22	27	23	23	23	400 to 500	400 to 500	400 to 500
Main engine second start:									
Acceleration, g's	(d)	0.66	(d)	0.7	0.6	0.6	(c)	0.5	(c)
Frequency, Hz	(d)	20 to 22	(d)	20 to 30	30	23	(c)	400 to 500	(c)
Main engine second cutoff:									
Acceleration, g's	(d)	0.97	(d)	0.9	0.9	0.9	1.1	1.5	3
Frequency, Hz	(d)	24	(d)	30	30	30	480	480	400 to 500

^aMaximum shock and vibration levels at mark events are given in terms of maximum single amplitude (in g's) and the most predominant frequency (in Hz) except for rms levels which represent maximum levels observed at launch.

^bA nonstandard Interrange Instrumentation Group filter of 600 Hz was used to analyze launch data on AC-13, AC-14, and AC-15. All other postlaunch data were analyzed with a 330-Hz filter.

^cNo detectable response.

^dSingle-burn missions.

TABLE VI-VIII, - Concluded. COMPARISON OF MAXIMUM SHOCK AND VIBRATION LEVELS AT MARK EVENTS

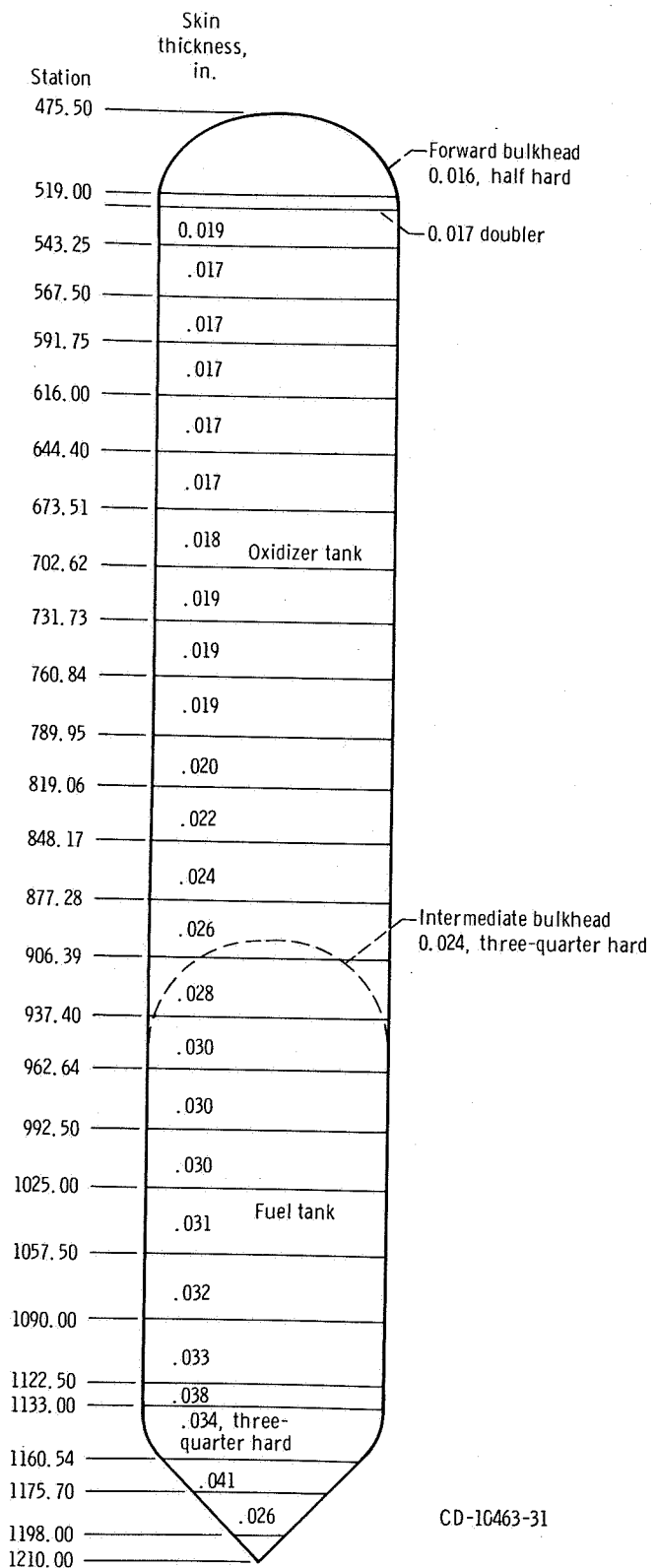
(b) AC-16 (OAO-II) mission

Flight event	Accelerometer location									
	Centaur station 68 (+x axis); frequency response, 2100 Hz (amplifier filter)			Centaur station 85						
				+y axis	+x axis	-y axis	+y axis	-y axis	-x axis	
	Accelerator system response limited to -									
	Analysis band, Hz			100 Hz			70 Hz			
	10 to 330	10 to 790		Telemetry channel filter frequency limited to -						
				110 Hz	160 Hz	220 Hz	330 Hz	450 Hz	-----	
Accelerometer range, g's										
	±10	±20		-2.88 to 8.88		-3.00 to 9.00		-1.17 to 1.17	-1.16 to 1.17	-1.17 to 1.17
Launch:										
Acceleration, g's	2.5 (rms)	2.6 (rms)	2.6 (rms)	-----	-----	-----	-----	-----	-----	-----
Frequency, Hz	6.1 310	6.5 280	8.9 280	1.5 100 to 600	1.3 100 to 600	1.4 100 to 600	0.7 100 to 600	0.6 100 to 600	0.5 100 to 600	0.5 100 to 600
Booster engine cutoff:										
Acceleration, g's	1.0	(c)	(c)	0.65	0.65	0.60	0.51	0.56	0.56	0.56
Frequency, Hz	8 to 9	(c)	(c)	12	12	12	90	90	90	90
Booster jettison acceleration ^e , g's	0.5	(c)	(c)	0.2	0.2	0.2	0.36	0.25	0.22	0.22
Installation panel jettison:										
Acceleration, g's	11	24	24	1.7	1.5	1.3	0.43	0.35	0.45	0.45
Frequency, Hz	600 to 700	600 to 700	600 to 700	(e)	(e)	(e)	(e)	(e)	(e)	(e)
Sustainer engine cutoff:										
Acceleration, g's	(c)	(c)	(c)	0.1	0.8	0.1	0.8	0.16	0.14	0.36
Frequency, Hz	(c)	(c)	(c)	20	90	20	90	20	90	90
Atlas-Centaur separation acceleration ^e , g's	5.5	12	19	1.1	1.2	0.8	0.3	0.3	0.45	0.45
Main engine start:										
Acceleration, g's	(c)	(c)	(c)	0.11	0.11	0.11	0.11	0.14	0.11	0.11
Frequency, Hz	(c)	(c)	(c)	21	21	21	(e)	(e)	(e)	(e)
Nose fairing jettison acceleration ^e , g's	13	23	24	2.1	1.4	2.6	0.47	0.51	0.54	0.54
Main engine cutoff:										
Acceleration, g's	0.5	(c)	1.9	0.35	0.55	0.40	0.27	0.27	0.23	0.23
Frequency, Hz	320	(c)	(e)	(e)	(e)	(e)	(e)	(e)	(e)	(e)
Spacecraft separation:										
Acceleration, g's	12	(f)	(f)	2.6	1.4	2.1	1.0	1.0	0.5	0.5
Frequency, Hz	600 to 700	(f)	(f)	(e)	(e)	(e)	(e)	(e)	(e)	(e)

^cNo detectable response.

^eFrequency response at amplitude noted was ≥100 Hz and <1000 Hz.

^fInvalid data.



CD-10463-31

Figure VI-30. - Atlas propellant tanks, AC-16.

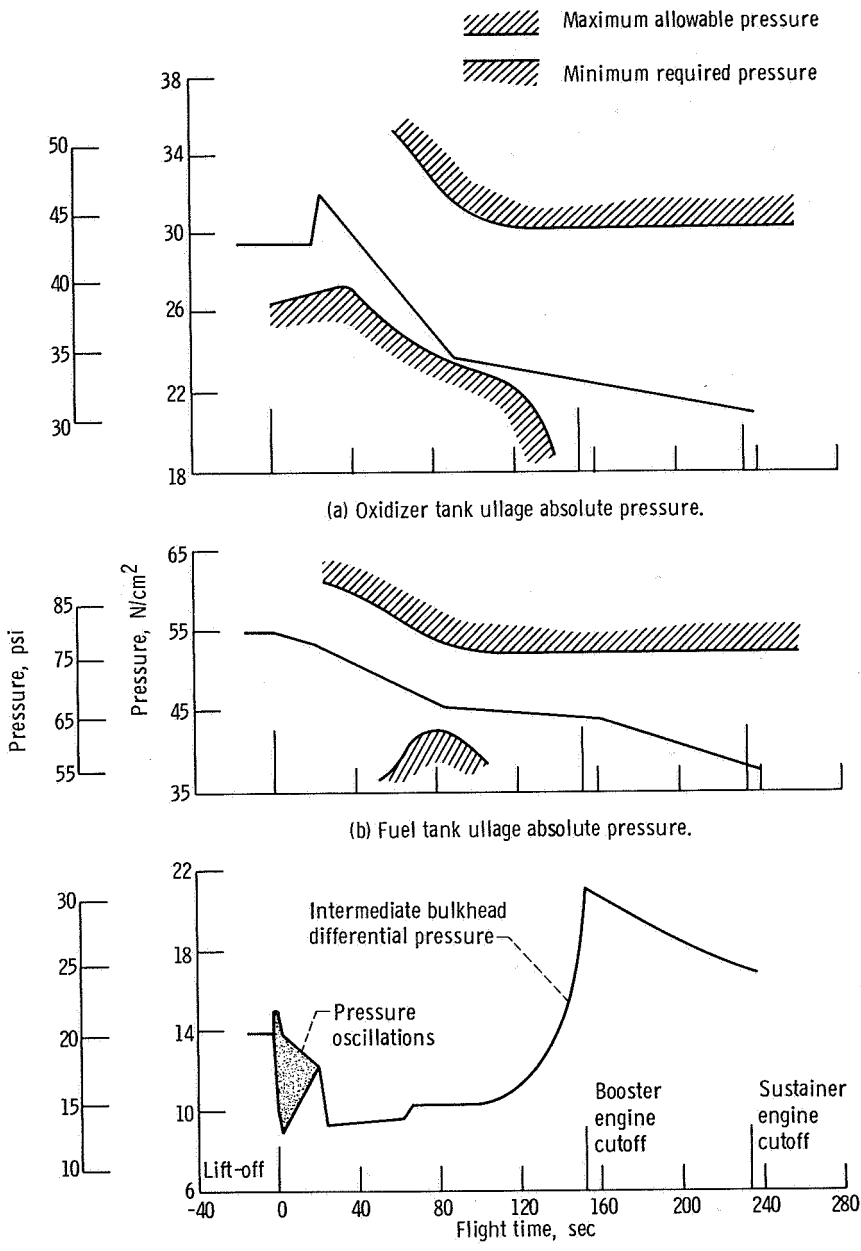


Figure VI-31. - Atlas fuel and oxidizer tank pressures, AC-16.

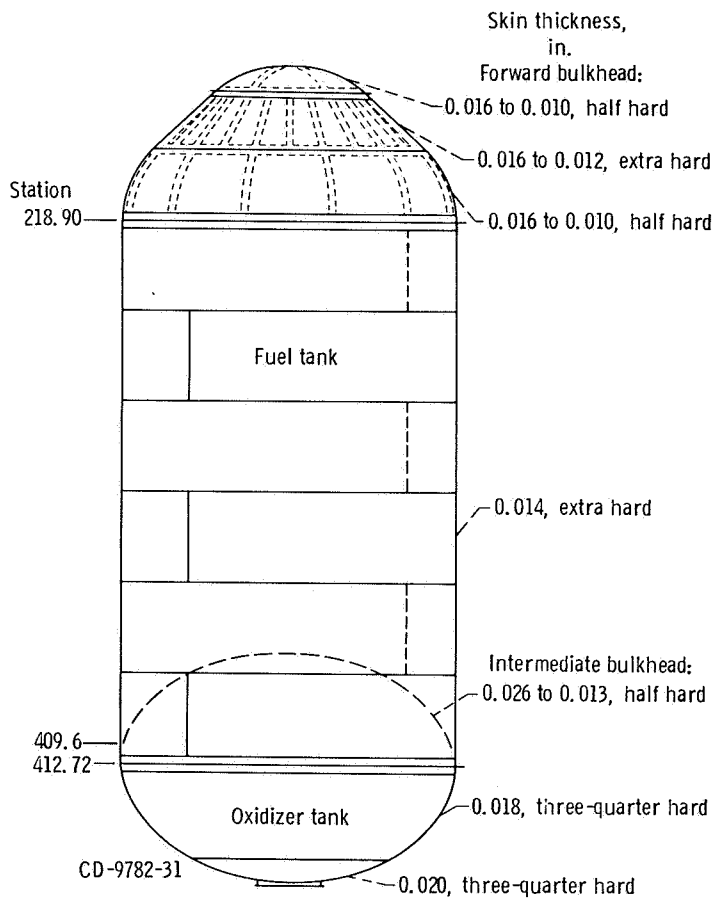


Figure VI-32. - Centaur propellant tanks, AC-16.
 (All material 301 stainless steel, of hardness indicated.)

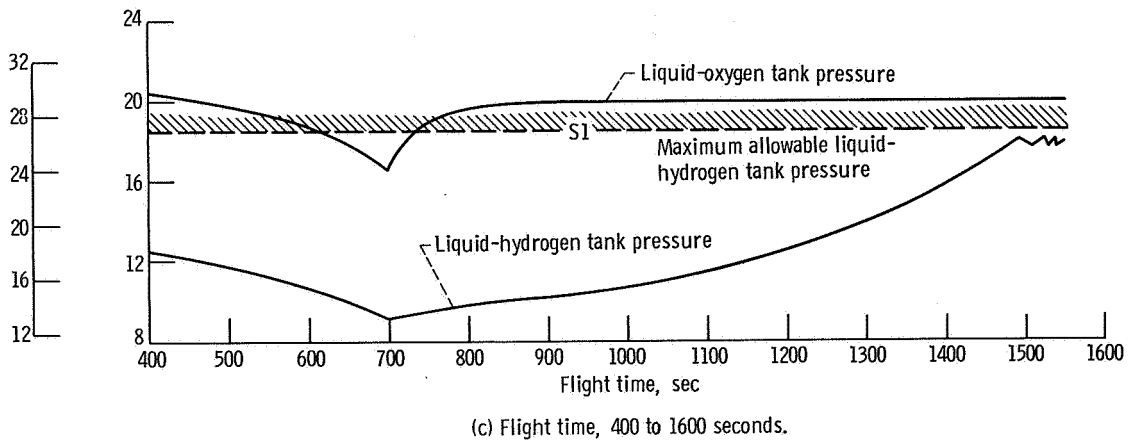
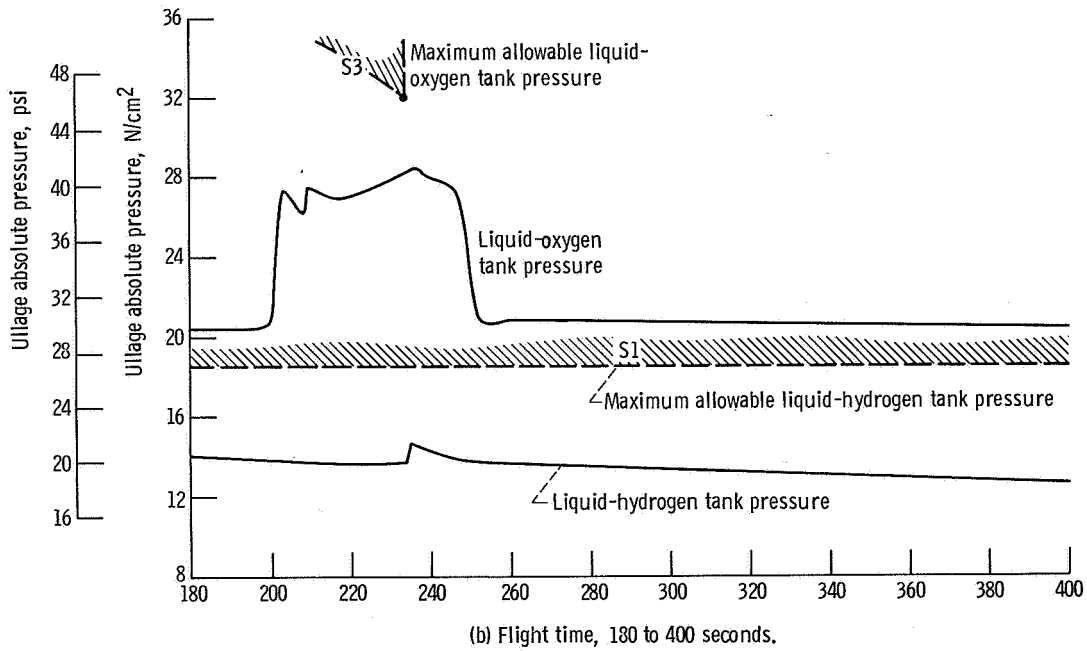
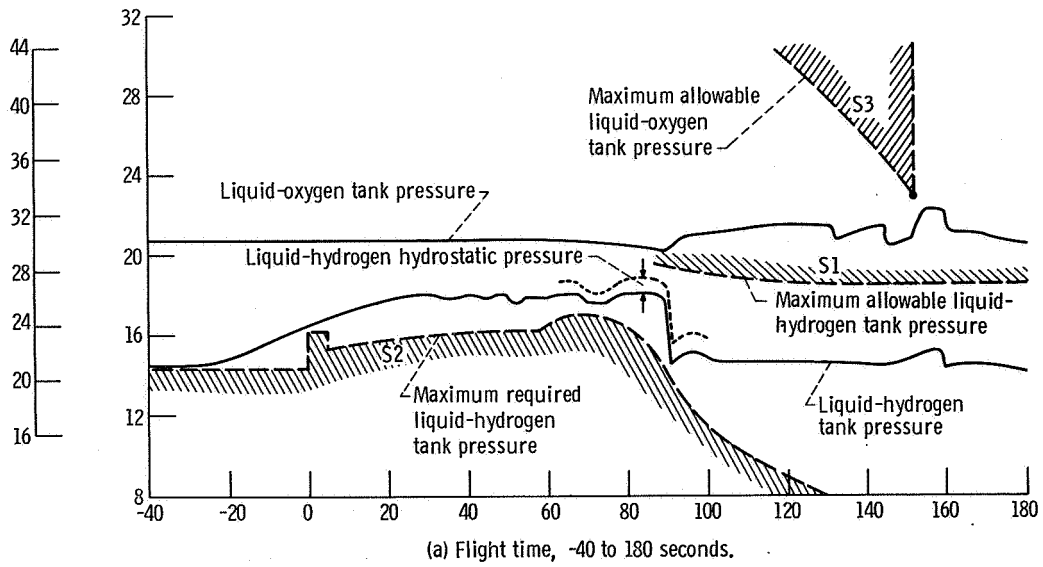


Figure VI-33. - Centaur fuel and oxidizer tank pressure, AC-16. S1, S2, etc., indicate tank structure areas which determine allowable tank pressure (see fig. VI-34).

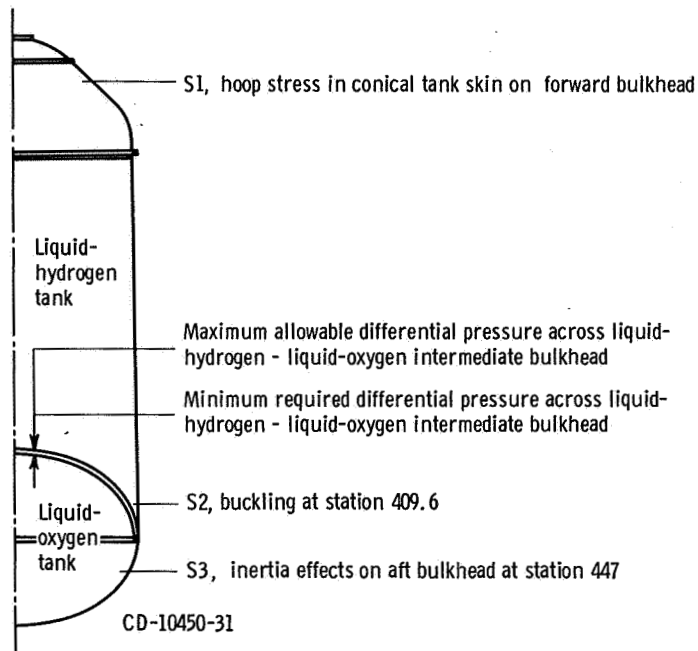


Figure VI-34. - Tank locations and criteria which determine allowable pressures, AC-16.

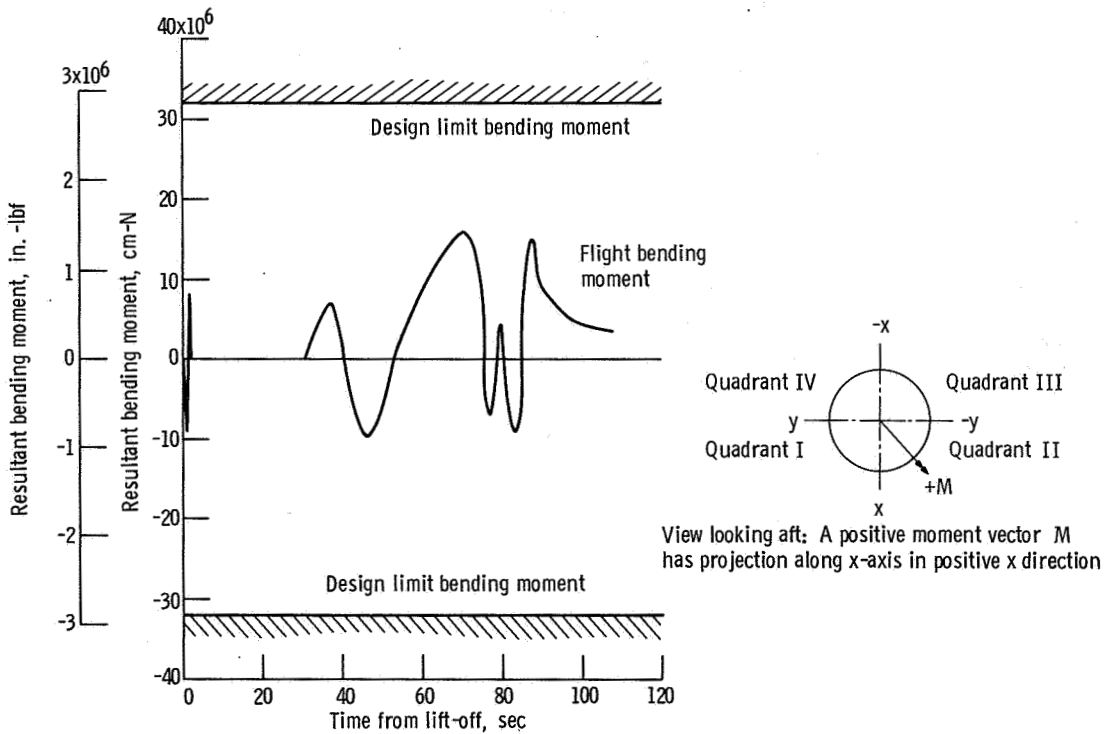


Figure VI-35. - Bending moment, fixed fairing at Centaur station 125, AC-16.

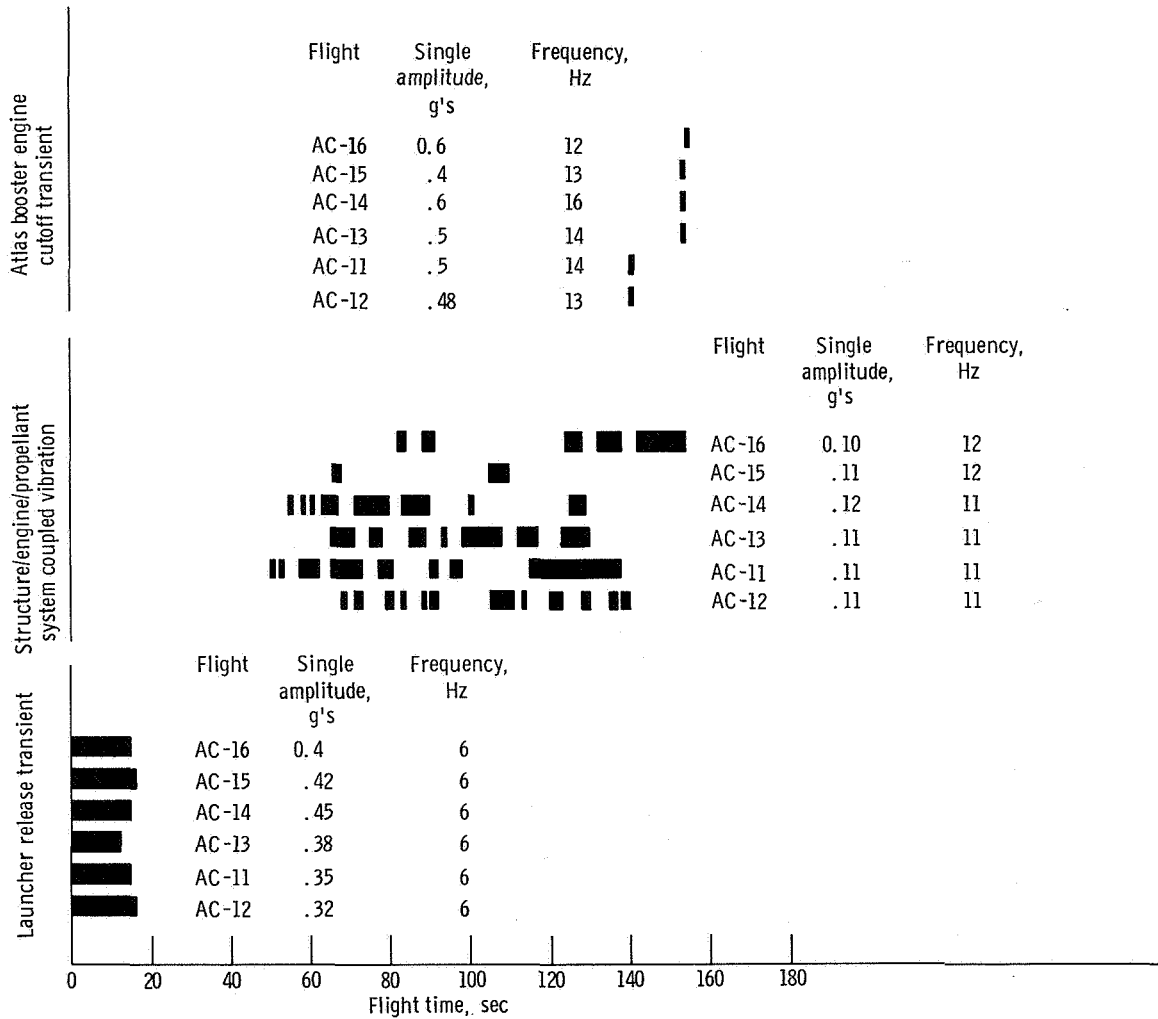


Figure VI-36. - Longitudinal vibrations for Atlas-Centaur flights.

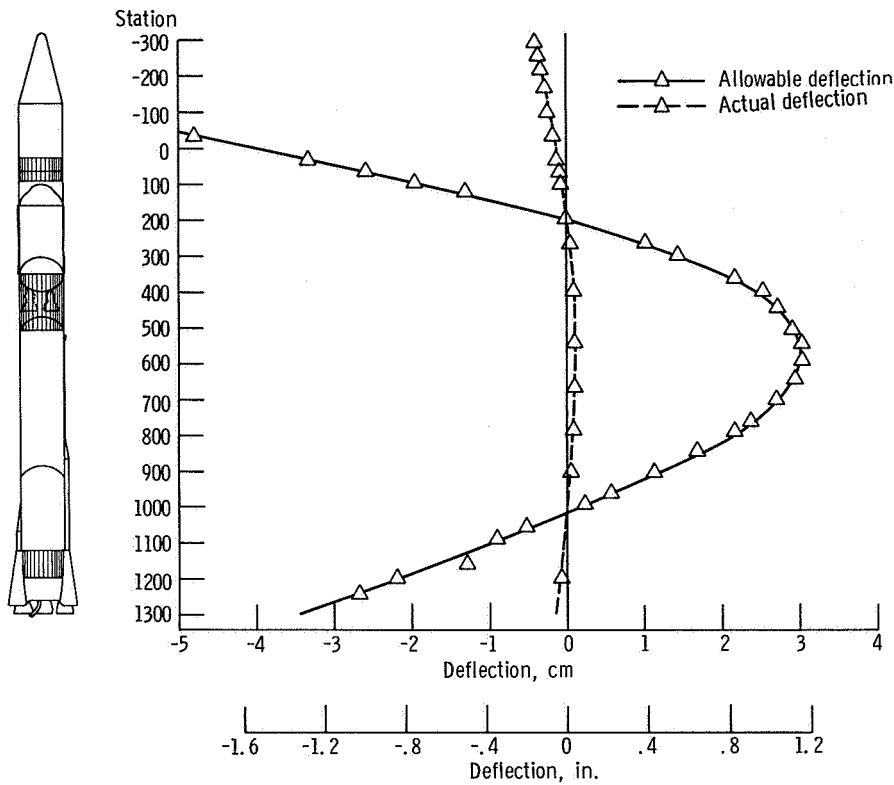


Figure VI-37. - Maximum pitch plane first-bending-mode amplitudes at T + 132 seconds, AC-16.

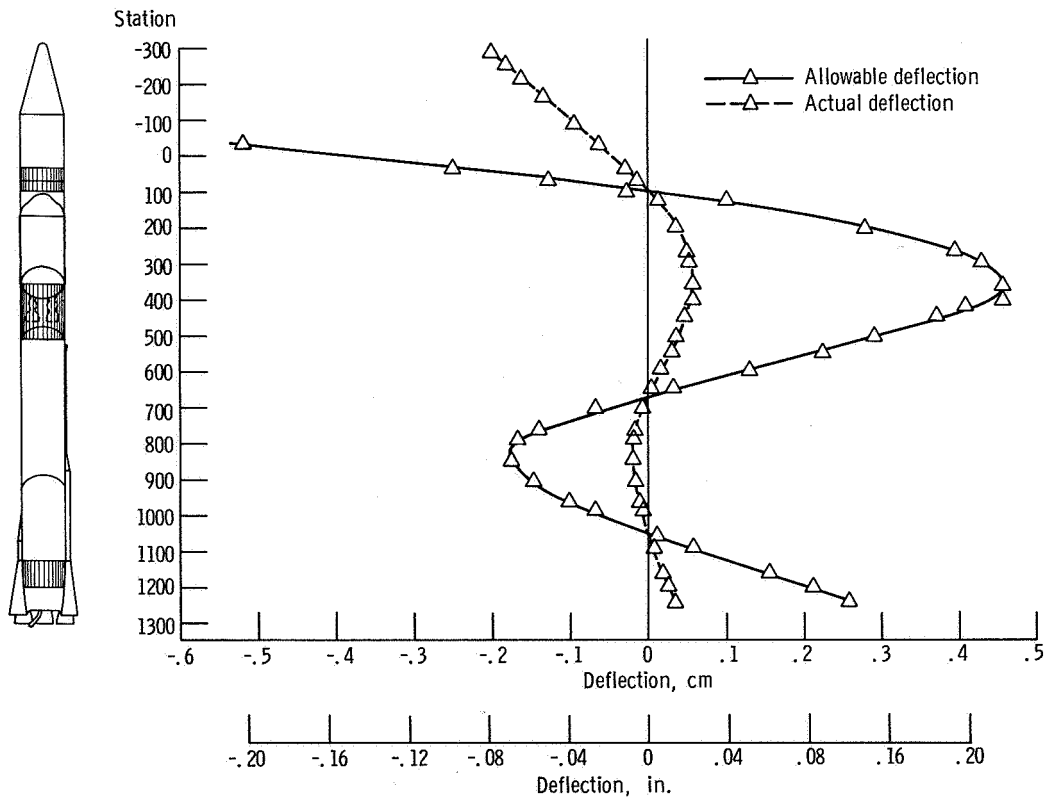


Figure VI-38. - Maximum pitch plane second-bending-mode amplitudes at T + 42 seconds, AC-16.

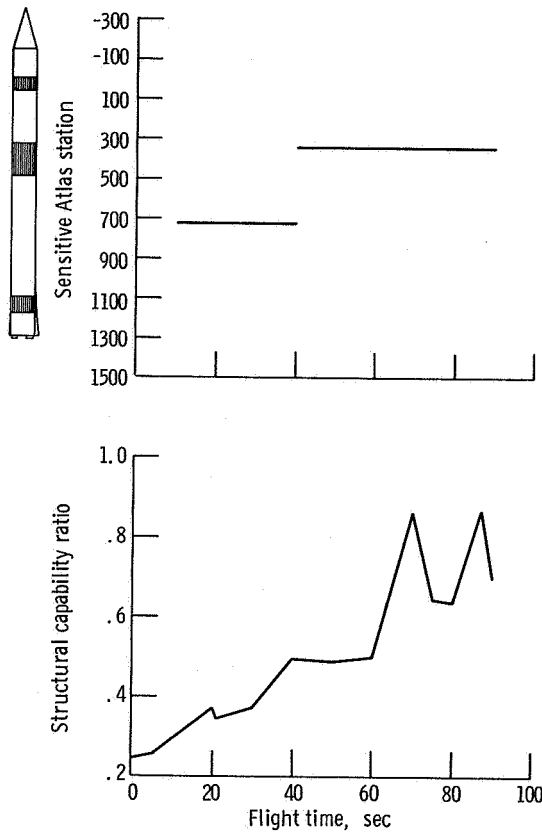


Figure VI-39. - Maximum predicted structural capability ratio, (total equivalent predicted bending moment)/(bending moment allowable), and sensitive station, AC-16.

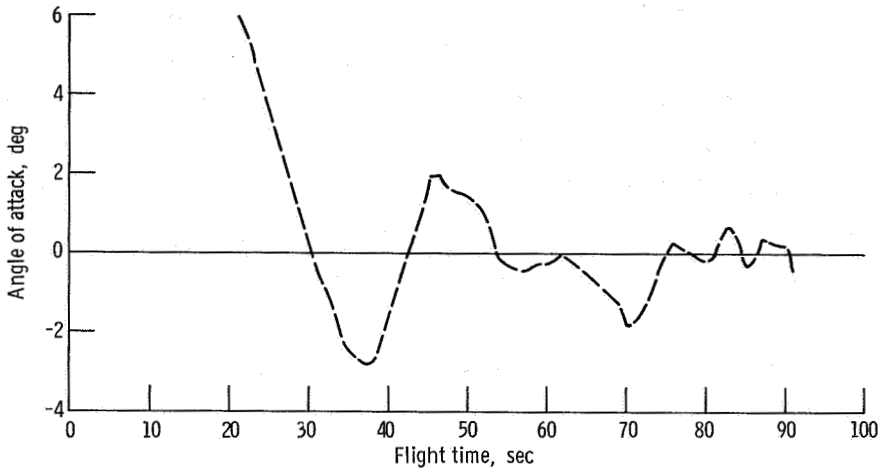


Figure VI-40. - Predicted pitch angles of attack, AC-16.

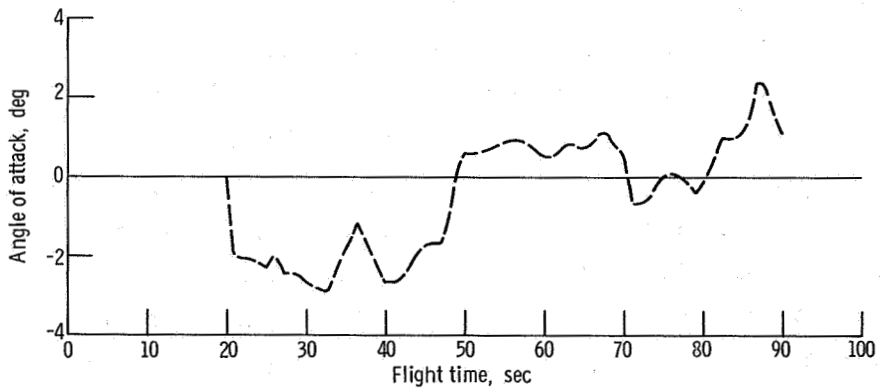


Figure VI-41. - Predicted yaw angles of attack, AC-16.

SEPARATION SYSTEMS

by Thomas L. Seeholzer, Charles W. Eastwood, and William M. Prati

Stage Separation

System description. - The Atlas-Centaur vehicle requires systems for Atlas booster engine section separation, Atlas-Centaur separation, and Centaur-spacecraft separation.

The Atlas booster engine stage separation system consists of 10 helium-gas-operated latch mechanisms. These latches (figs. VI-42 and VI-43) are located circumferentially around the Atlas aft bulkhead thrust ring at station 1133. An explosive valve supplies 2068-newton-per-square-centimeter (3000-psig) helium through the distribution manifold. When actuated, this results in the disengagement of the booster engine from the Atlas vehicle. Two tracks which extend from the thrust ring (fig. VI-44) are used to guide the booster engine section as it separates from the Atlas.

Atlas-Centaur staging systems (fig. VI-45) consist of a flexible, linear, shaped charge mounted circumferentially which severs the forward end of the interstage adapter at station 413; separation force is provided by eight retrorockets mounted on the aft end of the Atlas.

The OAO-II spacecraft is separated from Centaur by release of a four-segment band that clamps the spacecraft to the payload adapter. Release of the segmented band is accomplished by activation of four pyrotechnically operated latches. Separation force is provided by four mechanical spring assemblies, each having an 11.9-centimeter (4.7-in.) stroke, mounted on the payload adapter (fig. VI-46).

System performance. - Atlas booster engine section staging occurred 3 seconds after booster engine cutoff. This event was verified by data from instrumentation on the B-1 pitch actuator and from the vehicle axial (fine) accelerometer.

Atlas-Centaur staging was initiated at $T + 236.4$ seconds by the firing of the shaped charge which severed the interstage adapter at station 413. The eight retrorockets, mounted around the aft end of the Atlas, fired 0.1 second later to decelerate the Atlas and provide separation from the Centaur. Accelerometer and other data indicated that all eight retrorockets functioned as expected. Figure VI-47 shows the separation distance as a function of time after shaped-charge firing between the Atlas and the Centaur vehicle.

The yaw displacement gyros indicated that the Atlas rotated 0.39° about the yaw axis at the time the forward end of the interstage adapter cleared the Centaur engine nozzles. This resulted in a clearance loss in the minus yaw direction of 9.9 centimeter (3.9 in.) (fig. VI-47). The pitch rate gyros indicated 0.09° rotation about the pitch axis at the

time the interstage adapter cleared the Centaur engine nozzles. This resulted in a clearance loss in the minus pitch direction of 2.3 centimeters (0.9 in.) (fig. VI-47). The resultant pitch and yaw clearance losses decreased the clearance (shown pictorially in fig VI-45) between the interstage adapter and Centaur engine nozzles from 27.9 to 24.1 centimeters (11 to 9.5 in.).

The latch pyrotechnics on the spacecraft clamping band were fired at T + 748.3 seconds, and the spacecraft separated from the Centaur vehicle.

Jettisonable Structures

System description. - The Atlas-Centaur vehicle jettisonable structures consists of hydrogen tank insulation panels, a nose fairing, and related separation systems.

The hydrogen tank insulation is made up of four polyurethane-foam-filled fiber glass honeycomb panels bolted together along the longitudinal axis to form a cylindrical cover around the Centaur tank. The panels are bolted at their aft end to a support on the Centaur vehicle. At the forward end, a circumferential Tedlar and fiber glass laminated cloth forms a seal between the panels and the base of the nose fairing at station 219. Separation of the four insulation panels is accomplished by firing the flexible, linear, shaped charges located at the forward, aft, and longitudinal seams. Immediately following shaped-charge firing, the panels rotate at their aft end about hinge points (fig. VI-48) because of the preload hoop tension, the center-of-gravity offset, and the in-flight residual purge pressure. The panels jettison free of the Centaur vehicle after approximately 45° of panel rotation on the hinge pins.

The vehicle nose fairing was a 3.05-meter - (10-ft-) diameter assembly approximately 12.2 meters (40 ft) long, consisting of a nonjettisonable section and a jettisonable section. The nonjettisonable section was composed of a fiber glass cylindrical barrel subassembly 1.83 meters (6 ft) long mounted on the forward flange of the Centaur tank and a metallic cylindrical fixed fairing subassembly 68.6 centimeters (27 in.) long bolted to the forward end of the barrel section. The jettisonable section consists of a metallic cylindrical split fairing subassembly 91.4 centimeters (36 in.) long bolted to a fiber glass cylindrical-to-conical configuration nose cone subassembly 8.84 meters (29 ft) long. This jettisonable section was assembled from two longitudinal halves joined by latch mechanisms. Each longitudinal half of the jettisonable section was attached to the fixed fairing subassembly with two hinges (fig. VI-49). The fairing hinges were each instrumented with biaxial strain gages (fig. VI-50) for jettison load measurements. Sheet cork on the exterior of the fiber glass section of the jettisonable nose fairing provided environmental protection to the spacecraft compartment and limited the fairing temperature to assure structural integrity. Separation of the nose

fairing halves was accomplished by the firing of 10 pyrotechnically operated release latches along the split line and six release latches at the aft circumferential connection. Forces necessary to accomplish fairing jettison were applied by two preloaded compression spring assemblies mounted in the forward end, one in each fairing half. Upon release of the separation latches, the springs imparted the initial force to cause the fairing halves to pivot on their hinges. Each fairing half was free to leave the hinges after 30° of rotation (fig. VI-51).

System performance. - Flight data indicated that the four insulation panels were jettisoned satisfactorily. Insulation panel jettison sequence was commanded at T + 196.803 seconds. Data from axial accelerometers located on the spacecraft adapter indicated that the flexible, linear, shaped charges fired at T + 196.830 seconds. Event time data were provided by breakwire transducers to indicate 35° rotation of the panels. These breakwire transducers were attached to one hinge arm of each panel (fig. VI-52). Since these data were monitored on commutated channels, the panel 35° positive event times in the following table are mean times:

Panel location, quadrant	Instrumented hinge arm, quadrant	Event mean time, sec
I-II	I	T + 197.288
II-III	III	T + 197.394
III-IV	III	T + 197.296
IV-I	I	T + 197.348

Average angular velocities of the panels, assuming first motion at shaped-charge firing, were determined from the mean times of the 35° position. Panel velocities are compared in the following table with values from three previous flights:

[Minimum allowable rotation velocity, 40 deg/sec.]

Panel location, quadrant	Average rotation velocities from shaped-charge firing to mean time of 35° position, deg/sec			
	AC-16	AC-13	AC-14	AC-15
I-II	76.5	83.8	82.6	87.5
II-III	62.1	83.8	76.5	77.5
III-IV	75.2	82.6	84.3	82.5
IV-I	67.6	79.4	78.0	76.5

The rate for each panel was 10 to 20 percent lower than that observed on earlier flights. This was due in part to the lower jettison force resulting from a lower axial acceleration of the vehicle at panel jettison. A slightly lower fuel tank pressure at the event time resulted in a lower panel hoop tension and thereby also contributed to a lower jettison force. However, this combined force reduction did not account for the full difference in rotational rates. Another possible cause, and probably the major contributor, was variation within the allowed limits for panel installation pretension. The observed velocities were, however, considered to be well within design limits. Vehicle rates and dynamics at the event time indicated a completely satisfactory panel jettison sequence.

The nose fairing was jettisoned satisfactorily following issuance of the jettison command at T + 257.6 seconds. The pyrotechnically actuated unlatching mechanisms fired at T + 257.983 seconds and permitted the jettison springs to start rotation of the fairing halves. The times that fairing halves rotated 13.5°, 15°, and 45° are shown in the following table:

Fairing half	Angle of fairing rotation, deg		
	13.5	15	45
	Nose fairing rotation event time, sec		
+Y (without cap)	T + 258.494	T + 258.656	T + 259.628
-Y (with cap)	T + 258.494	T + 258.622	T + 259.627

The elapsed times of the fairing rotation events as determined from the flight data compared very well with data from the nose fairing jettison ground tests. These tests were full-scale, jettison system functional performance tests conducted at simulated altitude; the 1-g earth gravitational field approximated the vehicle longitudinal acceleration of 0.8 g expected at the time of nose fairing jettison. Comparable elapsed times of fairing rotation positions during flight and during ground test are summarized in the following table:

Fairing jettison event	Elapsed time from latch pyrotechnic firing to nose fairing rotation position, sec			
	-Y fairing half (with cap)		+Y fairing half (without cap)	
	AC-16	Test	AC-16	Test
Unlatch firing	0	0	0	0
13.5° Rotation	.511	.585	.511	.579
15° Rotation	.639	.723	.673	.691
45° Rotation	1.644	1.667	1.645	1.660
Last detected hinge load	2.240	2.180	2.135	2.130

The strain gage flight data indicated that the hinge loads were as predicted and had close similarity to the fairing jettison test data.

The +Y fairing (without cap) commenced a buildup of hinge loads 0.025 seconds after fairing latch pyrotechnic firing. Hinge 1 reached a maximum axial compressive loading of 4670 newtons (1050 lbf) at latch firing plus 0.072 second. Hinge 2 experienced 6894 newtons (1550 lbf) of axial compressive load at latch firing plus 0.128 second. The loading of hinges 1 and 2 then went out of phase, indicating rocking of the fairing half on the hinges. This rocking motion was at approximately 2 hertz and continued with decreasing magnitude until separation of the hinge at latch pyrotechnic firing plus 2.13 seconds. The out-of-phase loading on the hinges is shown in figure VI-53. Oscillations at a frequency of 25 hertz were evident on both hinges for the first 1.5 seconds of rotation. Neither hinge experienced any axial tension loads, but the loading on both hinges decreased to zero several times as a result of the rocking action. Radial loads on the +Y fairing hinges indicated the rocking effect also. Maximum radial loads on both hinges were always less than 2224 newtons (500 lbf).

On the -Y fairing (with cap), hinge 4 began to experience an axial compressive load at latch firing plus 0.025 second. Oscillations at a frequency of 20 hertz were evident for 0.5 second of rotation. A maximum axial load of 9341 newtons (2100 lbf) occurred at latch pyrotechnic firing plus 0.350 second.

Hinge 3 had essentially no axial load buildup for 0.55 second of fairing rotation. The data indicated that the -Y fairing also rocked on the hinges at a frequency of 2 hertz from first rotation to hinge separation at latch pyrotechnic firing plus 2.24 seconds. Oscillations at a frequency of 25 hertz also were evident on this fairing. The maximum axial compressive load on hinge 3 was 4893 newtons (1100 lbf) at 0.605 second after latch pyrotechnic firing. This hinge did experience some small axial tension loads which did not exceed 445 newtons (100 lbf). Hinge 4 axial loads did diminish to zero several times

but never went into tension from the rocking action. Radial loads on this fairing half also showed the rocking effect. On hinges 3 and 4 the radial loads were not over 2669 newtons (600 lbf) at any time.

Jettison of the fairing did result in some vehicle transients, principally roll oscillations. The rocking action of the fairing halves was in phase on opposite hinges and produced roll torques. This resulted in roll oscillations of approximately the same frequency and duration as the hinge load fluctuations, 2 hertz for 2 seconds.

The hinge loads at nose fairing jettison during flight were well within the design limits and were similar to those generated in the ground jettison test as shown in the following table:

Type of load	Units	Maximum hinge loads at nose fairing jettison, AC-16							
		During flight ^a				During ground test ^b			
		Hinge							
		1	2	3	4	1	2	3	4
Maximum axial compression	N	4670	6894	4893	9341	6405	8006	5338	6316
	lbf	1050	1550	1100	2100	1440	1800	1200	1420
Maximum radial acting inboard	N	1801	1312	2513	1023	1334	2268	1557	1913
	lbf	405	295	565	230	300	510	350	430
Maximum radial acting outboard	N	1557	2068	1913	2291	2046	2180	1690	1824
	lbf	350	465	430	515	460	490	380	410
		Combined hinges, fairing half -							
		+Y		-Y		+Y		-Y	
Maximum axial compression	N	10 898		9118		12 677		11 565	
	lbf	2 450		2050		2 850		2 600	
Maximum radial acting inboard	N	1 957		3269		1 423		3 247	
	lbf	440		735		320		730	
Maximum radial acting outboard	N	2 669		2291		3 158		3 514	
	lbf	600		515		710		790	

^aOnly hinge 3 experienced axial tension loads; maximum value was 445 N (100 lbf).

^bThese values are the maximum values obtained during the series of three ground tests.

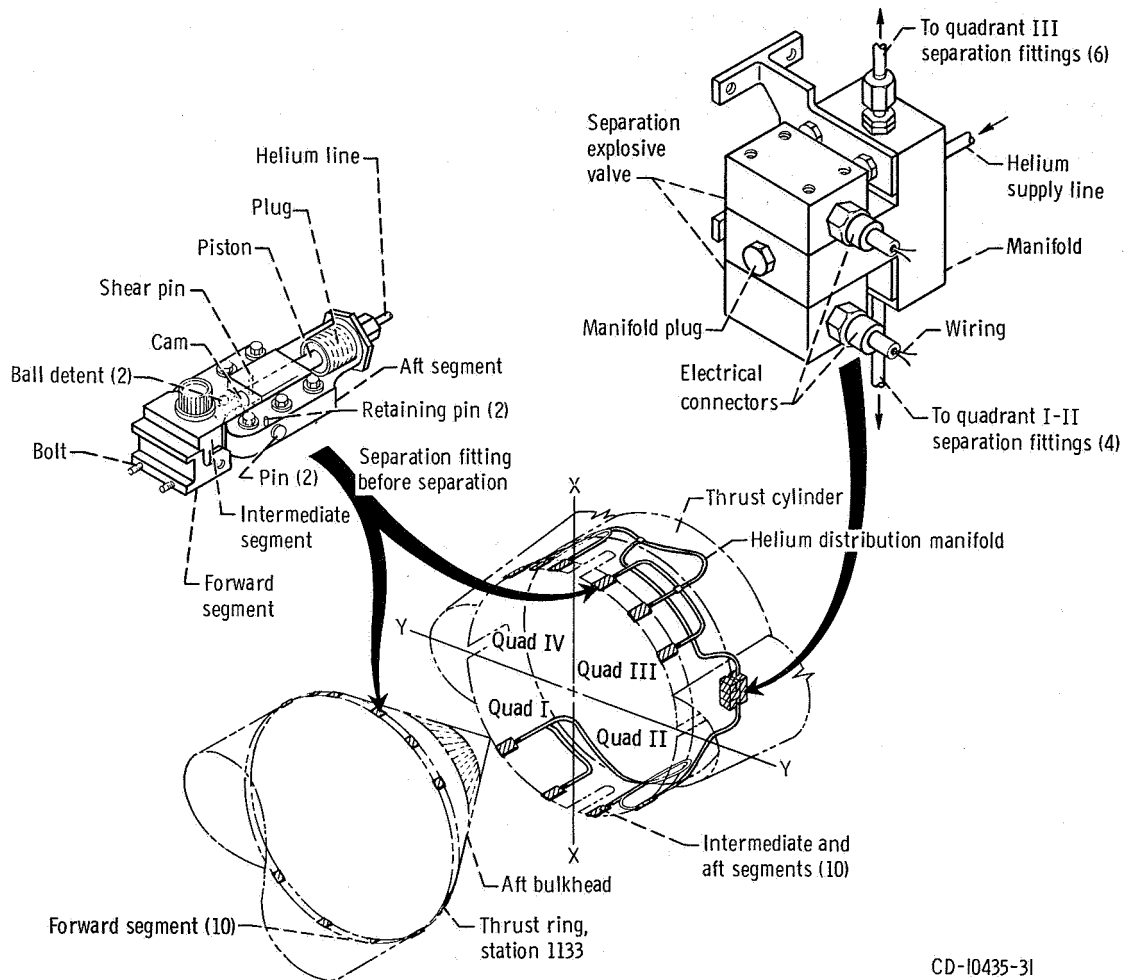


Figure VI-42. - Atlas booster engine section separation system details, AC-16.

CD-10435-31

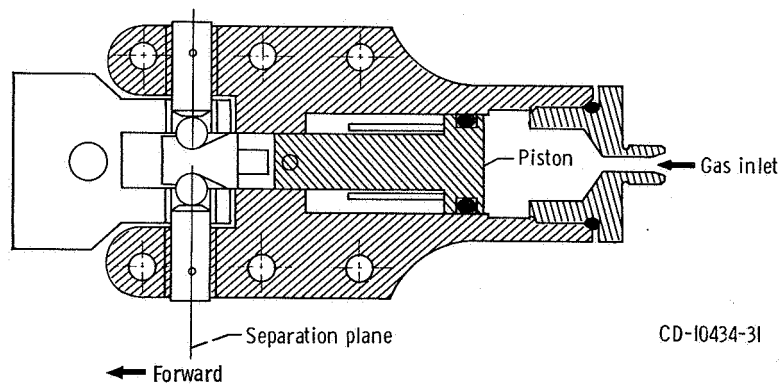


Figure VI-43. - Atlas booster engine section separation fitting, AC-16.

CD-10434-31

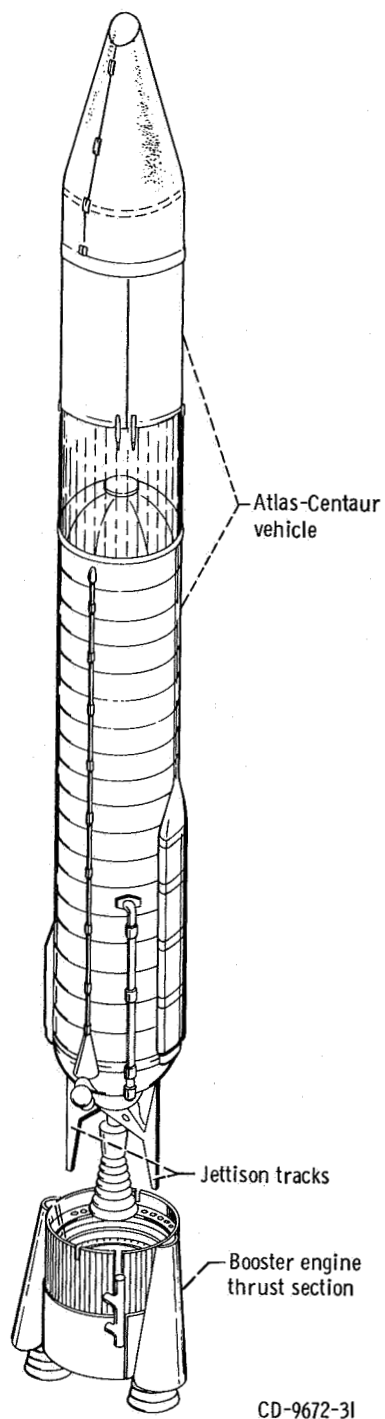
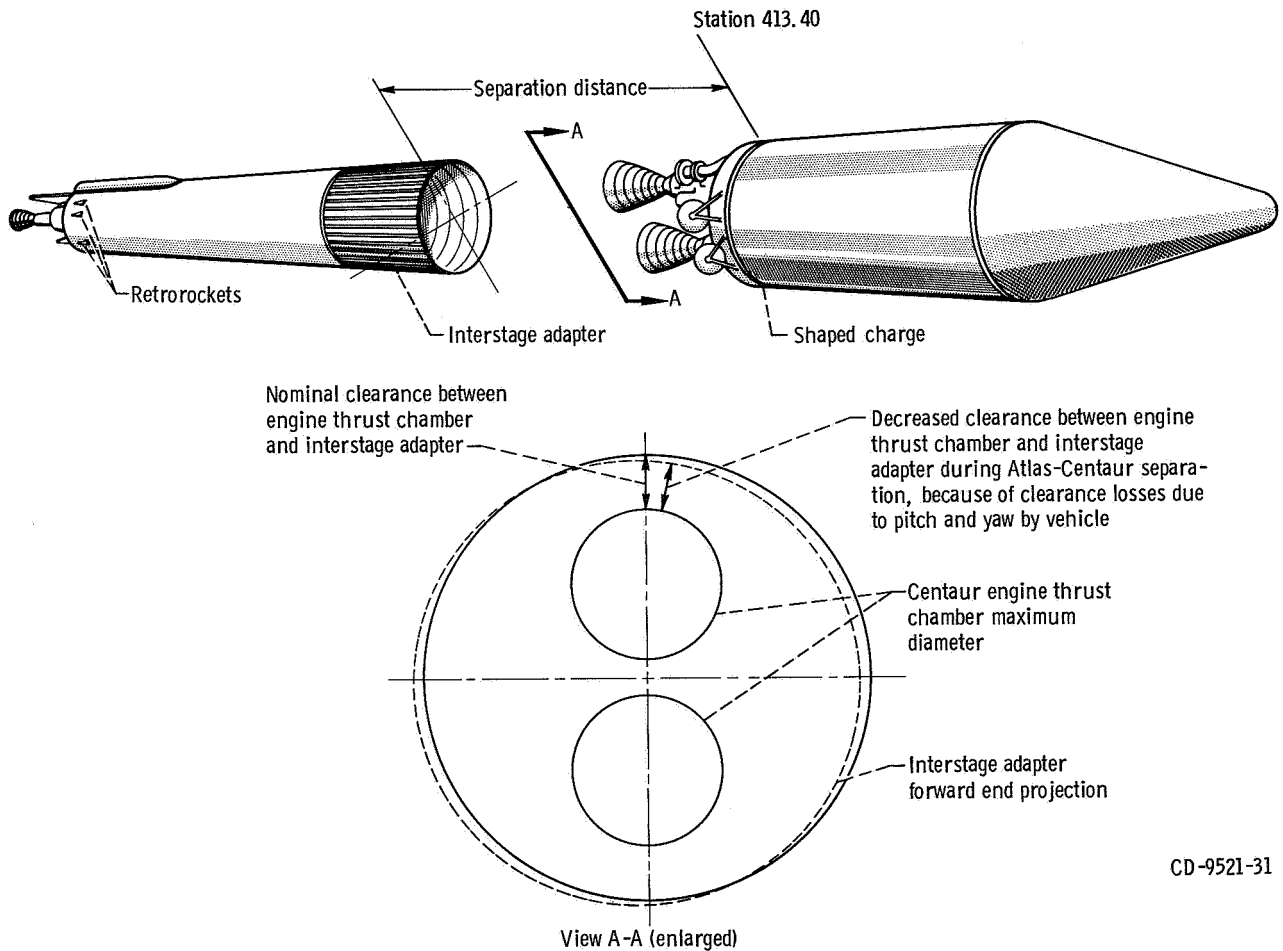


Figure VI-44. - Atlas booster engine section staging system, AC-16.



CD-9521-31

Figure VI-45. - Atlas-Centaur separation system, AC-16.

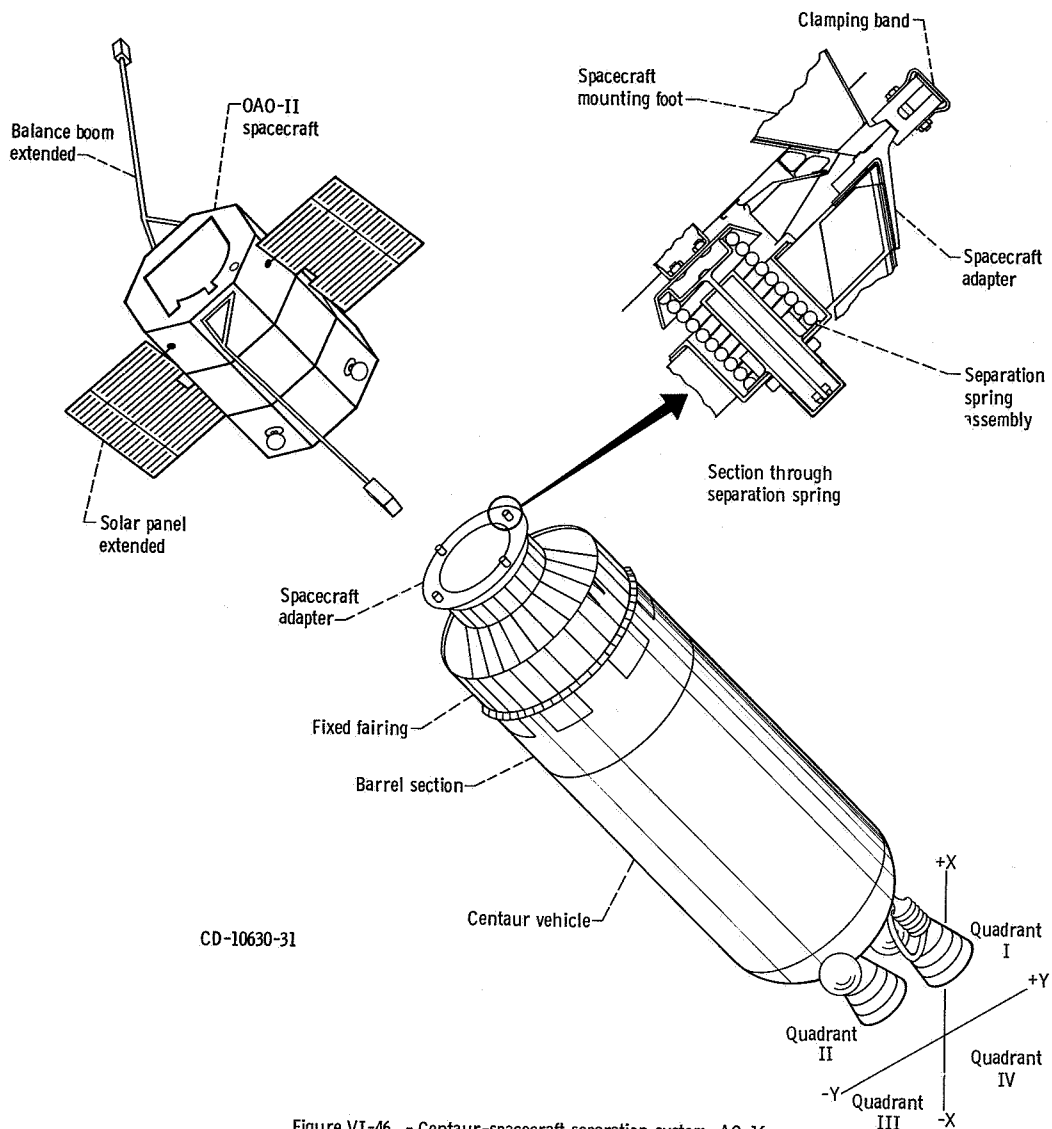


Figure VI-46. - Centaur-spacecraft separation system, AC-16.

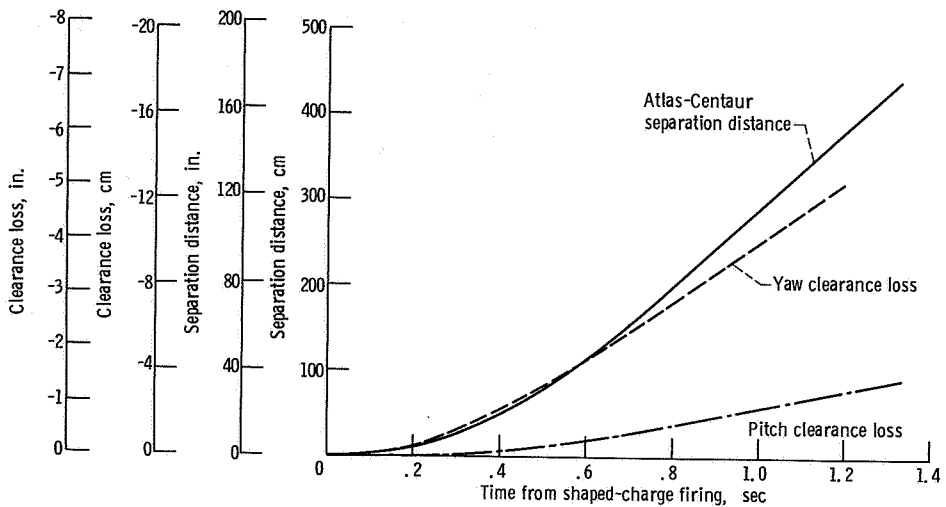


Figure VI-47. - Atlas-Centaur separation distances, AC-16. All clearance losses referenced to forward end of interstage adapter (station 413).

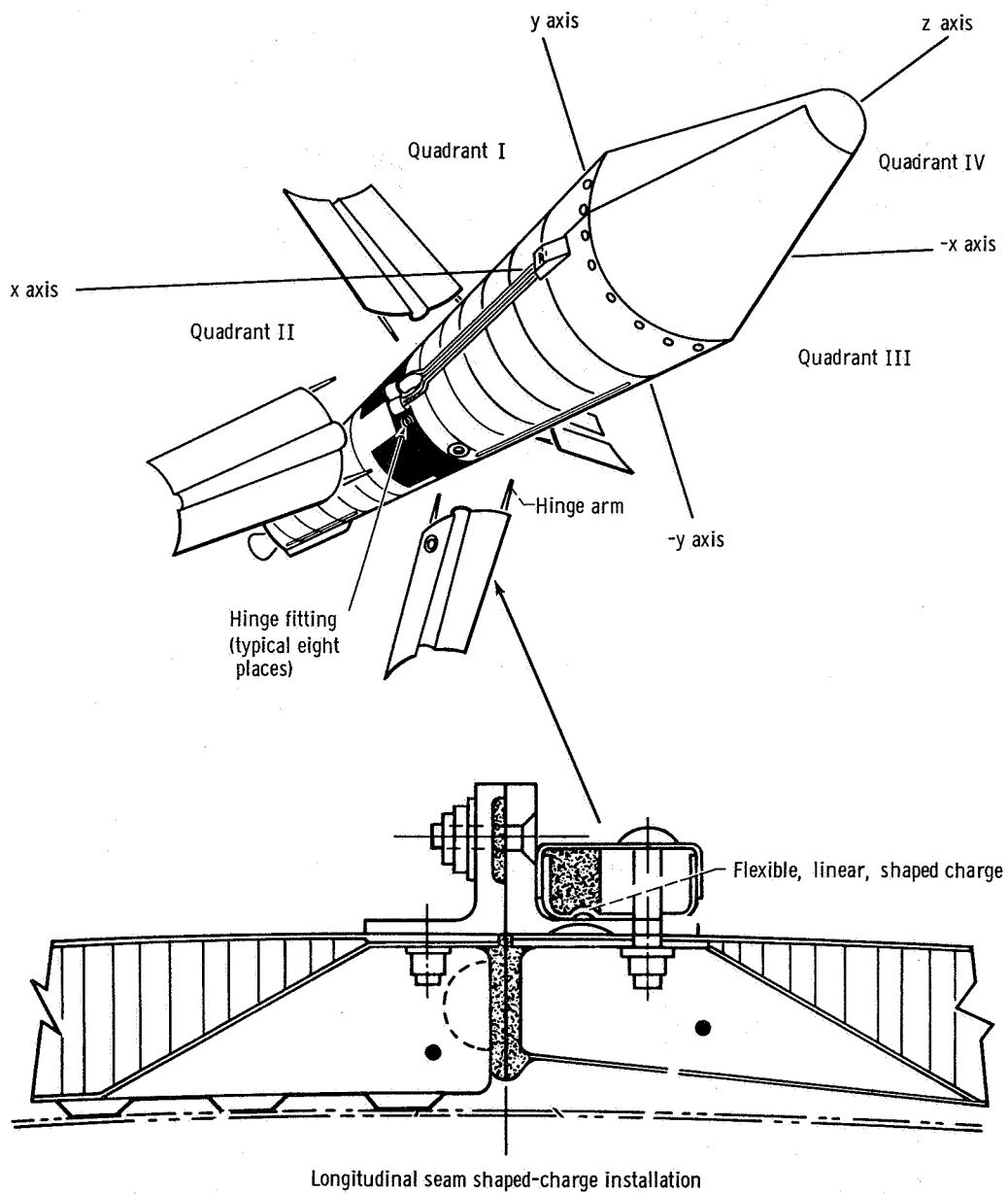


Figure VI-48. - Hydrogen tank insulation jettison system, AC-16.

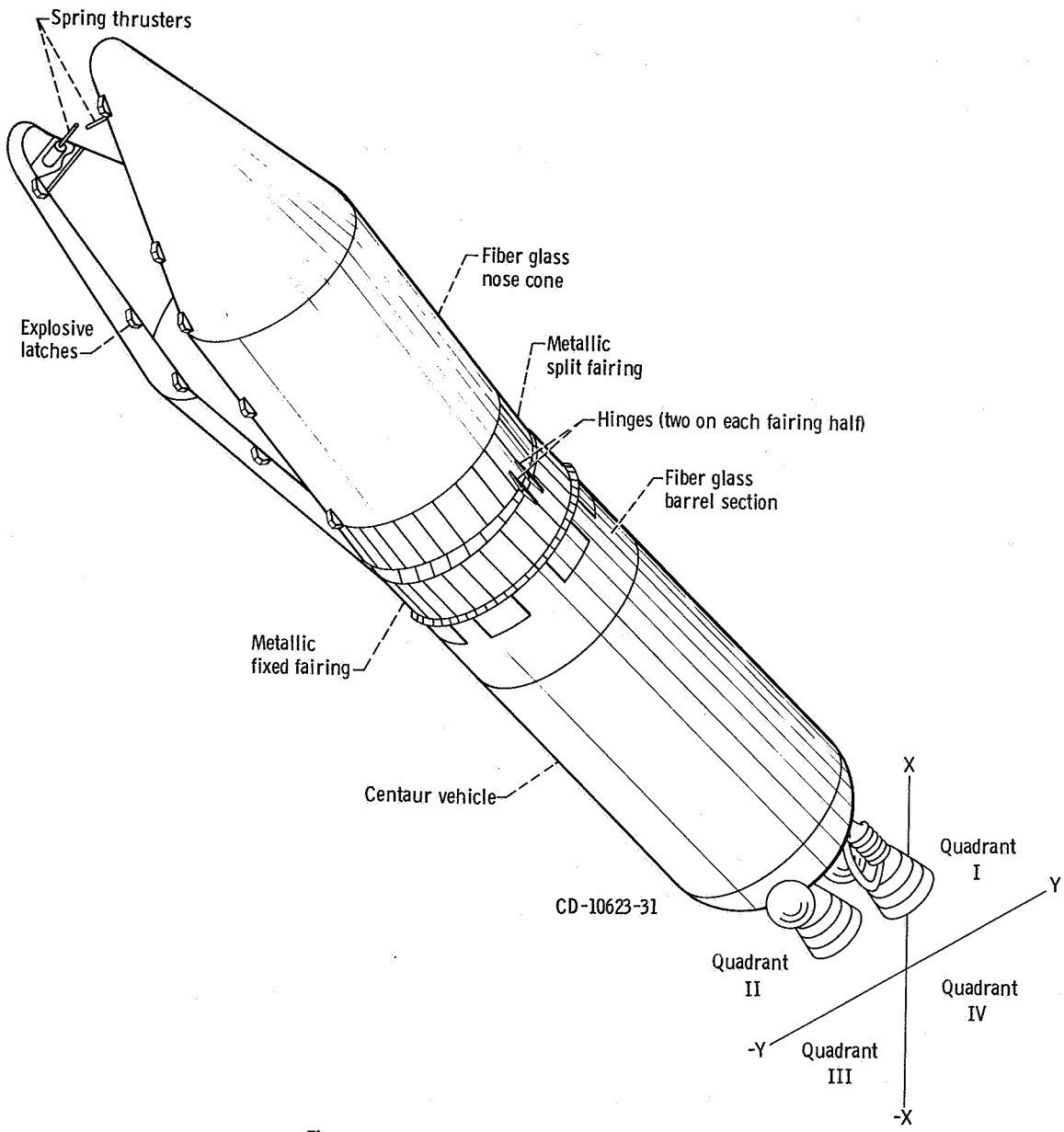
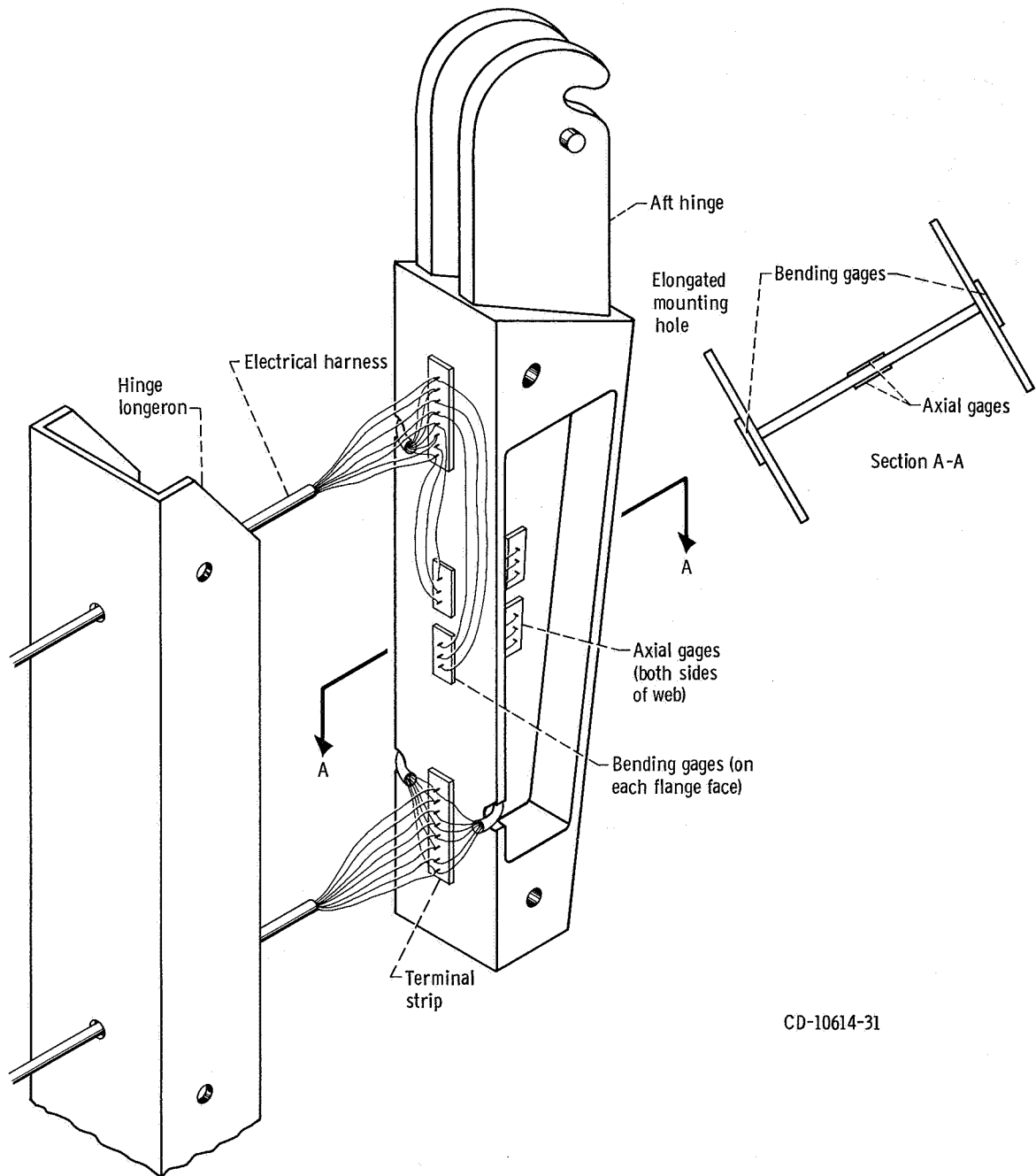
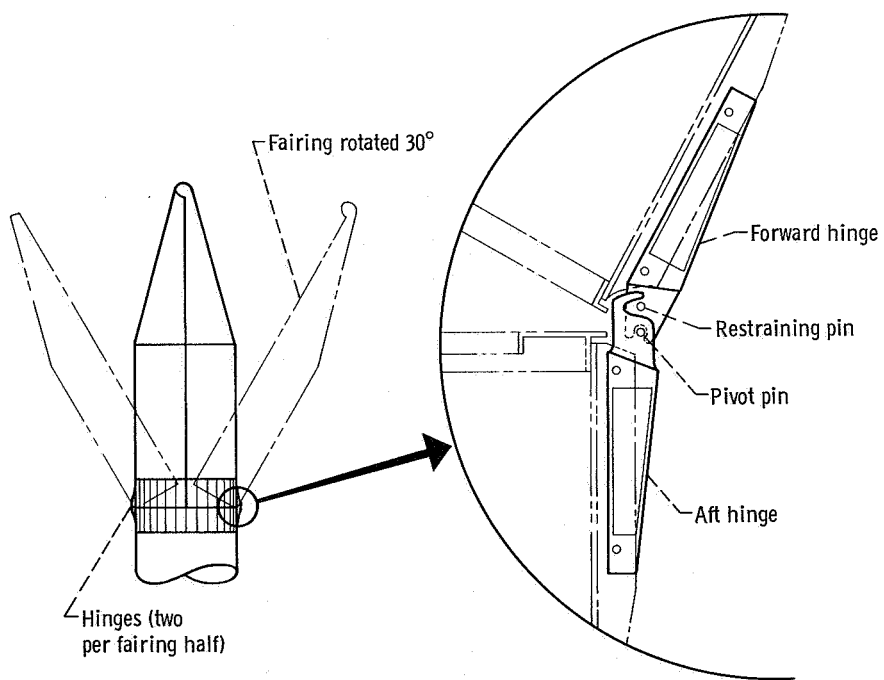


Figure VI-49. - Nose fairing jettison system, AC-16.



CD-10614-31

Figure VI-50. - Nose fairing hinge strain gages, AC-16. (Typical for four hinges.)



CD-10613-31

Figure VI-51. - Nose fairing hinges, AC-16.

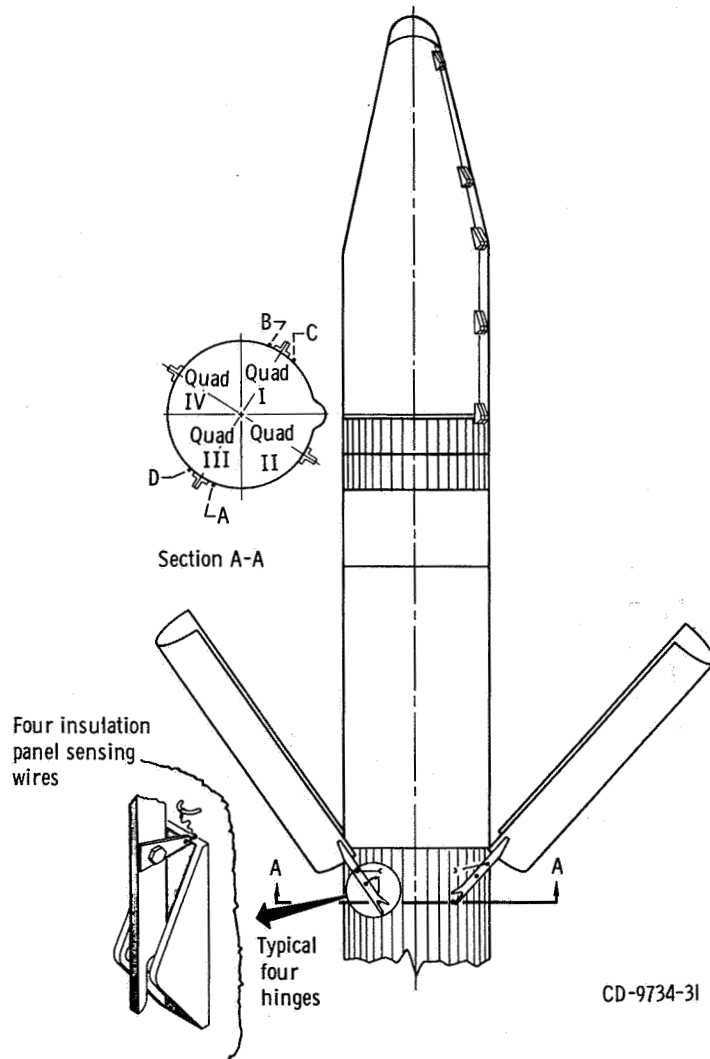
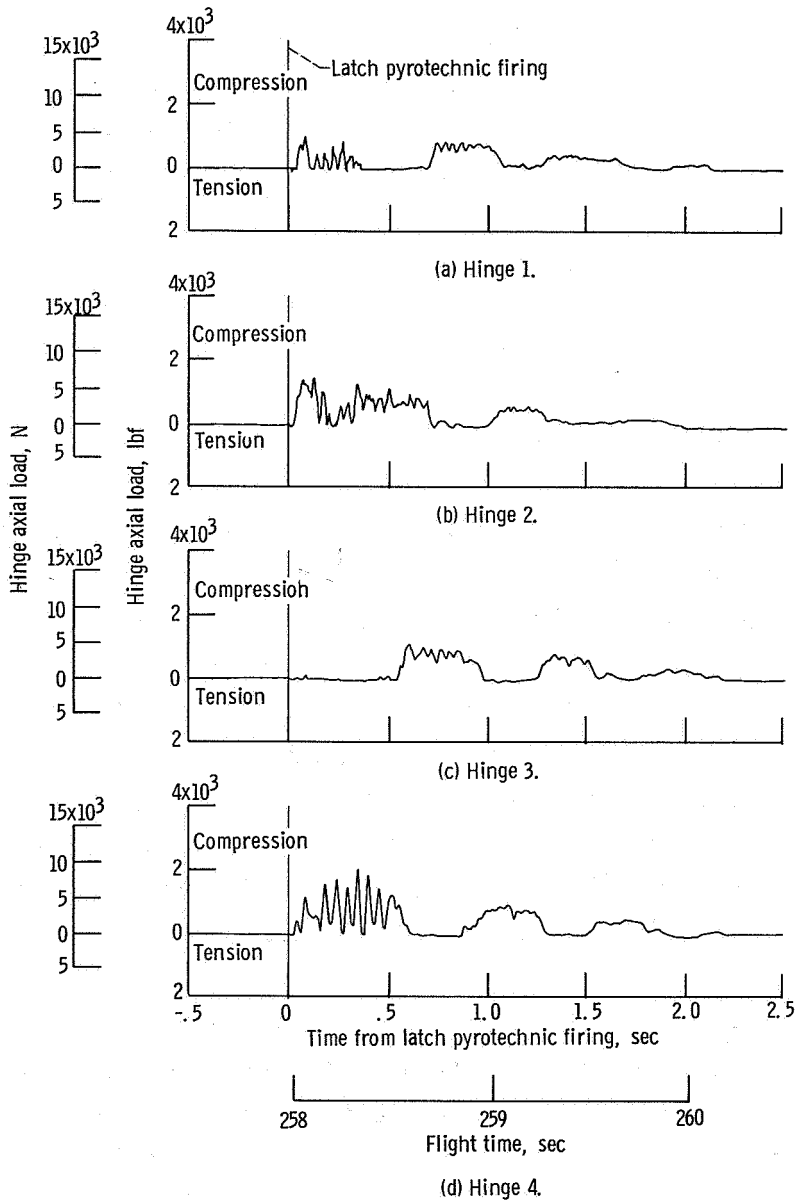
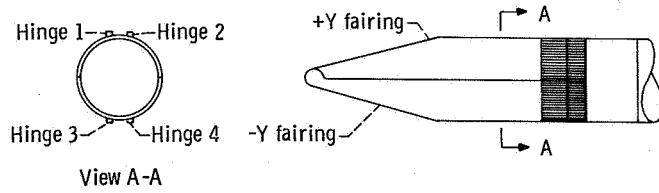


Figure VI-52. - Insulation panel breakwire locations, AC-16.



ELECTRICAL SYSTEMS

by John M. Bulloch and John B. Nechvatal

Power Sources and Distribution

System description - Atlas. - The power supply consists of a power changeover switch, one main battery, one telemetry battery, two independent range safety command (vehicle destruct) system batteries, and a three-phase 400-hertz rotary inverter.

System performance - Atlas. - Transfer of the Atlas electrical load from external to internal power was accomplished by the main power changeover switch at T - 2 minutes. Performance of the Atlas electrical system was normal throughout the flight. Voltages and current levels furnished to the dependent systems were within specification limits.

The Atlas main battery supplied the requirements of the user systems at normal levels (25 to 30 V). The battery voltage was 28.1 volts at lift-off and 28.4 volts at sustainer engine cutoff. This is a normal rise of voltage, and is caused by battery temperature increase.

The telemetry battery and the two range safety command batteries provided normal voltage levels throughout Atlas flight. The voltages at lift-off were 28.4 volts for the telemetry system, and 29.4 and 29.7 volts for the two range safety command systems.

The Atlas rotary inverter supplied 400-hertz power within specified voltages and frequency limits. The voltage at lift-off was 115.1 volts and decreased to 114.7 volts at the end of Atlas powered flight (234.5 sec). The inverter frequency at lift-off was 401.8 hertz and increased to 402.8 hertz by the end of Atlas flight. The gradual rise in frequency is typical of the Atlas inverter. The required frequency difference range of 1.3 to 3.7 hertz between the Atlas and Centaur inverter frequencies was properly maintained. Operation in this range prohibits the possibility of generating undesirable beat frequencies within the flight control system, thereby precluding the chance of resonant excitation of propellant "slosh" modes or natural frequencies of the vehicle structure.

System description - Centaur. - The electric power system consists of a power changeover switch, a main battery, two independent range safety command (vehicle destruct) batteries, two pyrotechnic system batteries, and a solid-state inverter supplying 400-hertz current to the guidance, flight control, and propellant utilization systems.

System performance - Centaur. - Performance of the Centaur electrical system was satisfactory throughout the flight. Transfer of the Centaur electric load from external power to the internal battery was accomplished at T - 4 minutes by the power change-

over switch in 250 milliseconds (specification value, 2.00 sec max.). The maximum voltage excursion at power transfer was 0.5 volt, which is considered negligible.

The main battery voltage at lift-off was 27.9 volts. It decreased to 27.2 volts at Centaur main engine start (T + 246.0 sec), and rose to a steady-state level of 28 volts during Centaur powered flight. Following main engine cutoff the voltage increased to 28.2 volts and remained constant throughout the coast phase. These values are consistent with normal battery regulation. The main battery voltage was 27.5 volts, with a sustained vehicle load of 50 amperes at the loss of telemetry data (T + 8100 sec). An approximate total of 115 ampere-hours had been expended from the battery. (Rated battery capacity is 100 A-hr.)

The flight current profile (fig. VI-54) was normal and correlated closely with tests prior to launch. At lift-off the current was 44 amperes, increasing to 61 amperes at Centaur engine start (T + 246.0 sec).

A series of current disturbances of 0.5 ampere peak-to-peak was observed, starting at T + 682.4 seconds. These small disturbances were not detrimental; their cause has not been determined. Simultaneous disturbances were also observed on the six spacecraft accelerometers at precisely the same time.

The voltages of the nose fairing pyrotechnic batteries were 34.85 and 34.9 volts at lift-off. These batteries had a higher capacity than those used in previous Centaur flights in order to meet the higher power requirements of the AC-16 nose fairing pyrotechnic system. Proper operation of the pyrotechnic system batteries and associated relays was verified by instrumentation and by the successful jettison of the insulation panels and the nose fairing.

Performance of the two range safety command system batteries was satisfactory. At lift-off the two battery voltages were 32.6 and 33.6 volts. The minimum specification limit is 30 volts.

The Centaur inverter operated satisfactorily throughout the flight. Telemetered voltage levels compared closely to values recorded during preflight testing. The inverter phase voltages at lift-off were as follows: Phase A, 115.3 volts; Phase B, 115.5 volts; and Phase C, 115.4 volts. Voltage changes during flight were small and well within expected values. Inverter frequency remained constant at 400.0 hertz throughout the flight. Inverter skin temperature was 304.2 K (88^o F) at lift-off and reached a high of 360 K (188^o F) by T + 8100 seconds.

Instrumentation and Telemetry

System description - Atlas. - The Atlas telemetry system (fig. VI-55) consists of a radiofrequency telemetry package, two antennas, a telemetry battery, and transducers.

It is a Pulse Amplitude Modulation/Frequency Modulation/Frequency Modulation (PAM/FM/FM) telemetry system and operates at a carrier frequency of 229.0 megahertz. The PAM technique used on all Atlas-Centaur commutated (sampled) channels makes possible a larger number of measurements on one subcarrier channel. This increases the data handling capability of the telemetry system. The FM/FM technique uses analog values from transducers to frequency modulate the subcarrier oscillators, which, in turn, frequency modulate the main carrier (radiofrequency link).

System performance - Atlas. - The 107 operational measurements shown in table VI-IX were transmitted through two antennas located on the two equipment pods. Satisfactory telemetry coverage was obtained to T + 813 seconds (fig. VI-56). All measurements provided useful data. Minor anomalies were experienced with the following three measurements:

(1) Sustainer hydraulic return line pressure measurement (Alt601P): Erratic data variations and "spiking" were experienced from approximately T + 37 to T + 57 seconds and from T + 92 to T + 158 seconds. The data at all other times were at expected levels and trends. The cause of the data variations is not known.

(2) Sustainer engine yaw position measurement (As256D): This measurement exhibited a bias condition of approximately 10-percent Information Band Width (IBW) below the expected 50 percent level prior to lift-off and during the flight. Other than the bias shift, data levels and trends were satisfactory. The cause of the bias shift was probably slippage of the sustainer engine yaw position transducer adjustment.

(3) Insulation panel 35°-of-rotation breakwire measurements (AA205X/AA208X) for quadrants III-IV and IV-I: The measurement AA205X indicated 35° of rotation of the quadrant III-IV insulation panel at T + 197.31 seconds (61-percent IBW). The 61-percent level also indicates the quadrant IV-I insulation panel had not rotated 35°. At T + 197.328 seconds the measurement AA208X indicated 35° of rotation of the quadrant IV-I insulation panel (37-percent IBW). The 37-percent IBW also indicated the quadrant III-IV insulation panel had not rotated. Subsequent data samples were at the correct level (80-percent IBW). The 80-percent IBW indicates both the quadrant III-IV and the quadrant IV-I insulation panels had rotated 35°. It is theorized that the quadrant III-IV insulation panel breakwire transducer opened, then momentarily closed, then opened again.

System description - Centaur. - The Centaur telemetry system (fig. VI-57) consists of two radiofrequency telemetry packages, one antenna (fig. VI-58), and transducers. It is a PAM/FM/FM system which operates at frequencies of 225.7 and 259.7 megahertz for radiofrequency telemetry package 1 (RF1) and radiofrequency telemetry package 2 (RF2), respectively. The RF1 telemetry package was used for vehicle operational measurements, and the RF2 telemetry package was installed in order to define (1) the low-frequency rigid-body vibration environment at the spacecraft interface,

(2) axial and radial loads on the nose fairing hinges, (3) vehicle bending modes in the fixed fairing, (4) nose fairing jettison separation rates and clearances, and (5) spacecraft acoustic environment.

System performance - Centaur. - A total of 181 measurements (table VI-X) were transmitted to the ground stations. Anomalies were experienced with the following measurements:

(1) Centaur engine C-1 thrust chamber jacket temperature measurements (CP63T) went off scale high at T + 264 seconds. This indicates an open circuit in either the transducer or the harnessing. No data were retrieved beyond this time.

(2) Centaur engine C-2 fuel pump case temperature measurement (CP122T) exhibited a slow response to temperature changes. This malfunction has been observed on previous flights, and the problem is believed to be caused by the temperature transducer losing its bond to the fuel pump case.

(3) Centaur engine C-2 hydraulic power package pressure measurement (CH3P) exhibited negative "spiking" of up to 8-percent IBW during the powered portion of flight. This is indicative of wiper arm lift-off in the transducer. No data were lost because of this malfunction.

(4) The six accelerometers mounted on the payload adapter exhibited small disturbances that coincided with a series of 0.5-ampere "spikes" on the battery current monitor. The cause of this anomaly has not been determined.

(5) Guidance digital data after approximately 92 minutes into the flight showed intermittent computer telemetry bits occurring during the telemetry work marker and immediately following some data words. The problem has been isolated to the telemetry output circuitry in the guidance computer being temperature sensitive. No data were lost because of this malfunction.

Satisfactory telemetry coverage was obtained to T + 8256 seconds as shown in figure VI-59. Location of the receiving stations are shown in figure VI-60.

Noisy data were experienced at Canary Island from approximately T + 1079 to T + 1161 seconds. Tananarive had intermittent noise from approximately T + 2351 to T + 2461 seconds. Carnarvon did not record radiofrequency link 1, channels 1, 2, 3, and 4, because of the ground equipment problems.

Tracking System

System description. - The tracking system consisting of an airborne C-band radar beacon subsystem (fig. VI-60), with associated radar ground stations (fig. VI-61), provided real-time position and velocity data to the range safety tracking system. These data were also used by the Manned Space Flight Network (MSFN) for assistance in

acquisition of the spacecraft and for guidance and flight trajectory data analysis. The airborne equipment includes a lightweight transponder, a circulator (to channelize receiving and sending signals), a power divider, and two antennas located on opposite sides of the Centaur vehicle. The locations of the C-band antennas are shown in figure VI-58.

System performance. - The C-band radar tracking was satisfactory; coverage was obtained up to $T + 7998$ seconds, as indicated in figure VI-62. Antigua, Canary Island, Tananarive, Carnarvon, and Hawaii provided data to verify orbital conditions. Merritt Island, Patrick, Grand Bahama Island, Grand Turk, and Bermuda provided coverage during Atlas-Centaur powered flight and data for orbit calculation. Merritt Island, Bermuda, and Canary Island also provided second orbital pass coverage.

Range Safety Command System

System description. - The Atlas and Centaur stages each contained independent vehicle destruct systems. Each system included redundant receivers, a power control unit, destructor, two antennas, and batteries which operate independently of the main vehicle power system. The location of the Centaur range safety antennas is shown in figure VI-58. Block diagrams of the Atlas and Centaur vehicle destruct systems are shown in figures VI-63 and VI-64, respectively. These systems were designed to function simultaneously upon command from the ground stations.

The Atlas and Centaur vehicle destruct systems provide a highly reliable means of shutting down the engine only, or shutting down the engines and destroying the vehicle, if it had left the safe flight corridor. To destroy the vehicle, the propellant tanks would be ruptured with an explosive charge and the liquid propellants of the Atlas and Centaur dispersed.

System performance. - The Atlas and Centaur vehicle destruct systems were prepared to execute destruct command throughout the flight. Engine cutoff or destruct commands were not sent by the range transmitter. The command from the Bermuda ground station to disable the range safety command system shortly after Centaur main engine cutoff was properly received and executed. Figure VI-65 depicts ground transmitter coverage to support the vehicle destruct systems.

The receiver signal strength measurements indicated a satisfactory received signal strength throughout the flight, with one exception at approximately $T + 107$ to $T + 112$ seconds. Just prior to the switching of the range transmitter from Cape Kennedy to Grand Bahama, the signal strength to all four receivers dropped below the 12-decibel gain margin above threshold required by the range for range safety operation. It is believed the signal strength decrease was due to inadequate signal strength at the vehicle,

which was caused by the range not switching the Cape Kennedy range transmitter from low power (600 W) to high power (10 000 W). Upon switching to the Grand Bahama transmitter at T + 112 seconds, the signal strength at all four receivers increased substantially. Telemetered data indicated that both the Centaur receivers were deactivated at approximately T + 705 seconds, thus confirming that the disable command was transmitted from the Bermuda station.

TABLE VI-IX. - ATLAS MEASUREMENT SUMMARY, AC-16

System	Measurement type										Totals
	Vibra- tion	Accelera- tion	Rotation rate	Displace- ment	Pres- sure	Fre- quency	Rate	Tempera- ture	Volt- age	Dis- cretes	
Airframe	2	1			3			2		4	12
Range safety									3	1	4
Electrical						1			4		5
Pneumatics					7			1			8
Hydraulics					6						6
Dynamics		1								2	3
Propulsion			3	3	18			6		6	36
Flight control				11			3		4	11	29
Propellants		1			2				1		4
Totals	2	3	3	14	36	1	3	9	12	24	107

TABLE VI-X. - CENTAUR MEASUREMENT SUMMARY, AC-16

System	Measurement type														Totals
	Acous- tical	Strain	Accelera- tion	Rotation rate	Cur- rent	Displace- ment	Vibra- tion	Pres- sure	Fre- quency	Rate	Tempera- ture	Digi- tal	Volt- age	Dis- cretes	
Airframe		11	7			1					2			6	27
Range safety													2	3	5
Electrical					1				1		2		4		8
Pneumatics									6		4			2	12
Hydraulics									2		2				4
Guidance											1	1	16		18
Propulsion				4					12		28			10	54
Flight control										3			4	30	37
Propellant						2							2		4
Spacecraft	1						3	1			1			6	12
Totals	1	11	7	4	1	3	3	21	1	3	40	1	28	57	181

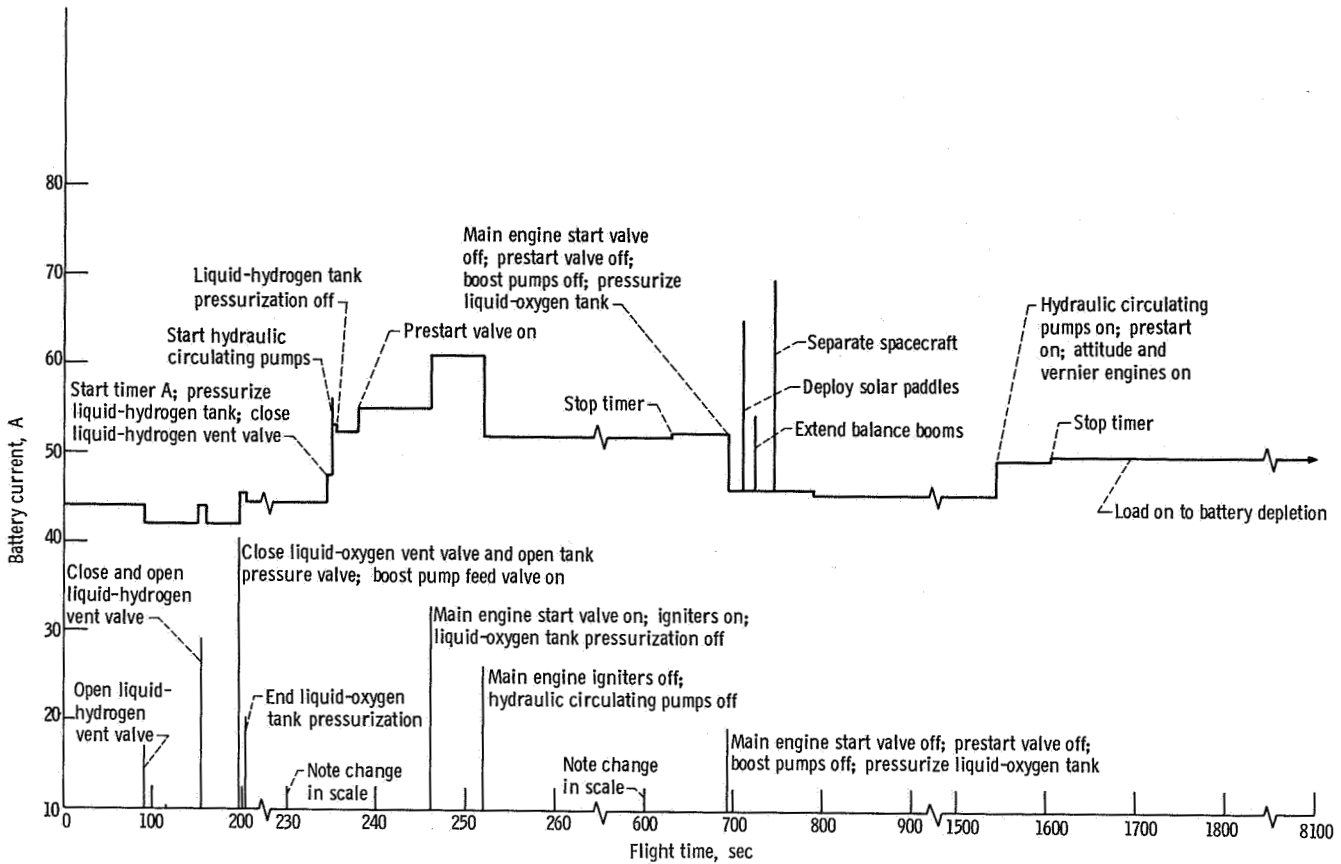


Figure VI-54. - Centaur main battery current profile, AC-16.

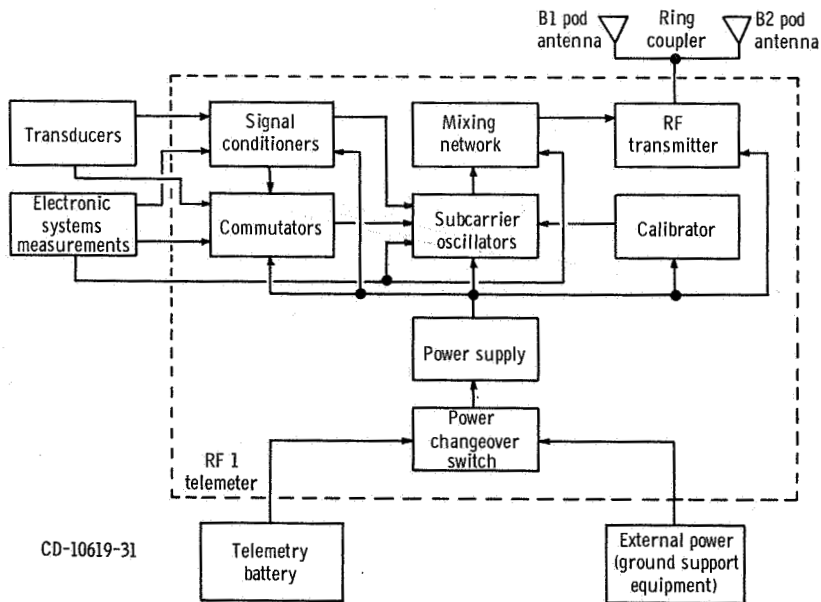


Figure VI-55. - Atlas telemetry system block diagram, AC-16.

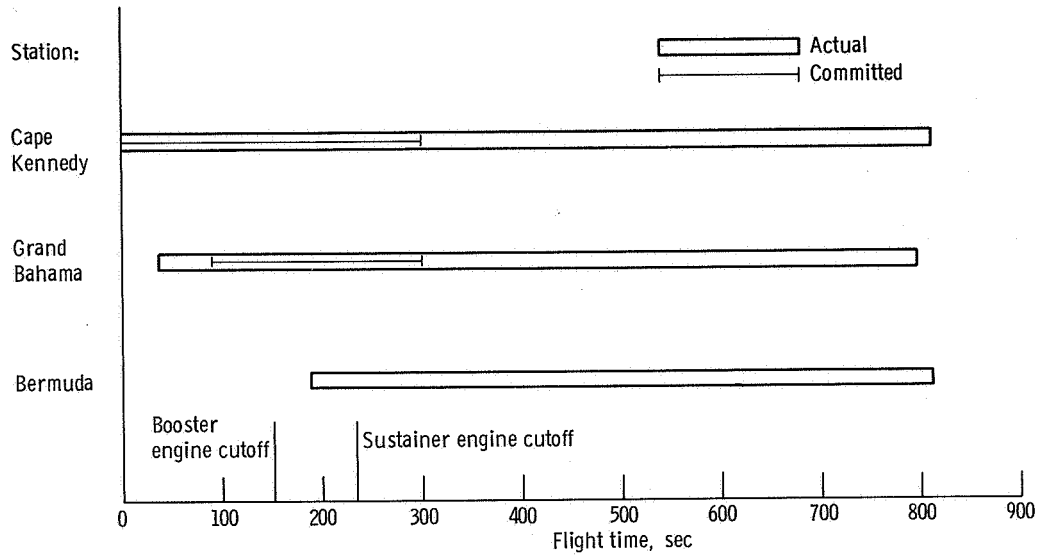


Figure VI-56. - Atlas telemetry coverage, AC-16.

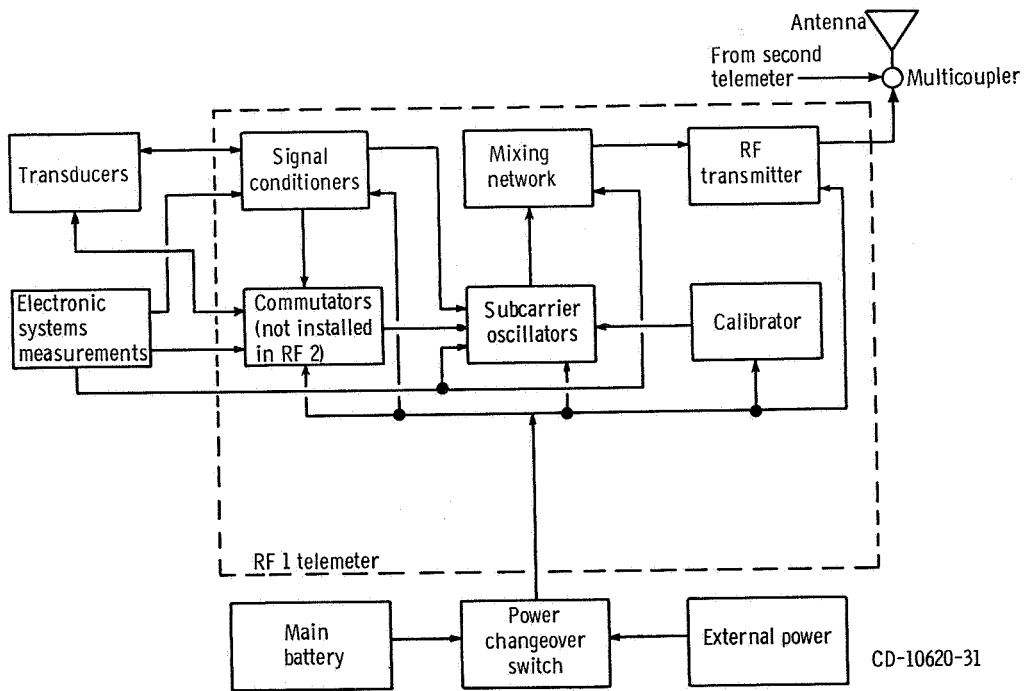


Figure VI-57. - Centaur telemetry system, typical both telemeters, AC-16.

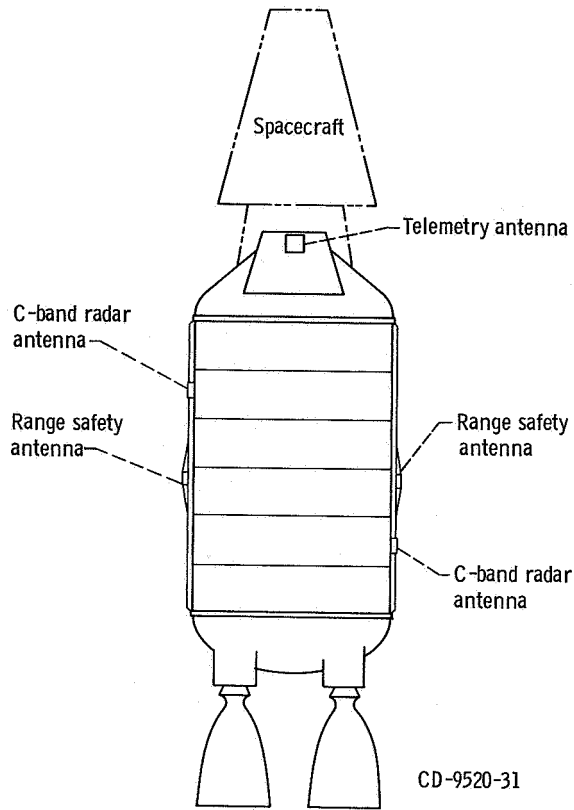


Figure VI-58. - Location of Centaur antennas, AC-16.

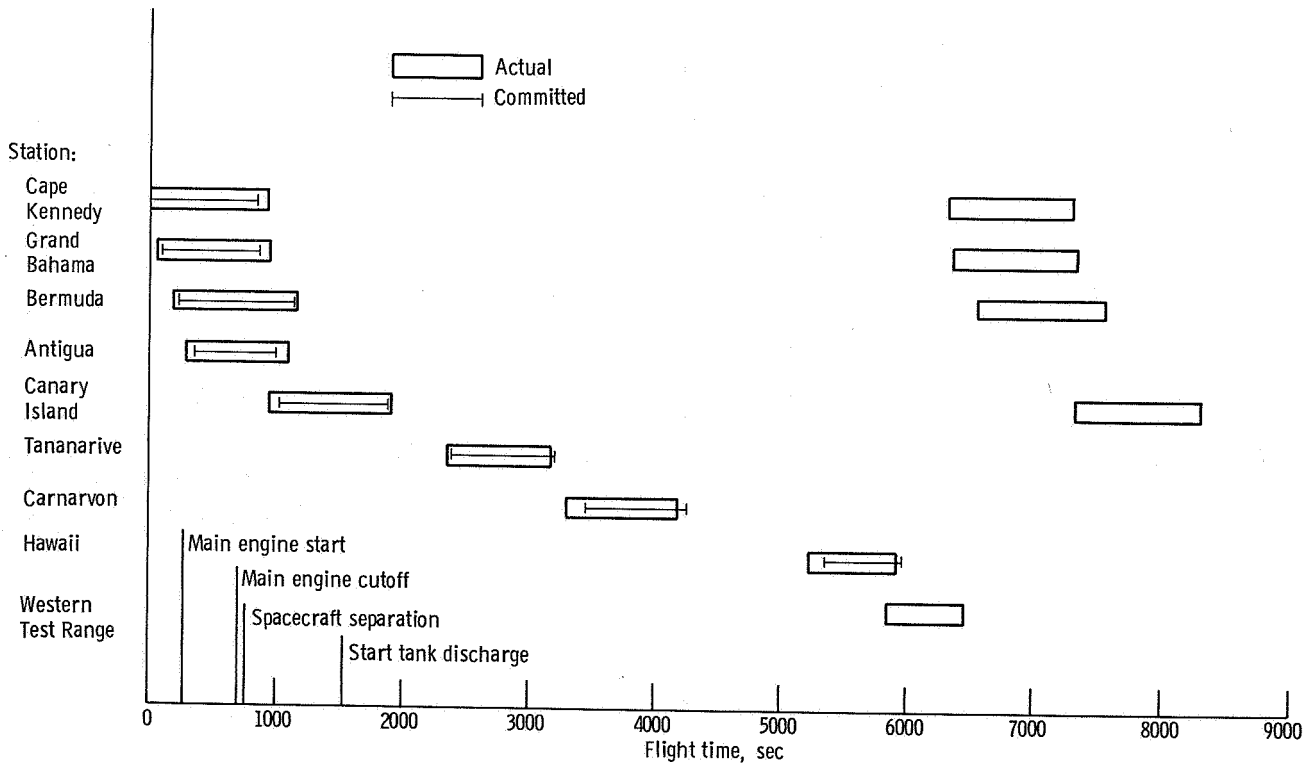


Figure VI-59. - Centaur telemetry coverage, AC-16.

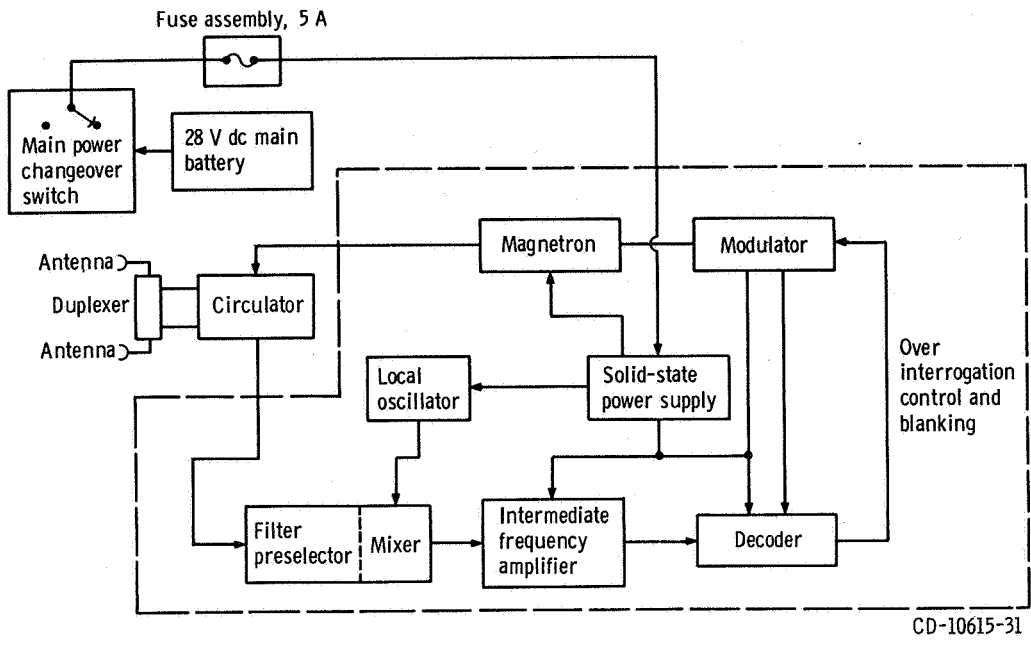


Figure VI-60. - Centaur C-band beacon subsystem, AC-16.

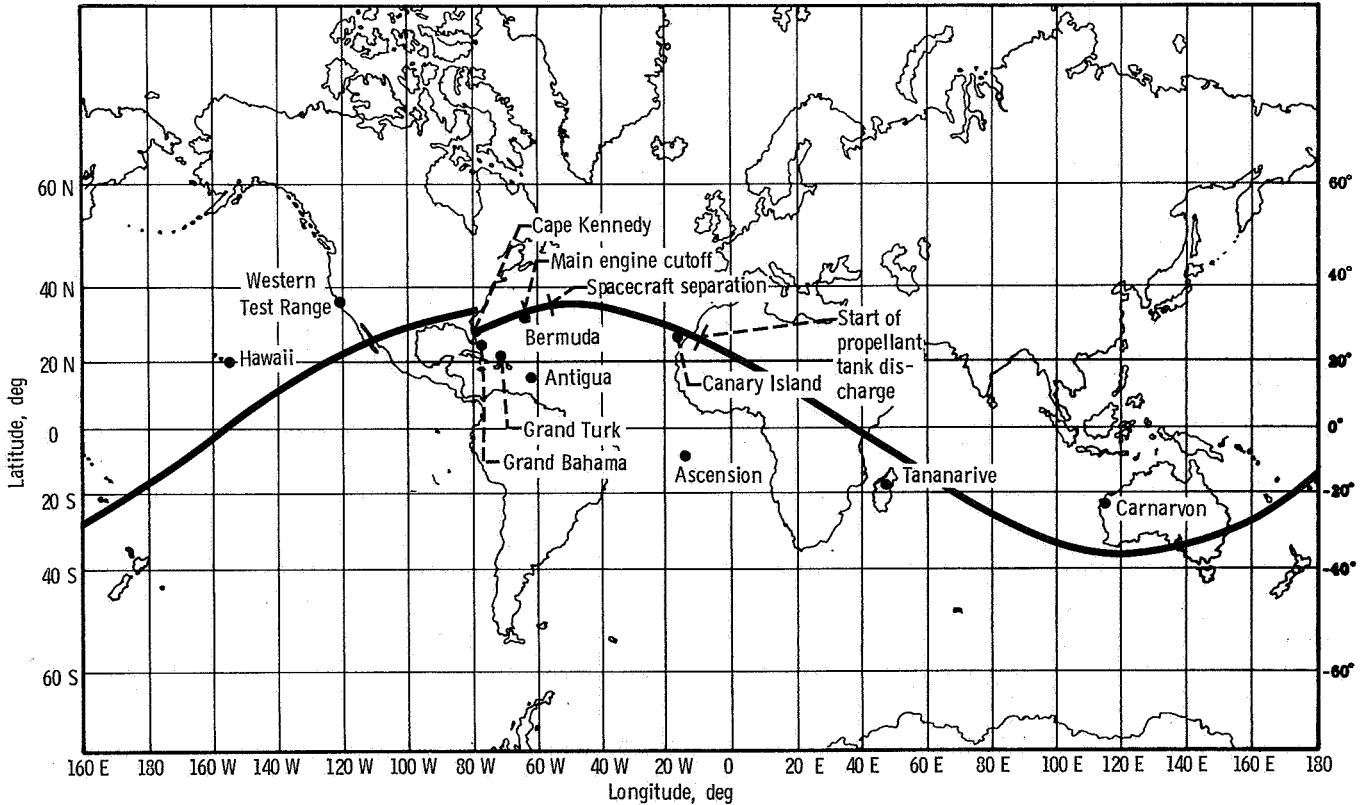


Figure VI-61. - Tracking station location and vehicle trajectory Earth track, AC-16.

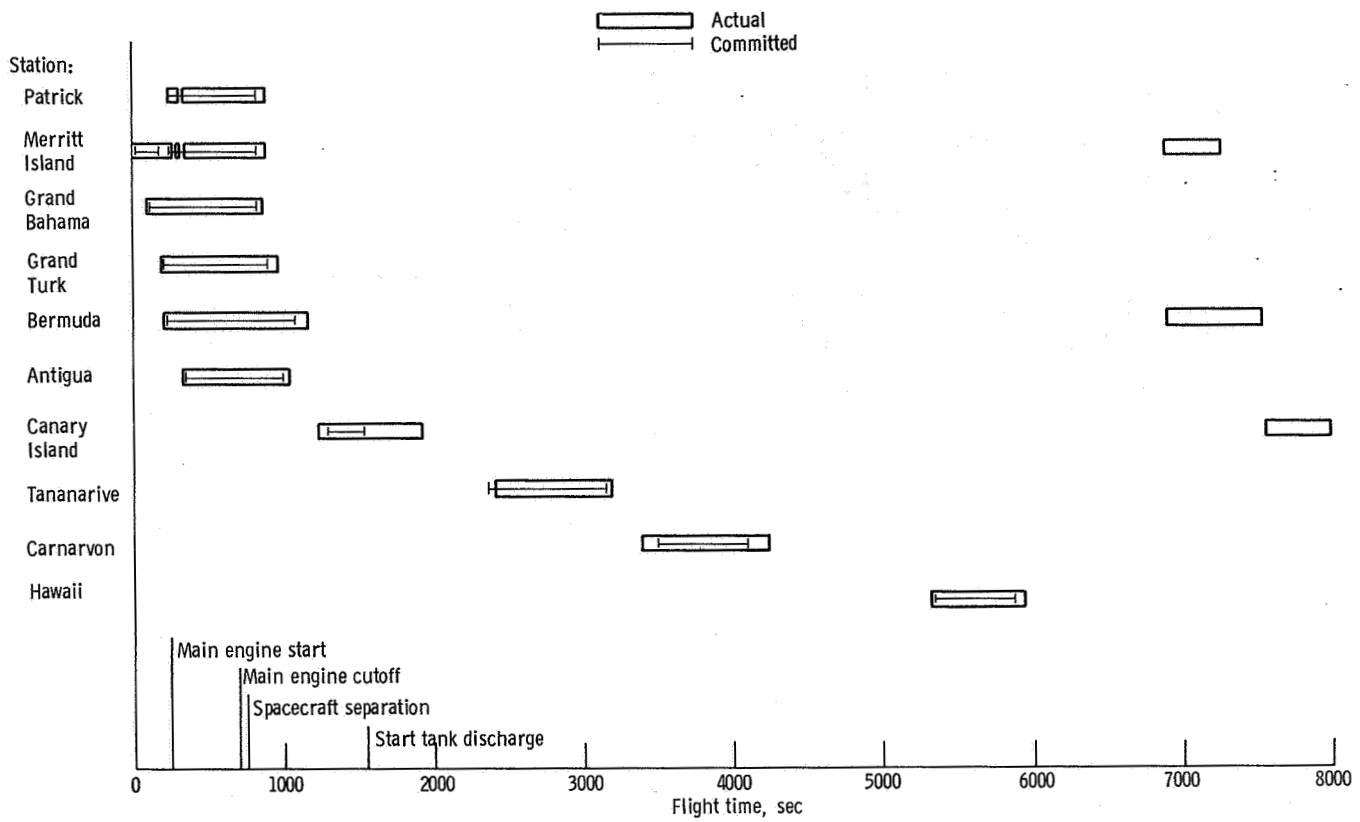


Figure VI-62. - C-Band radar coverage, AC-16. Coverage shown is for autobeacon track only.

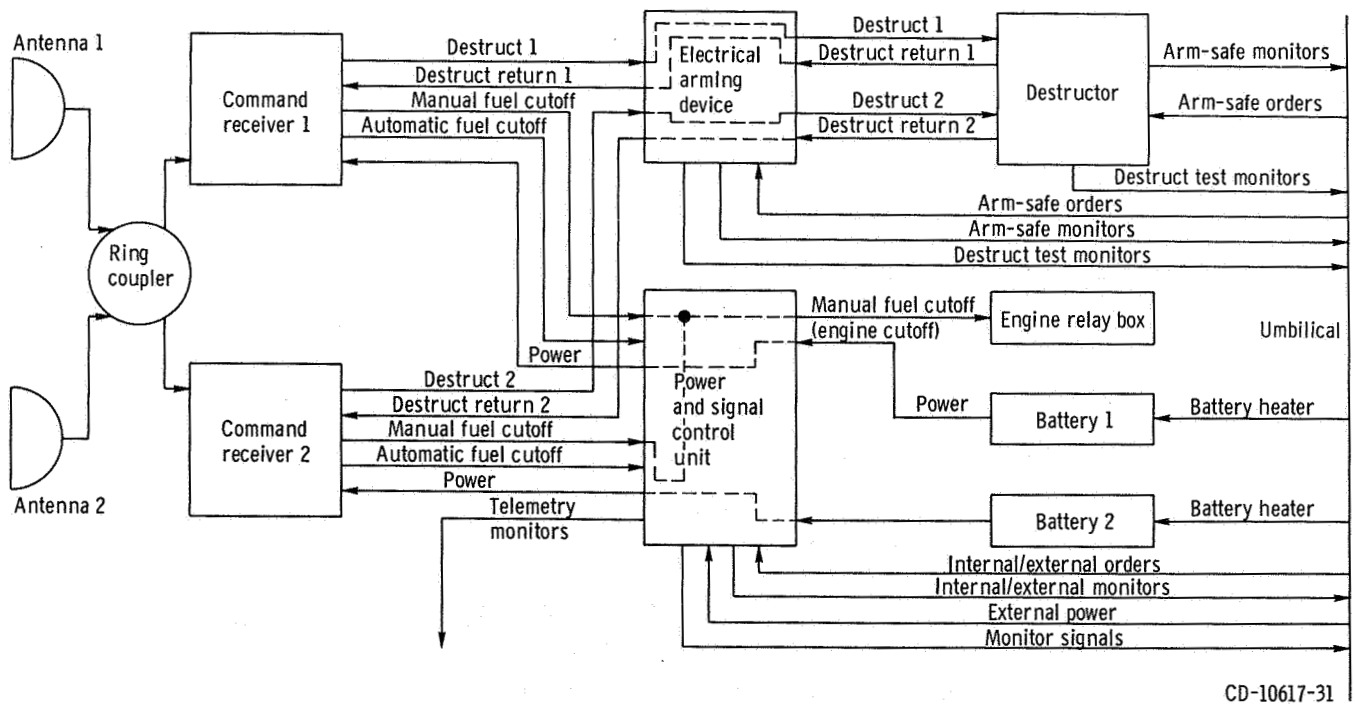


Figure VI-63. - Atlas vehicle destruct system block diagram, AC-16.

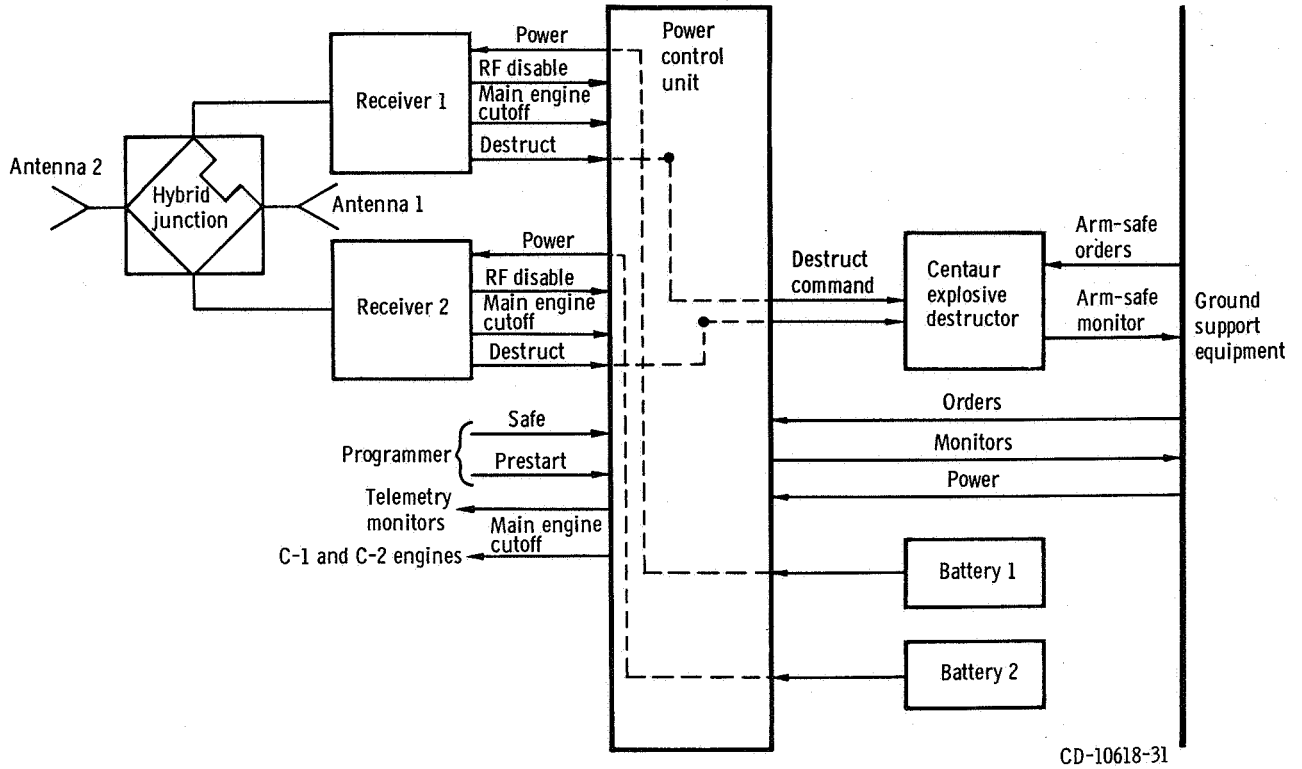


Figure VI-64. - Centaur vehicle destruct subsystem block diagram, AC-16.

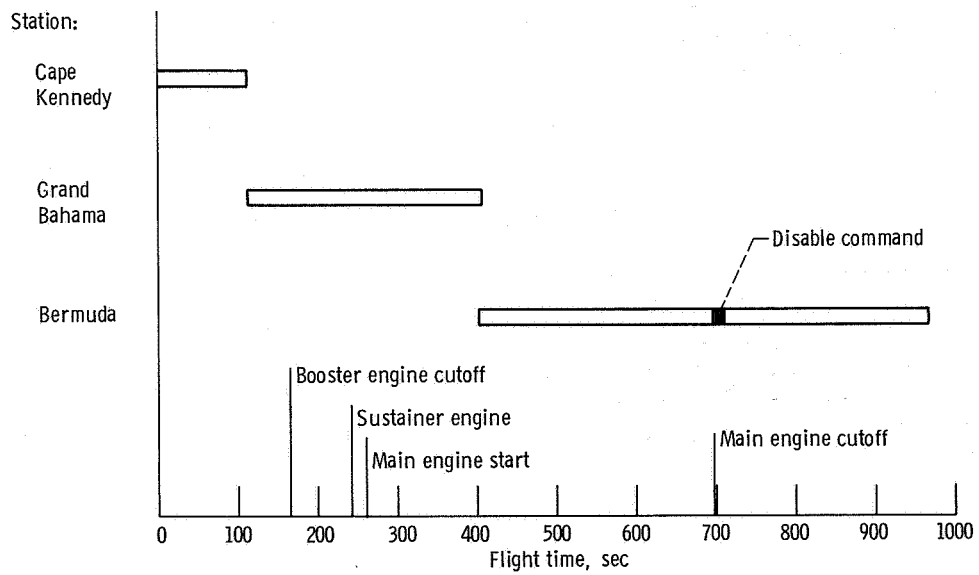


Figure VI-65. - Range safety command system transmitter utilization, AC-16.

GUIDANCE AND FLIGHT CONTROL SYSTEMS

by Paul W. Kuebeler, William J. Middendorf, and Corrine Rawlin

The objectives of the guidance and flight control systems are to guide the launch vehicle to the orbit injection point and establish the vehicle velocity necessary to place the spacecraft in the desired orbit. To accomplish these objectives, the guidance and flight control systems provide vehicle stabilization, control and guide the vehicle along the flight path, and sequence flight events of the launch vehicle. These functions are performed at specified time periods from vehicle lift-off through completion of the Centaur retromaneuver after spacecraft separation. An inertial guidance system is installed on the Centaur stage. Separate flight control systems are installed on the Atlas and on the Centaur stages. The guidance system, operating with the flight control systems, provides the capability to stabilize the vehicle and compensate for trajectory dispersions resulting from thrust misalignment, winds, and vehicle performance variations.

Three modes of operation are used for stabilization, control, and guidance of the launch vehicle. These modes are rate stabilization only, rate stabilization and attitude control, and rate stabilization and guidance control. Block diagrams of the three modes are shown in figure VI-66. The flight times during which a particular mode is used are shown in figure VI-67. Figure VI-67 also shows the modes of operation of the Centaur hydrogen peroxide attitude control system which are discussed later in this section.

The Atlas flight control system controls the Atlas-Centaur vehicle by gimbaling the Atlas main and vernier engines to provide thrust vector control. The Centaur flight control system controls the Centaur vehicle by gimbaling the main engines to provide thrust vector control while the main engines are firing or by commanding various combinations of the hydrogen peroxide attitude control engines on or off during coast periods, when the main engines are not firing.

The rate-stabilization-only mode stabilizes the roll axis of the Centaur stage continuously after Atlas-Centaur separation. This mode is also used to stabilize the pitch and yaw axes of the Centaur stage for 15.5 seconds following Atlas-Centaur separation. In this mode, output signals from rate gyros are used to control the vehicle. The output signal of each rate gyro is proportional to the angular rate of rotation of the vehicle about the input axis of the gyro. The vehicle angular rates are minimized by the flight control system to stabilize the vehicle. Rate stabilization is also combined with position (attitude) information in the other two modes of operation.

The rate-stabilization-and-attitude-control mode is used for pitch, yaw, and roll control during the Atlas booster phase of flight and for roll control only during the Atlas sustainer phase. This mode is termed attitude control since the displacement gyros (one each for the pitch, yaw, and roll axes) provide a reference attitude to which the

vehicle is to be aligned. However, if the actual flight path differs from the desired flight path, there is no way of determining the difference and correcting the flight path. The reference attitude is programmed to change during booster phase. These changes in reference attitude cause the vehicle to roll to the programmed flight azimuth angle and to pitch downward. Vehicle stabilization is accomplished in the same manner as in the rate-stabilization-only mode. The rate stabilization signals are algebraically summed with the attitude reference signals. These resultant signals are used to control and stabilize the vehicle.

The rate-stabilization-and-guidance-control mode is used for the pitch and yaw axes during Atlas sustainer phase, Centaur main engine firing, and the coast period following main engine cutoff. In this mode, the guidance system provides the attitude and direction reference. If the resultant flight path, as measured by the guidance system, is not the desired flight path, the guidance system issues steering signals to direct the vehicle to the desired flight path. Vehicle stabilization is accomplished in the same manner as in the rate stabilization only mode. The pitch and yaw rate stabilization signals are algebraically summed with the appropriate pitch and yaw steering signals from the guidance system. These resultant signals are used to control and stabilize the vehicle.

Figure VI-68 is a simplified diagram of the interface between the guidance system and the flight control system.

Guidance System

System description. - The guidance system performs the following functions:

- (1) Measures vehicle acceleration in fixed inertial coordinates
- (2) Computes the values of actual vehicle velocity and position, and computes the vehicle flight path to attain the trajectory injection point
- (3) Compares the actual position to the desired flight path and issues steering signals
- (4) Issues discrete commands

The Centaur guidance system is an inertial system which becomes completely independent of ground control approximately 12 seconds before lift-off of the vehicle. The guidance system consists of five separate units. Three of the units form an inertial measurement group. A simplified block diagram of the guidance system is shown in figure VI-69.

Inertial measurement group: Vehicle acceleration is measured by the following three units:

- (1) The inertial platform unit, which contains the platform assembly, gyros, and accelerometers

- (2) The pulse rebalance, gyro torquer, and power supply unit, which contains the electronics associated with the accelerometers
- (3) The platform electronics unit, which contains the electronics associated with the gyros

The platform assembly uses four gimbals which provide a three-axis coordinate system. The use of four gimbals, instead of three, allows complete rotation of all three vehicle axes about the platform without gimbal lock. Gimbal lock is a condition in which two axes coincide, causing loss of one degree of freedom. A gimbal diagram is shown in figure VI-70. The azimuth gimbal is isolated from movements of the vehicle airframe by the other three gimbals. The inertial components (three gyros and three accelerometers) are mounted on the azimuth or inner gimbal. A gyro and an accelerometer are mounted as a pair with their sensing axes parallel. The gyro and accelerometer pairs are also aligned on three mutually perpendicular (orthogonal) axes corresponding to the three axes of the platform.

The three gyros are identical and are of the single-degree-of-freedom, floated-gimbal, rate integrating type. Each gyro monitors one of the three axes of the platform. These gyros are elements of control loops, the sole purpose of which is to maintain each axis fixed in inertial space. The output signal of each gyro is connected to a servoamplifier whose output controls a direct-drive torque motor which moves a gimbal of the platform assembly. The orientation of the azimuth gimbal is fixed in the inertial space and the outer roll gimbal is attached to the vehicle. The angles between the gimbals provide a means for transforming steering signals from inertial coordinates to vehicle coordinates. The transformation is accomplished by electromechanical resolvers, mounted between gimbals, to produce analog electrical signals proportional to the sine and cosine functions of the gimbal angles. These electrical signals are used for an analog solution of the mathematical equations for coordinate transformation by interconnecting the resolvers in a multiple resolver chain.

The three accelerometers are identical and are of the single-axis, viscous-damped, hinged-pendulum type. The accelerometer associated with each axis measures the change in vehicle velocity along that axis by responding to acceleration. Acceleration of the vehicle causes the pendulum to move off center. The associated electronics then produce precise current pulses to recenter the pendulum. These rebalance pulses are either positive or negative depending on an increase or decrease in vehicle velocity. These pulses, representing changes in velocity (incremental velocity), are then routed to the navigation computer unit for computation of vehicle velocity.

Proper flight operation requires alignment and calibration of the inertial measuring unit during launch countdown. The azimuth of the platform, to which the desired flight trajectory is referenced, is aligned by ground-based optical equipment. The platform is aligned perpendicular to the local vertical by using the two accelerometers in the horizontal plane. Each gyro is calibrated to determine its characteristic constant torque

drift rate and mass unbalance along the input axis. The scale factor and zero bias offset of each accelerometer is determined. These prelaunch-determined calibration constants and scale factors are stored in the navigation computer for use during flight.

Navigation computer unit: The navigation computer unit is a serial, binary, digital machine with a magnetic drum memory. The memory drum has a capacity of 2816 words (25 bits/word) of permanent storage, 256 words of temporary storage, and six special-purpose tracks. Permanent storage is prerecorded and cannot be altered by the computer. The temporary storage is the working storage of the computer.

Incremental velocity pulses from the accelerometers are the information inputs to the navigation computer. The operation of the navigation computer is controlled by the prerecorded program. This program directs the computer to use the prelaunch equations, navigation equations, and guidance equations.

The prelaunch equations establish the initial conditions for the navigation and guidance equations. Initial conditions include (1) a reference trajectory, (2) launch site values of geographical position, and (3) initial values of navigation and guidance functions. Based on these initial conditions, the guidance system starts flight operation approximately 12 seconds before lift-off.

The navigation equations are used to compute vehicle velocity and actual position. Velocity is determined by algebraically summing the incremental velocity pulses from the accelerometers. An integration is then performed on the computed velocity to determine actual position. Corrections for the prelaunch-determined gyro and accelerometer constants are also made during the velocity and position computation to improve the navigation accuracy. For example, the velocity data derived from the accelerometer measurements are adjusted to compensate for the accelerometer scale factors and zero offset biases measured during the launch countdown. The direction of the velocity vector is also adjusted to compensate for the gyro constant torque drift rates measured during the launch countdown.

The guidance equations continually compare actual position and velocity with the position and velocity desired at the time of injection. Based upon this position comparison, steering signals are generated to guide the vehicle along an optimized flight path to obtain the desired injection conditions. The guidance equations are used to generate four discrete commands: (1) booster engine cutoff, (2) sustainer engine cutoff backup, (3) Centaur main engine cutoff, and (4) "null" the propellant utilization system. The booster engine cutoff command and the sustainer engine cutoff backup commands are issued when the measured vehicle acceleration equals predetermined values. The Centaur main engine cutoff command is issued when the extrapolated vehicle orbital angular momentum equals that required for injection into orbit. The command to "null" the propellant utilization system is issued 15 seconds before the Centaur main engine cutoff command.

During the booster phase of flight, the navigation computer supplies incremental pitch and yaw signals for steering the Atlas stage. From a series of predetermined programs, one pitch program and one yaw program are selected based on prelaunch upper-air wind soundings. The selected programs are entered and stored in the computer during launch countdown. The program consists of discrete pitch and yaw turning rates for specified time intervals from T + 15 seconds until booster engine cutoff. These programs permit changes to be made in the flight reference trajectory during countdown to reduce anticipated aerodynamic heating and structural loading conditions on the vehicle.

Signal conditioner unit: The signal conditioner unit is the link between the guidance system and the vehicle telemetry system. This unit modifies and scales guidance system parameters to match the input range of the telemetry system.

System performance. - The performance of the guidance system was as follows:

Accuracy: The performance of the guidance system was satisfactory, as indicated by the following orbital parameters:

Parameter	Units	Predicted value	Actual value		Error, predicted value minus BET value	Estimated 3-sigma errors
			GRT ^a	BET ^b		
Injection ^c	km	772.676	772.716	772.768	0.092	1.46
	n mi	416.930	416.952	416.980	.050	.79
Apogee minus perigee	km	1.275	1.188	3.154	1.879	10.23
	n mi	.688	.592	1.702	1.014	5.52
Eccentricity	----	.000089	.000083	.00022	-----	-----
Inclination	deg	34.9982	34.9990	34.9811	0.017	0.035

^aGuidance Reconstructed Trajectory obtained from telemetered guidance data.

^bBest Estimated Trajectory obtained from radar tracking data.

^cSee V. TRAJECTORY AND PERFORMANCE for details on injection altitude.

Discrete commands: All discrete commands were issued properly. Table VI-XI lists the discrettes, the criteria for the issuance of the discrettes, and the computed values at the time the discrettes were issued. Actual and predicted times from lift-off are also shown for reference only.

Guidance steering loop: The pitch and yaw steering signals issued by the guidance system are proportional to the components of the steering vector (desired vehicle pointing vector) along the vehicle pitch and yaw axes. In this section of the report, the steering signals have been converted into the approximate angular attitude errors between the steering vector and the vehicle roll axis (vehicle pointing vector) in the pitch and yaw planes. During the sustainer phase of flight and during Centaur main engine

firing, the attitude errors remained less than 2.5° in pitch and 1° in yaw, except during periods when guidance steering was deactivated or when a large sudden change in the steering vector occurred.

Attitude errors at guidance steering activation are given in the following table:

Event	Time, sec	Attitude displacements, deg	
		Pitch	Yaw
Sustainer phase	T + 160	1 (nose below)	<1 (nose right)
Centaur powered flight	T + 250	1.5 (nose below)	2.2 (nose right)

At T + 267.1 seconds the guidance system issued a nose right command of approximately 14° in the inertial coordinate system. The resultant command in the vehicle coordinate system was approximately 13.8° nose right and 4.5° nose down. The retro-maneuver command was issued at T + 1055.2 seconds, and the vehicle began to align to approximately the negative of the instantaneous radius vector.

Accelerometer loops and gyro control loops: The accelerometer loops operated satisfactorily. The accelerometer pendulum offsets from "null" remained within a band of approximately 2 arc-seconds.

The gimbal control loops operated satisfactorily, and the inertial platform remained stable throughout the flight. The fourth gimbal uncaged at T + 82 seconds, when the vehicle had pitched over approximately 23° as planned. The maximum gimbal displacement errors are given in the following table:

Gimbal	Maximum displacement errors, arc-sec	
	Through main engine cutoff	After main engine cutoff
1	7.8, ^a -8.0	7.8, -7.8
2	7.4, -8.0	5.5, -7.3
3	11.6, -7.6	12.0, -11.6
4	^a 335, -301	417, -668

^aExcludes gimbal 4 uncaging transient of -12.9 arc-sec for gimbal 1 and 2600 arc-sec for gimbal 4.

Other measurements: Except for the digital data, all of the guidance system signals and measurements which were monitored during the flight were normal and indicated

satisfactory operation of the guidance system. The skin temperature of the Pulse Rebalance Electronics was 288.2 K (59⁰ F) at lift-off and reached 302.1 K (84⁰ F) at the end of the first orbital pass.

After T + 92 minutes, an intermittent navigation computer malfunction resulted in incorrect digital telemetry data. Incorrect bits occurred, intermittently, during the telemetry work marker and the data words and following some of the data words. The malfunction affected only the telemetry output function of the computer. Otherwise, the computer performed normally. It is believed that the malfunction was the intermittent failure of the telemetry output flip-flop (located in the computer) to reset upon command, because of the temperature increase of the flip-flop during its extended operation. This specific malfunction has been reproduced in laboratory tests.

Flight Control Systems

System description - Atlas. - The Atlas flight control system provides the primary functions required for vehicle stabilization, control, sequencing, and execution of guidance steering signals, and consists of the following major units:

(1) The displacement gyro unit, which contains three single-degree-of-freedom, floated, rate integrating gyros and associated electronic circuitry for gain selection and signal amplification. These gyros are mounted to the vehicle airframe in an orthogonal triad configuration aligning the input axis of a gyro to its respective vehicle axis of pitch, yaw, or roll. Each gyro provides an electrical output signal proportional to the integral of the time rate of change of angular displacement from the gyro reference axis.

(2) The rate gyro unit, which contains three single-degree-of-freedom, floated, rate gyros and associated electronic circuitry. These gyros are mounted in the same manner as the displacement gyro unit. Each gyro provides an electrical output signal proportional to the angular rate of rotation of the vehicle about the gyro input (reference) axis. The AC-16 flight was the first wherein the Centaur provided both rate and position signals to the Atlas flight control system during the Atlas sustainer phase.

(3) The servoamplifier unit, which contains electronic circuitry to amplify, filter, integrate, and algebraically sum combined position and rate signals with engine position feedback signals. The electrical outputs of this unit direct the hydraulic actuators which gimbal the engines to provide thrust vector control.

(4) The programmer unit, which contains an electronic timer, arm-safe switch, high-, low-, and medium-power electronic switches, and circuitry to set the roll program from launch ground equipment. The programmer issues discrete commands to the following systems: other units of the Atlas flight control system, Atlas propulsion, Atlas pneumatic, vehicle separation systems, and Centaur flight control.

System performance - Atlas. - The flight control system performed satisfactorily throughout the Atlas phase of flight. Corrections required to control the vehicle because of disturbances were well within the system capability. Vehicle dynamic response resulting from each flight event was evaluated in terms of amplitude, frequency, and duration as observed on rate gyro data (table VI-XII). In this table, the control capability (in percent) is the ratio of engine gimbal angle used to the available total engine gimbal angle.

The programmer was started at 1.1-meter (42-in.) rise, which occurred at approximately $T + 1$ second. This permitted the flight control system to gimbal the engines and thereafter control the vehicle. The vehicle lift-off transients were damped out by $T + 4$ seconds using 12 percent of the control capability.

At $T + 2$ seconds the roll program was initiated and continued until $T + 20$ seconds; this was 5 seconds longer than for previous flights. This large roll maneuver was required for this flight to satisfy the Bermuda overflight constraints. (See V. TRAJECTORY AND PERFORMANCE for discussion of Bermuda overflight constraints.) Atlas and Centaur rate gyro data indicated that the vehicle rolled clockwise approximately 53° . This value compares favorably with an expected roll of 55° required to achieve the desired flight azimuth of 60° .

The pitch program was started at $T + 15$ seconds with a pitch rate of -0.36 degree per second.

Rate gyro data indicated that the period of maximum aerodynamic loading for this flight was approximately from $T + 75$ to $T + 95$ seconds. During this period, a maximum of 48 percent of the control capability was required to overcome both steady-state and transient loading.

Atlas booster engine cutoff occurred at $T + 152.1$ seconds. The angular rates imparted to the vehicle by this transient required 8 percent of the sustainer engine gimbal capability. The Atlas booster engines were jettisoned at $T + 155.2$ seconds. The maximum angular rate imparted by this disturbance was 3.11 degree per second in the yaw plane.

During the Atlas powered flight, the Atlas flight control system provided the attitude reference until $T + 160.2$ seconds; thereafter, the Centaur guidance system provided the attitude reference. Twenty percent of the total control capability was required to steer the vehicle to the new reference. The maximum vehicle angular rate transient during this change was a yaw rate of 1.64 degree per second, peak-to-peak, with a duration of 7 seconds.

Insulation panels were jettisoned at $T + 196.8$ seconds. The maximum vehicle angular rate transient observed due to this disturbance was a pitch rate of 2.32 degree per second, peak-to-peak, which utilized 20 percent of the control capability for correction.

Sustainer engine cutoff occurred at $T + 234.5$ seconds. Atlas-Centaur separation was smooth and resulting transients were under 0.5 degree per second.

System description - Centaur. - The Centaur flight control system provides the primary means for vehicle stabilization and control, execution of guidance steering signals, and timed switching sequences for programmed flight events. The Centaur flight control system (fig. VI-71) consists of the following major units:

(1) The rate gyro unit, which contains three single-degree-of-freedom, floated, rate gyros with associated electronics for signal amplification gain selection and conditioning of guidance steering signals. These gyros are mounted to the vehicle in an orthogonal triad configuration aligning the input axis of each gyro to its respective vehicle axis of pitch, yaw, or roll. Each gyro provides an electrical output signal proportional to the angular rate of rotation of the vehicle about the gyro input (reference) axis.

(2) The servoamplifier unit, which contains electronics to amplify, filter, integrate, and algebraically sum combined position and rate signals with engine position feedback signals. The electrical outputs of this unit issue signals to the hydraulic actuators which control the gimbaling of the engines. In addition, this unit contains the logic and threshold circuitry controlling the engines of the hydrogen peroxide attitude control system.

(3) The electromechanical sequence timer unit, which contains a 400-hertz synchronous motor to provide the time reference and 22 time slots capable of actuating 144 switches.

(4) The auxiliary electronics unit which contains logic, relay switches, transistor switches, power supplies, control circuitry for the electromechanical timer, circuitry for conditioning computer generated discrettes, and an arm-safe switch. The arm-safe switch electrically isolates valves and pyrotechnic devices from the control switches. The combination of the electromechanical timer units and the auxiliary electronics unit issues discrettes to the following systems: other units of the Centaur flight control, propulsion, pneumatic, hydraulic, separation, propellant utilization, telemetry, spacecraft, and electrical systems, and the Atlas flight control system.

Vehicle steering during Centaur powered flight is by thrust vector control through gimbaling of the two main engines. There are two actuators for each engine to provide pitch, yaw, and roll control. Pitch control is accomplished by moving both engines together in the pitch plane. Yaw control is accomplished by moving both engines together in the yaw plane, and roll control is accomplished by moving the engines differentially in the yaw plane. Thus, the yaw actuator responds to an algebraically summed yaw-roll command. By controlling the direction of thrust of the main engines, the flight control system maintains the flight of the vehicle on a trajectory directed by the guidance system. After main engine cutoff, control of the vehicle is maintained by the flight control system through selective firing of hydrogen peroxide engines. A more complete

description of the engines and the propellant supply for the attitude control system is presented in the section PROPULSION SYSTEMS.

The logic circuitry, which commands the 14 hydrogen peroxide engines either on or off, is contained in the servoamplifier unit of the flight control system. Figure VI-72 shows the alphanumeric designations of the engines and their locations on the aft end of the vehicle. Algebraically summed position and rate signals are the inputs to the logic circuitry. The logic circuitry provides five modes of operation designated: all off, separate on, A and P separate on, V half on, and S half on. These modes of operation are used during different periods of the flight and are controlled by the sequence timer unit. A summary of the modes of operation is presented in table VI-XIII. In this table "threshold" designates the vehicle rate in degrees per second that has to be exceeded before the engines are commanded "on."

System performance - Centaur. - The Centaur flight control system performance was satisfactory. Vehicle stabilization and control were maintained throughout the flight. All events sequenced by the timer were executed at the required times. (Refer to fig. VI-67 for the time periods of guidance - flight control mode of operation and attitude control system mode of operation. Vehicle dynamic responses for selected flight events are tabulated in table VI-XII.) The following evaluation of system performance is presented in the order of time sequenced portions of the flight.

Sustainer engine cutoff to Centaur main engine cutoff (T + 234.5 to T + 698.2 sec): The Centaur timer was started at Atlas sustainer engine cutoff by a command from the Atlas programmer. Appropriate commands were issued to separate the Centaur from the Atlas and to initiate the Centaur main engine firing sequence. Vehicle control was maintained during the period between sustainer engine cutoff and main engine start by gimbaling the main engines as they were discharging boost pump turbine exhaust and chilldown flow. There were no significant transients during separation. Centaur main engine start occurred at T + 246.0 seconds; only small transients were observed. Four seconds after main engine start the steering vector generated at sustainer engine cutoff was admitted and held until T + 267.1 seconds, 9.5 seconds after nose fairing jettison; this prevented the vehicle from turning during this time interval in order to minimize vehicle motion during the nose fairing jettison event. Nose fairing jettison occurred at T + 257.6 seconds with maximum response in roll, as expected. Nose fairing jettison was programmed to occur after Atlas-Centaur separation. At T + 267.1 seconds a yaw right maneuver was performed to achieve the required orbit inclination of 35° . The yaw right maneuver (dogleg) introduced a 2.94-degree-per-second yaw rate, which was damped in 7 seconds. Vehicle angular rates during the remainder of Centaur burn were larger than for previous flights. Angular rates as high as 1.66 degrees per second were observed during this time. This was partly due to the fact that the guidance compute cycle for AC-16 and AC-17 was on the order of three times larger than for previous Atlas-

Centaur flights. The long compute cycle caused the vehicle to steer along one vector for approximately 4.5 seconds while a new vector was being computed and commanded. The powered phase transients on AC-17 with a comparable compute cycle were smaller than for AC-16 because of the effect of larger end-to-end position gains for the AC-16 autopilot. At all times the transients were well within the vehicle control capability.

Centaur main engine cutoff to retrothrust (T + 698.2 to T + 1548.2 sec): The hydrogen peroxide attitude control system was activated at the time of main engine cutoff in the A and P separate-on mode. Angular rates imparted to the vehicle due to the differences in the shutdown characteristics of the two Centaur main engines were reduced to acceptable control levels in 1 second. During the time from main engine cutoff to spacecraft separation, the vehicle aligned to the separation vector. Also during this time interval the spacecraft solar paddles were deployed, and the balance booms were extended. These events were initiated at T + 708.2 and T + 723.2 seconds, respectively. The only significant angular rate due to these disturbances was a roll rate of 1.69 degrees per second due to solar paddle deployment. Only small angular rates were observed when the spacecraft was separated from the Centaur at T + 748.3 seconds.

At T + 1055.2 seconds the Centaur began its reorientation to align its axis along the approximately negative geocentric radius vector. The purposes of the retromaneuver were to minimize the impingement of Centaur exhaust on the spacecraft and to provide a difference between the orbital periods of the Centaur and the OAO spacecraft. The attitude control system then switched to the V half-on mode for 50 seconds. This was followed by the S half-on mode which lasted until the initiation of retrothrust. The attitude control system sequence was so designed because of the viewing constraints (cone angle) imposed upon the Centaur by the spacecraft. (See V. TRAJECTORY AND PERFORMANCE for discussion on viewing constraints (cone angles).) Unbalanced venting of hydrogen began during the S half-on mode. Venting started at approximately T + 1493 seconds, which was 58 seconds prior to "blowdown." Rate gyro data indicated that the V engines came on to control about 1.5 seconds after venting began. A peak disturbance torque of approximately 289 newton-meters (2560 in.-lbf) was calculated from yaw rate gyro data. The disturbing torque exceeded the control torque for about 3 seconds. The maximum angular rate due to this disturbance was approximately 0.58 degree per second.

At about T + 1548 seconds the engine prestart valves were opened to allow the residual propellants to discharge through the main engines.

TABLE VI-XI. - DISCRETE COMMANDS, AC-16

Discrete command	Criteria for discrete to be issued	Discrete issued at this computed value	Actual time, T + sec	Predicted time, T + sec
Booster engine cutoff	When square of vehicle thrust acceleration is greater than $27.53 (g's)^2$ ^a $(5.25 g's)^2$	$31.92 (g's)^2$ $(5.65 g's)^2$	152.1	153
Sustainer engine cutoff backup	When square of vehicle thrust acceleration is less than $0.53 (g's)^2$	$0.36 (g's)^2$	238	240
Null propellant utilization system	Fifteen seconds before main engine cutoff discrete	16.7 sec	681.5	671

^aThis value is lower than the vehicle thrust acceleration of $5.7 \pm 0.113 g$ required for issuing the discrete to allow for time delays between the time the computer determines the criteria is satisfied until the discrete is actually issued.

TABLE VI-XII. - VEHICLE DYNAMIC RESPONSE TO FLIGHT DISTURBANCES

Event	Flight time, T + sec	Measurement	Rate gyro peak-to-peak amplitude, deg/sec	Transient frequency, Hz	Transient duration, sec	Required control capability, percent	Event	Flight time, T + sec	Measurement	Rate gyro peak-to-peak amplitude, deg/sec	Transient frequency, Hz	Transient duration, sec	Required control capability, percent		
Lift-off	0	Pitch	0.50	(b)	----	(c)	Atlas-Centaur separation	236.6	Pitch	0.33	-----	0.3	--		
		Yaw	.49	(b)	----	(c)				.49	-----	.3	--		
		Roll	.48	(b)	----	(c)				(i)	-----	(i)	--		
42-inch (1.1-m) rise	1	Pitch	3.31	5	4	12	Main engine start	247.2	Pitch	0.66	20	2.9	18		
		Yaw	.49	-----	----	4				.99	4	2.9	18		
		Roll	1.77	1.43	1	4				.65	20	2.9	24		
Region of maximum aerodynamic pressure	82 87 83	Pitch	1.98	0.20	(d)	44	Admit guidance	250.1	Pitch	0.66	0.5	7.5	26		
		Yaw	1.47	.22	(d)	48				1.14	.5	5.5	46		
		Roll	1.12	.42	(d)	48				(i)	(i)	-----	--		
Booster engine cutoff	152.2	Pitch	1.32	10	(e)	8	Nose fairing jettison	258	Pitch	1.16	25	1	4		
		Yaw	1.14	10	(e)	4				1.06	25	1.4	12		
		Roll	1.28	10	(e)	8				1.76	2	2	12		
Booster engine jettison	155.1	Pitch } Yaw } Roll } frequency	1.66	3.3	10	(f)	Transient due to holding attitude for nose fairing jettison	267.1	Pitch	1.96	(i)	7	70		
			2.29	3.3	12	(f)				2.94	(j)	7	76		
			2.41	20	1	(f)				.32	(i)	7	76		
		Pitch } Yaw } Roll } frequency	1.49	.67	10	(f)			Main engine cutoff	698.3	Pitch	3.81	30	1	8
			3.11	.72	12	(f)						3.76	30	1	8
			1.12	.63	12	(f)						1.28	30	5	8
Admit guidance	160.2	Pitch } Yaw } Roll } frequency	1.32	0.35	5	8	Deploy solar paddles	708.3	Pitch	(k)	(k)	-----	-----		
			1.64	.20	7	20				(k)	(k)	-----	-----		
			(b)	(b)	(h)	8				1.69	-----	6	-----		
Insulation panel jettison	196.8	Pitch } Yaw } Roll } frequency	2.32	25	0.6	20	Extend balance booms	726.3	Pitch	(k)	(k)	-----	-----		
			.98	25	.6	6				0.25	1.43	5	-----		
			.40	25	1	6				.16	1.43	10	-----		
Sustainer engine cutoff	233.4	Pitch } Yaw } Roll } frequency	0.50	20	1.5	25	Spacecraft separation	748.3	Pitch	0.50	40	3	-----		
			.49	20	1.5	20				.65	25	3	-----		
			(i)	(i)	-----	8				.48	1.25	6	-----		

^aTime of transient as indicated on rate gyro data.

^bToo varied to measure.

^cAutopilot not yet active.

^dTransients during period from T + 75 to T + 95 sec.

^eNearly damped by time of booster engine jettison.

^fSustainer engine control inactive during booster engine jettison.

^gAppears to be damped rate from booster engine jettison.

^hOnly damped rate from booster engine jettison remains.

ⁱNo measurable transient.

^jDifficult to determine - odd shape.

^kToo small to measure.

TABLE VI-XIII. - DESCRIPTION OF ATTITUDE CONTROL SYSTEM MODES OF OPERATION, AC-16

[V engines, 222.4 N (50 lbf) thrust; S engines, 13.3 N (3.0 lbf) thrust; A engines, 15.6 N (3.5 lbf) thrust; P engines, 26.7 N (6.0 lbf) thrust.]

Mode	Flight period	Description
All off	Powered phases	This mode inhibits the operation of all attitude control engines.
Separate on	From 850 sec after main engine cutoff until retrothrust	When in the separate-on mode, a maximum of two V and two A engines and one P engine fire. These engines fire only when appropriate error signals surpass their respective threshold. A engines: When 0.2-deg/sec threshold is exceeded, suitable A engines fire to control in yaw and roll. A_1A_4 and A_2A_3 combinations are inhibited. P engines: When 0.2-deg/sec threshold is exceeded, suitable P engine fires to control in pitch. P_1P_2 combination is inhibited. S engines: Off V engines: When 0.3-deg/sec threshold is exceeded, suitable V engines fire (as a backup for higher rates). V_1V_3 and V_2V_4 combinations are inhibited.
A and P separate on	For 451 sec after main engine cutoff	This mode is the same as separate-on mode, except V engines are inhibited.
V half on	From 451 until 500 sec after main engine cutoff	A engines: When 0.2-deg/sec threshold is exceeded, suitable A engines fire to control in roll only. P engines: Off S engines: Off V engines: When there are no error signals, V_2V_4 combination fires continuously. The continuous firing provides lateral and added longitudinal separation between Centaur and spacecraft. When 0.2-deg/sec threshold is exceeded, a minimum of two and a maximum of three V engines fire to control in pitch and yaw.
S half on	From 500 until 850 sec after main engine cutoff	A engines: When 0.2-deg/sec threshold is exceeded, suitable A engines fire to control in roll only. P engines: Off S engines: When there are no error signals, S_2S_4 combination fires continuously. When 0.2-deg/sec threshold is exceeded, a minimum of two and a maximum of three engines fire to control in pitch and yaw. V engines: When 0.3-deg/sec threshold is exceeded, a minimum of one and a maximum of two V engines fire to control in pitch and yaw. When a V engine fires, the corresponding S engine is commanded off.

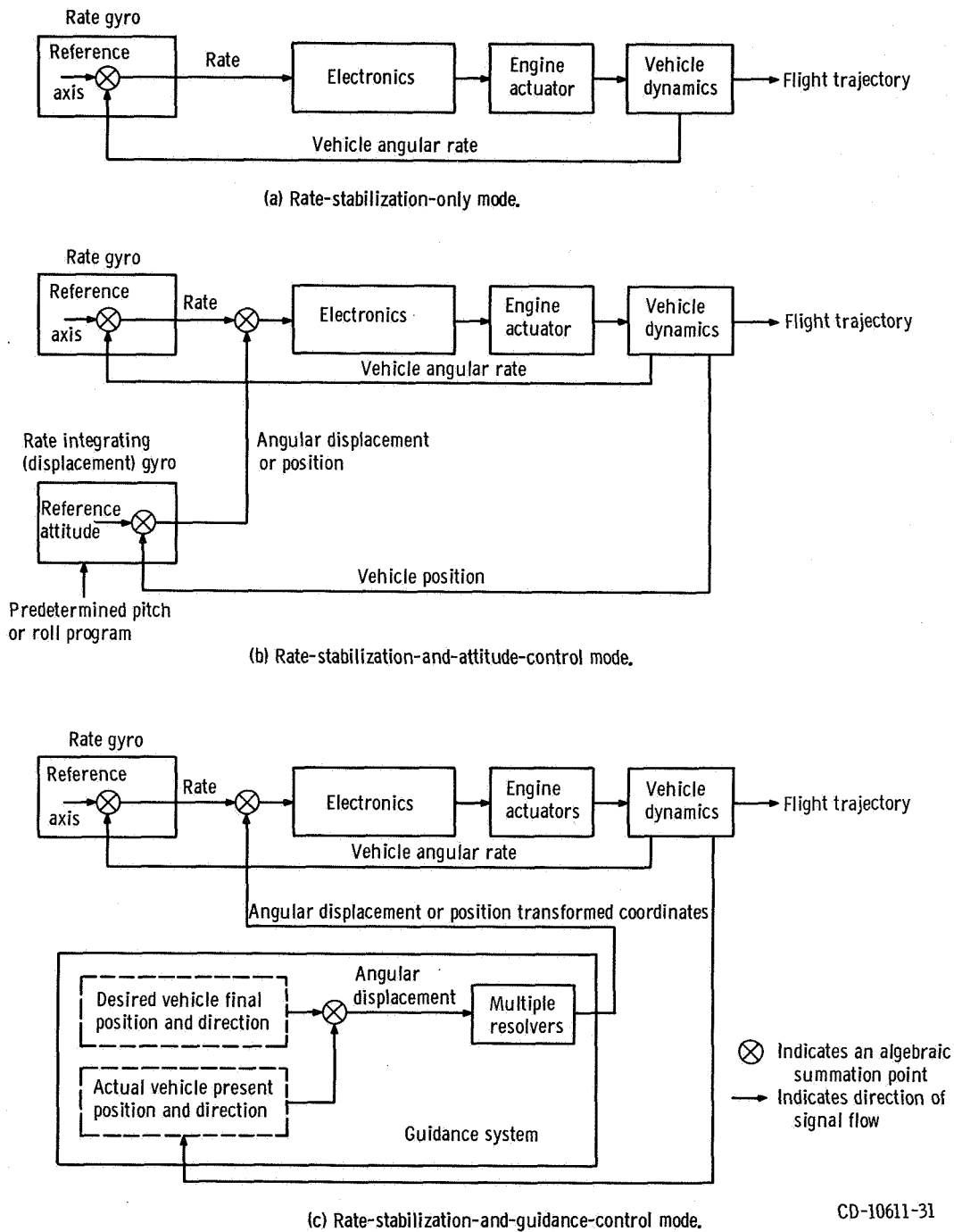


Figure VI-66. - Guidance and flight control modes of operation, AC-16.

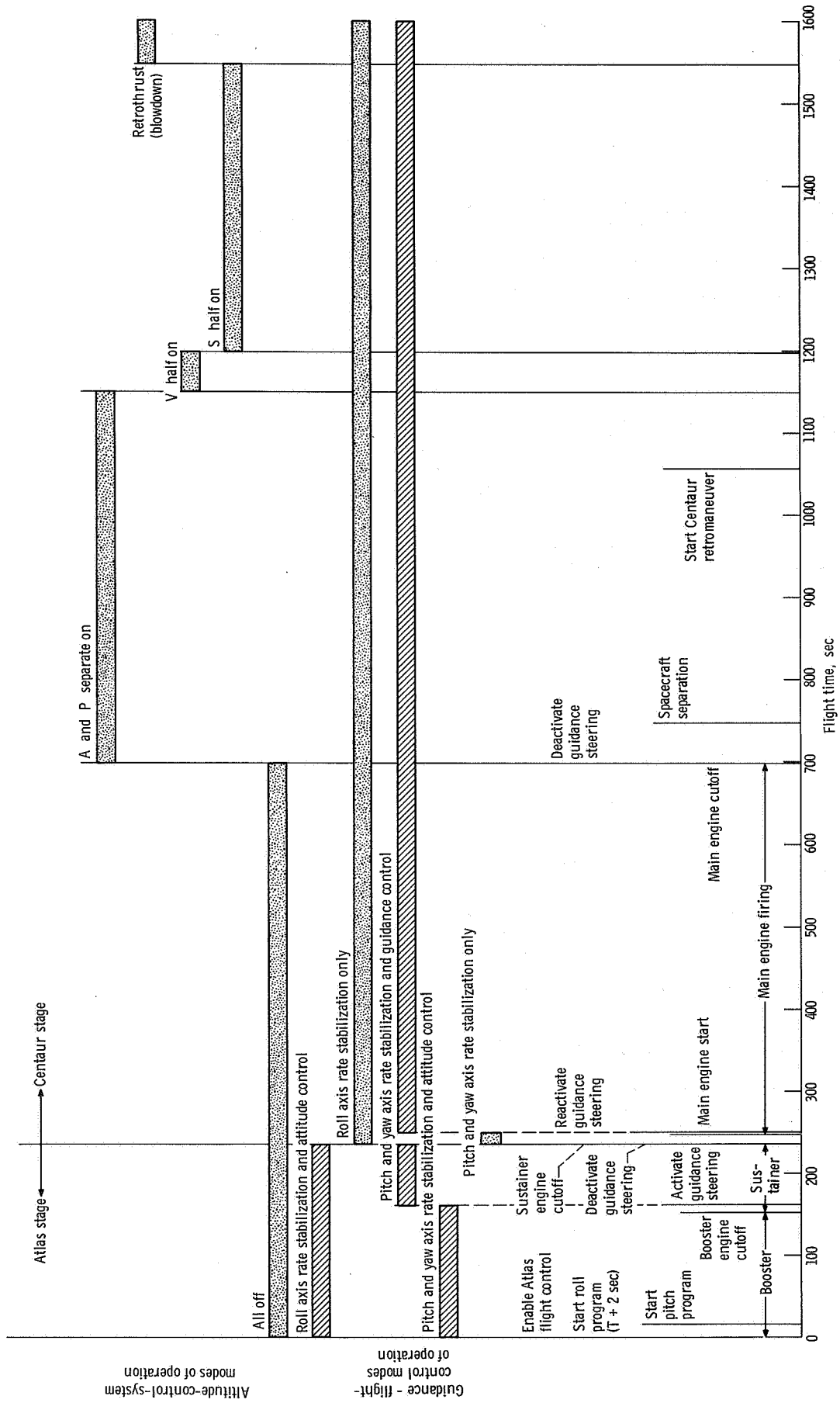
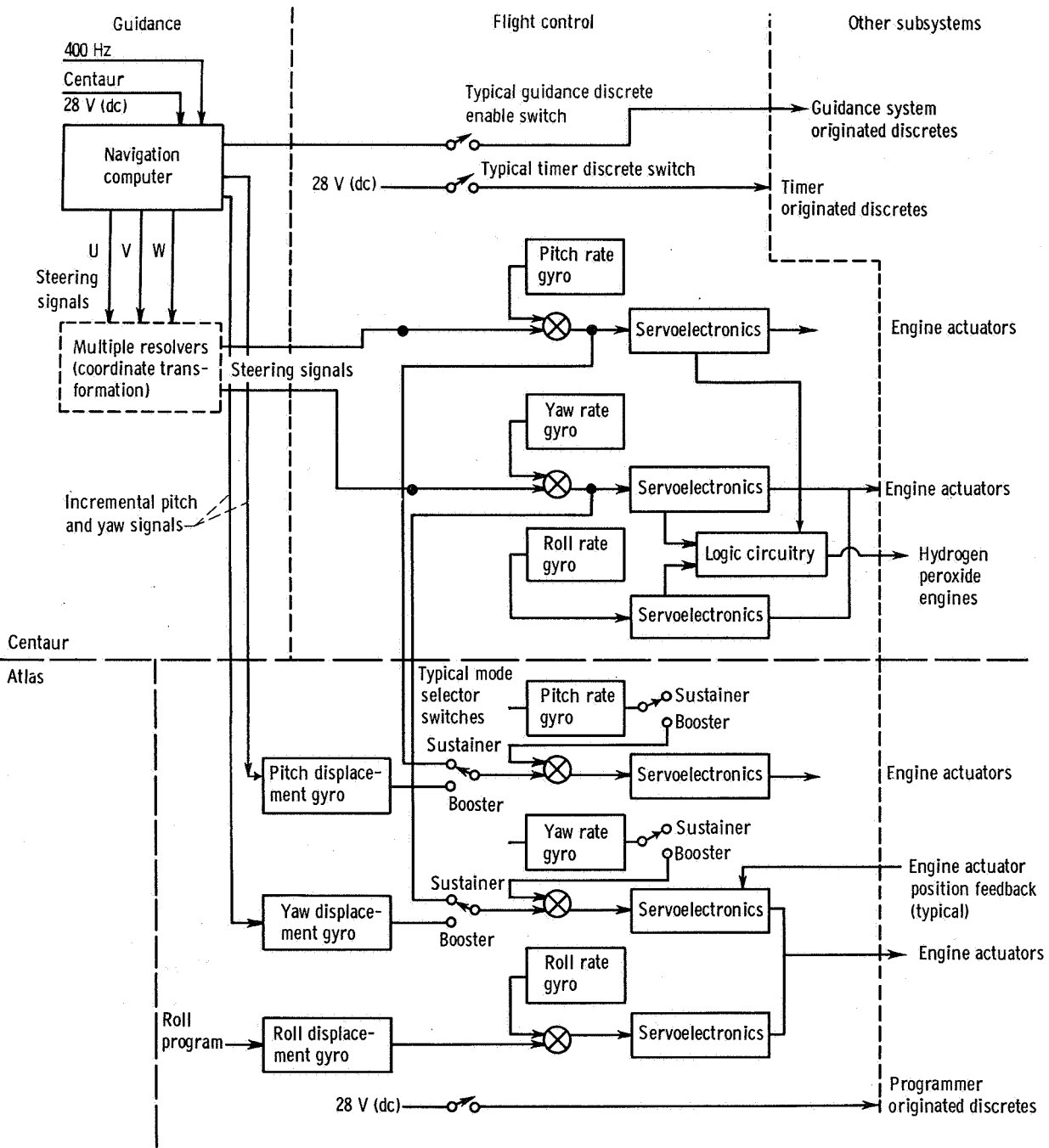


Figure VI-67. - Time periods of guidance - flight-control modes and attitude-control-system modes of operation. (There is no rate control during a 3.5-second period following sustainer engine cutoff because the engines are not developing thrust.)



⊗ Algebraic summation point

CD-10622-31

Figure VI-68. - Simplified guidance and flight control systems interface, AC-16.

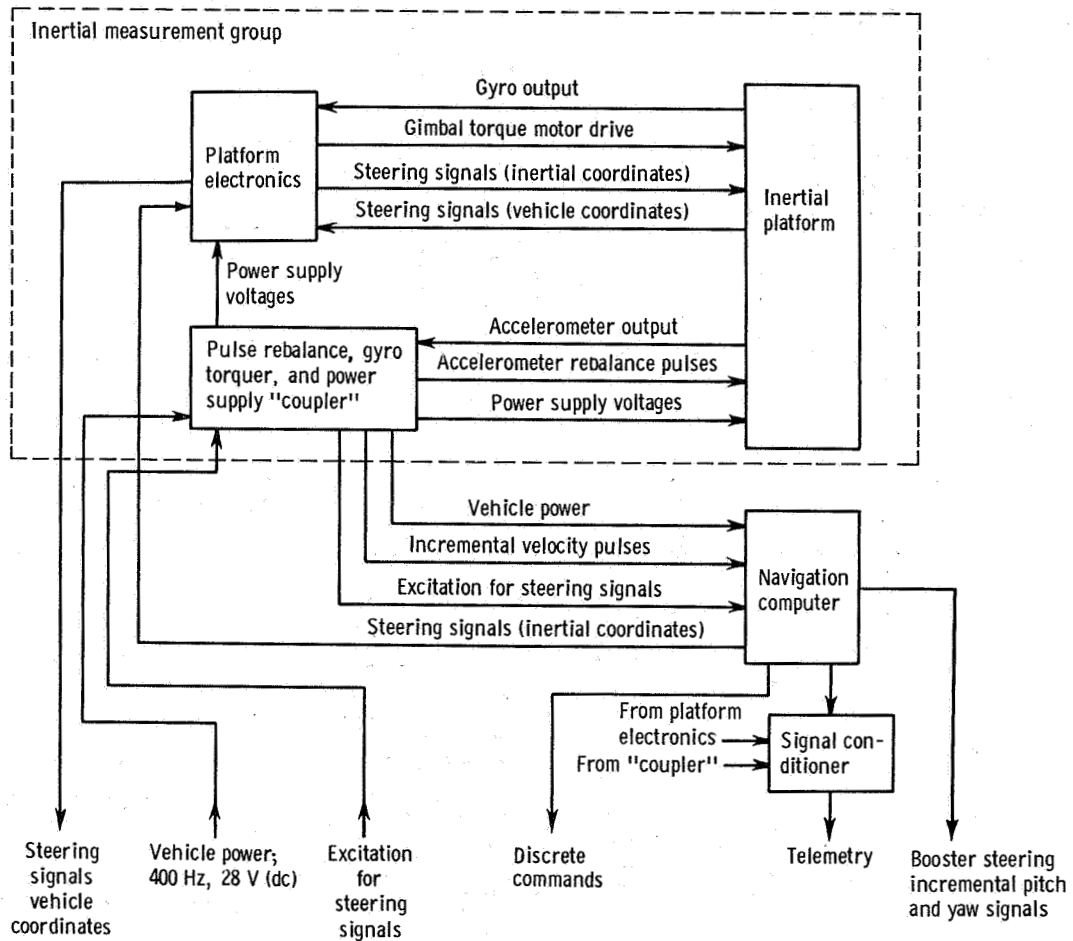


Figure VI-69. - Simplified block diagram of Centaur guidance system, AC-16.

CD-10616-31

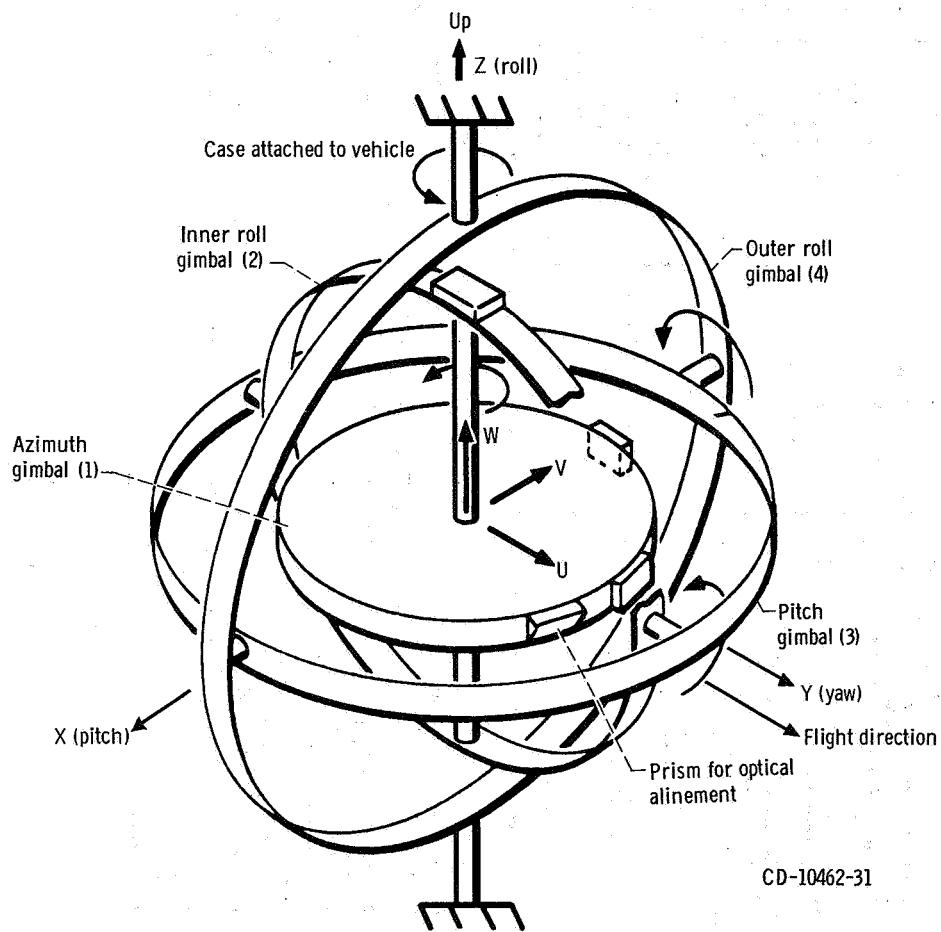


Figure VI-70. - Gimbal diagram, AC-16. Launch orientation: inertial platform coordinates, U, V, and W; vehicle coordinates, X, Y, and Z.

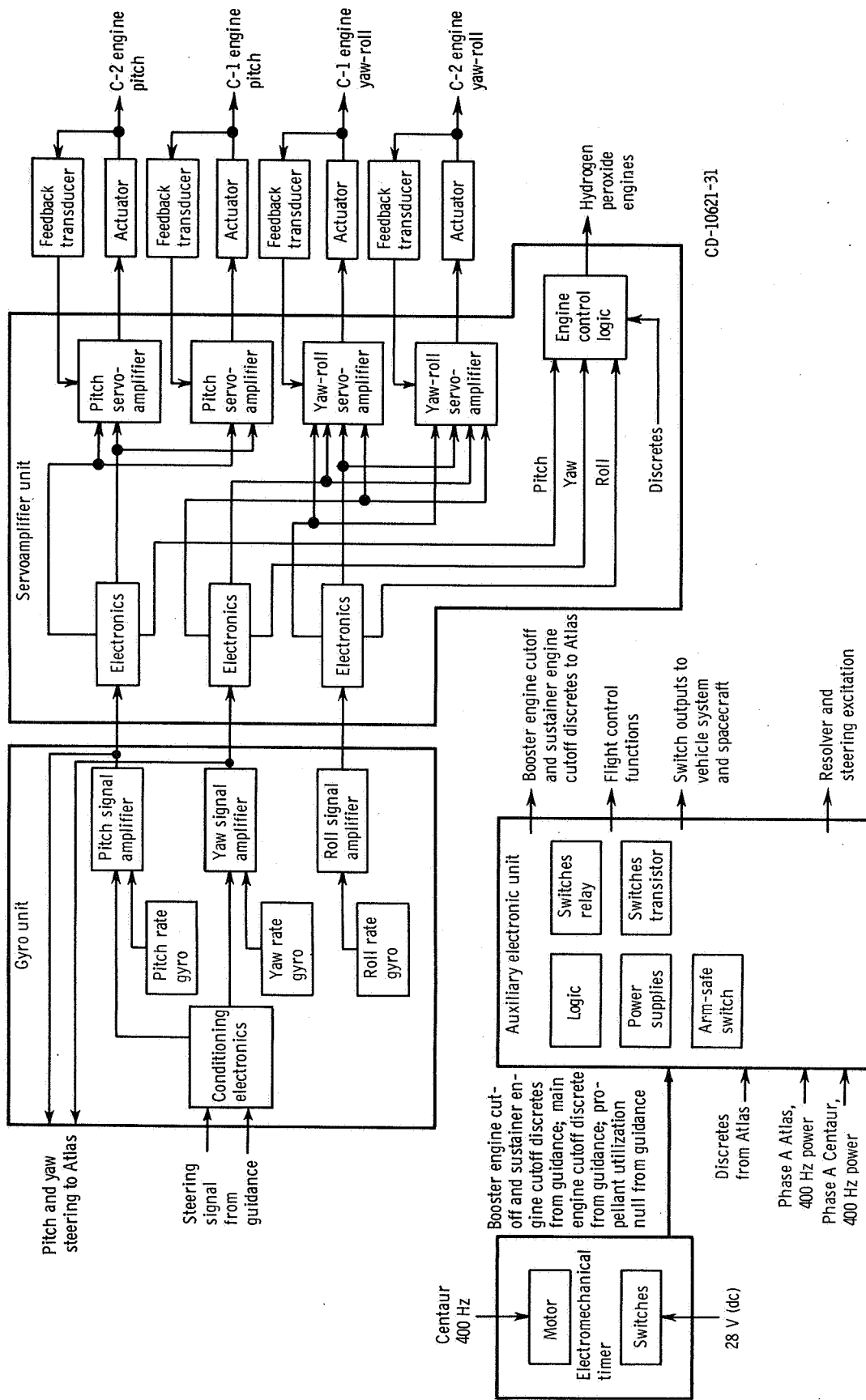


Figure VI-71. - Centaur flight control system, AC-16.

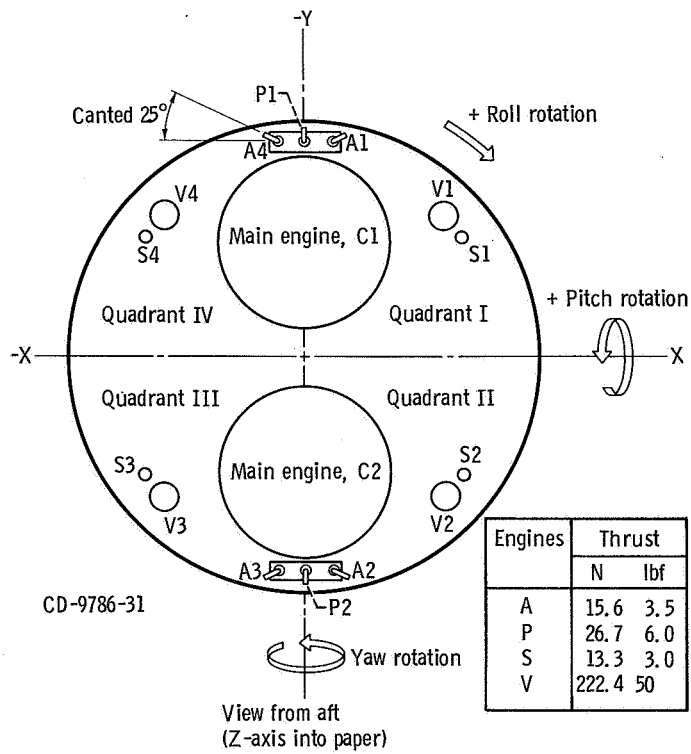


Figure VI-72. - Attitude engines alphanumeric designations and locations, AC-16. Signs of axes are convention for flight control system.

VII. CONCLUDING REMARKS

The OAO-II, launched in December 1968, was injected into the desired circular Earth orbit at an altitude of 772 kilometers and an inclination of 35° to the equator. For this mission the Atlas-Centaur flew a steeper ascent than for any previous Atlas-Centaur flight. All launch vehicle systems performed satisfactorily. The AC-16 flight proved the capability of the Atlas-Centaur to perform with a heavier payload and a longer nose fairing than those flown on previous missions. The OAO spacecraft was larger than the Surveyor spacecraft, requiring a 5.5-meter-longer nose fairing. Payload weight increase over previous missions was about 1000 kilograms.

The objectives of the star-studying observatory OAO-II, carrying 11 telescopes, were to investigate and study the young stars in the ultraviolet spectrum, to map the stars, and to further extend our knowledge of the makeup of the solar system. Many of these stars are not visible from Earth-based observatories because of the distorting effect of the Earth's atmosphere. The success of the OAO-II mission represents a significant breakthrough in the field of observational astronomy.

Lewis Research Center,
National Aeronautics and Space Administration,
Cleveland, Ohio, October 14, 1969,
491-02.

APPENDIX A

SUPPLEMENTAL LAUNCH AND WEIGHTS DATA

by John J. Nieberding

Launch Window and Countdown History

There was no specific launch opportunity, or specified number of days, for the OAO-II mission. Launch could occur on any day. The opening of the launch window on a given launch day was determined by a spacecraft constraint which would not permit spacecraft separation to occur until the spacecraft had been in sunlight for at least 1 minute. This constraint is reflected in the earliest possible lift-off time for the December 7, 1968, launch of 0340 eastern standard time. Launch window durations were chosen by the Goddard Space Flight Center to be 4 hours long.

AC-16 was launched on the first attempt. The countdown started on time at 2055 eastern standard time on December 6, 1968. Planned holds of 60 minutes duration at T - 90 minutes and 10 minutes duration at T - 5 minutes were observed as scheduled. No additional holds or recycles were required, and the countdown proceeded smoothly to vehicle lift-off at 0340:09.165 eastern standard time.

The Atlas and Centaur postflight vehicle weight summaries are presented in tables A-I and A-II.

TABLE A-I. - ATLAS POSTFLIGHT VEHICLE

WEIGHT SUMMARY, AC-16

Item	Weight	
	kg	lb
Booster jettison weight:		
Booster dry weight	2 850	6 283
Booster residuals	472	1 041
Unburned lubrication oil	16	36
Total	3 338	7 360
Sustainer jettison weight:		
Sustainer dry weight	2 700	5 953
Sustainer residuals	388	856
Interstage adapter	482	1 062
Unburned lubrication oil	8	18
Total	3 578	7 889
Flight expendables:		
Main impulse fuel (RP-1)	36 842	81 222
Main impulse oxygen	82 997	182 977
Helium panel purge	2	5
Oxygen boiloff and vent loss	229	504
Lubrication oil	82	182
Total	120 152	264 890
Ground expendables:		
Fuel (RP-1)	640	1 412
Oxygen	1 874	4 132
Lubrication oil	2	5
Exterior ice	24	54
Liquid nitrogen in helium shrouds	113	250
Total	2 653	5 853
Total Atlas tanked weight	129 721	285 992
Minus ground run	2 655	5 853
Total Atlas weight at lift-off	127 066	280 139

TABLE A-II. - CENTAUR POSTFLIGHT VEHICLE

WEIGHT SUMMARY, AC-16

Item	Weight	
	kg	lb
Basic hardware:		
Body	498	1 098
Propulsion group	501	1 105
Guidance group	143	315
Fluid systems group	116	256
Electric group	110	243
Separation group	47	103
Basic flight instrumentation	108	239
Total	1 523	3 359
Mission peculiar hardware, total	933	2 056
Hardware jettisoned in boost phase:		
Insulation panels	526	1 159
Ablated ice	23	50
Total	549	1 209
Hardware jettisoned in Centaur phase:		
Nose fairing	947	2 088
Split fairing and separation equipment	168	370
Total	1 115	2 458
Centaur residuals:		
Liquid hydrogen	86	190
Liquid oxygen	265	584
Gaseous hydrogen	39	85
Gaseous oxygen	71	169
Hydrogen peroxide	88	193
Helium	2	5
Ice	5	12
Total	556	1 238
Centaur expendables:		
Main impulse hydrogen	2 199	4 847
Main impulse oxygen	11 137	24 553
Gas boiloff on ground, hydrogen	8	17
Gas boiloff on ground, oxygen	0	0
In-flight chill, hydrogen	10	23
In-flight chill, oxygen	14	31
Booster phase vent, hydrogen	28	61
Booster phase vent, oxygen	30	66
Sustainer phase vent, hydrogen	14	30
Sustainer phase vent, oxygen	27	60
Engine shutdown loss, hydrogen	3	6
Engine shutdown loss, oxygen	6	13
Hydrogen peroxide	19	42
Helium	1	1
Total	13 496	29 750
Total Centaur weight at lift-off	18 172	40 070
Spacecraft	2 017	4 447
Total Atlas-Centaur-spacecraft weight at lift-off	147 255	324 656

APPENDIX B

CENTAUR ENGINE PERFORMANCE CALCULATION

by Ronald W. Ruedelee

The method of calculation used was the Pratt & Whitney C* technique. This technique is an iteration process for determining engine performance parameters. Flight data are used with calibration coefficients obtained from the engine acceptance tests. Calculations are made to determine C*, individual propellant weight flow rates, and subsequently, specific impulse and engine thrust. The procedure is as follows:

- (1) Calculate the hydrogen flow rate by using acceptance test calibration data and venturi measurements of pressure and temperature as obtained from telemetry.
- (2) Assume a given mixture ratio and calculate corresponding oxidizer flow rate and total propellant flow rate.
- (3) Obtain C* ideal from performance curve as a function of mixture ratio.
- (4) Correct to C* actual by using characteristic exit velocity efficiency factor obtained from acceptance test results.
- (5) Calculate total propellant flow rate, using C* actual;

$$\dot{\omega}_t = \frac{P_o A_t g}{C^*}$$

where $\dot{\omega}_t$ is the total engine propellant flow rate, P_o is the measured chamber pressure from telemetry, A_t is the thrust chamber throat area, g is the gravitational constant (32.17 ft/sec/sec), and C^* is the characteristic (actual) exhaust velocity.

- (6) Determine the mixture ratio by using the calculated total propellant flow rate and the measured hydrogen flow rate.
- (7) Compare the calculated mixture ratio with that assumed in step (2).
- (8) If two values of mixture ratio do not agree, assume a new value of the mixture ratio and repeat the process until agreement is obtained.
- (9) When the correct mixture ratio is determined, obtain the ideal specific impulse from the performance curve as a function of actual mixture ratio.
- (10) Correct to actual specific impulse by using specific impulse efficiency factor determined from acceptance test results.
- (11) Calculate engine thrust as a product of propellant flow rate and specific impulse.

REFERENCES

1. Gerus, Theodore F.; Housely, John A.; and Kusic, George: Atlas-Centaur-Surveyor Longitudinal Dynamics Test, NASA TM X-1459, 1967.
2. Foushee, B. R.: Liquid Hydrogen and Liquid Oxygen Density Data for Use in Centaur Propellant Loading Analysis. Rep. AE62-0471, General Dynamics Corp., May 1, 1962.
3. Pennington, K., Jr.: Liquid Oxygen Tanking Density for the Atlas-Centaur Vehicles. Rep. BTD65-103, General Dynamics Corp., June 3, 1965.